An Experimental Evaluation of S-Duct Inlet-Diffuser Configurations for Turboprop Offset Gearbox Applications

Final Report

Paul L. McDill
Boeing Commercial Airplane Company
Seattle, Washington

Date for general release February 1989

FOREWORD

This report was prepared by the Boeing Commercial Airplane Company, Seattle, Washington, for the NASA-Lewis Research Center, Cleveland, Ohio, under a Memorandum of Understanding and Agreement. George L. Stefko was program manager for the NASA-Lewis Research Center, and Paul L. McDill was program manager for the Boeing Commercial Airplane Company.

TABLE OF CONTENTS

LIST OF FIGURES

LIST OF TABLES

1.0 SUMMARY

With the current interest in turboprop-powered airplanes, specific inlet configurations must be designed that cannot be readily designed by existing procedures. Since existing techniques employ computer codes for design and analysis for all early configuration development, these codes must be adapted to the complex geometry of turboprop inlets. These adapted codes must be used in the design of turboprop inlet/diffuser systems, and the resulting designs must be tested before a great deal of confidence can be placed in them.

The design procedure discussed in this document employed an adapted design code to design a series of inlet/diffusers with a fixed system of constraints based on engine-gearbox and overall nacelle geometry. The design code used the superellipse to define mathematically all cross sections, and duct centerline shape was a spline fit to a small number of specified end points.

An arbitrary superellipse was defined for the diffuser throat, and the design code transitioned to the circular cross section at the compressor face. Since the plane of the throat need not be parallel to the compressor face plane, it could be canted to one side to accommodate swirl. The superellipse transition from throat to compressor face was made to follow a specified area progression.

The parametric design involved configurations that would investigate and establish trends in diffusion rate, cross-section aspect ratio, lip thickness, and shaft fairing geometry.

The results of the test program, run at tunnel Mach numbers to 0.35 and angles of attack to 15 deg, show that the lower 10% diffusion rate duct provides higher pressure recoveries particularly at angle of attack. The higher aspect ratio cross-section configuration had marginally higher pressure recovery than the low-aspect-ratio configuration. The very thin lip configuration separated at low forward speeds, however, above M=0.2 little difference between the three lips was experienced. Results indicate that the thin lip provides superior performance to either the very thin or thick lips. Of the shaft fairings tested, none were markedly superior indicating that shaft fairing configuration has a second-order effect on overall performance. The shaft fairing data indicates that careful design of cumulative diffusion (sum of duct diffusion and local diffusion from the shaft fairing) may improve compressor face distortion.

2.0 INTRODUCTION

The continuing advances in the capabilities of three-dimensional flow analysis codes have led to the reduced use of wind tunnel testing as an inlet development tool. Adding to this trend has been the increasing confidence in the inlet design procedures, developed over many years, used to design inlets for commercial airplanes.

With the recent increase of interest in turboprop-powered airplanes, inlets may be required that cannot be designed by existing procedures. The inlet/diffuser centerline may be highly curved, and the inlet/throat/diffuser cross-section may be far from round. To develop families of inlet/diffusers systematically, design codes have been written that subject lip shape, throat and diffuser cross-section shape, centerline shape, and area progression to mathematical formulation. Inlet/diffuser systems developed with these codes are designed for high total pressure recovery and low levels of compressor face distortion; however, since a large experimental data base does not exist, nor have the flow analysis codes been applied to inlets of these shapes, confidence in the design codes must be achieved through wind tunnel test correlation (see fig. 1, 2, and 3).

The wind tunnel test covered by this document provides data for this correlation, but because of the nature of the configurations tested, the parametric variations provide design trends for beginning the optimization process without a detailed knowledge of the design codes.

The most basic parameters of inlet design, inlet contraction ratio, throat Mach number for a given compressor face Mach number (diffusion rate), throat aspect ratio (height-to-width ratio), and shaft fairing shape, were varied parametrically to endeavor to establish performance trends to aid in the initial design process.

3.0 SYMBOLS AND ABBREVIATIONS

a	Semimajor axis of superellipse
Æ	Aspect ratio of throat cross section
b	Semiminor axis of superellipse
h	Total rake height
H	Total height of boundary-layer rake installed
L	Length
lb	Pounds mass
m	Exponent in equation for superellipse
M	Mach number
n	Exponent in equation for superellipse
P	Pressure
PT2	Compressor face total pressure
PTO	Freestream total pressure
r	Radius
R	Radius
W2CORR	Corrected airflow—lb/s
x	Axial distance
X	Axial distance
y	Height above surface—in
φ	Angle of attack—deg
ρ	Angle of yaw—deg
θ	Angle of rotation—clockwise looking aft—deg

3.1 Subscripts

C	Crown
H	Highlight
k	Keel
t	Total conditions
T	Throat
T_{AVG}	Average total
T_E	Trailing edge
T_{MAX}	Maximum total
T_{MIN}	Minimum total
t_{ref}	Reference total

4.0 APPROACH

4.1 CONFIGURATIONS

The design rationale for choosing the overall nacelle configuration, around which the parametric configuration variations were developed, was one of picking a configuration accommodating all of the design variables thought significant. The nacelle configuration was one in a series being investigated in the preliminary design phase of configuration development.

The design was of a wing mounted tractor installation employing a single rotation propeller and an offset gearbox. In order to keep the landing gear a reasonable length, while maintaining adequate propeller-ground clearance, the gearbox output shaft was not parallel to the engine centerline. This out of parallelism was termed spinner droop (fig. 4 and 5).

The specific design variables used in this study will be discussed in the paragraphs that follow.

4.1.1 Diffusion Rate

Even though little information was available on the relative flow angles in front of and aft of the propeller disk at angle-of-attack, it was thought that the propeller would attenuate angle-of-attack effects. In other words, the turboprop inlet in a tractor installation would not see the flow angles that turbofan inlets do for similar flight conditions. Propeller generated swirl will contribute to flow angularity at the inlet location, but since no propeller was used in this test, this effect could only be simulated through yawing the model.

With this thought in mind, it was deemed possible to not only make inlet lips sharper or thinner but to safely have higher throat Mach numbers. Two of the diffusers were designed for $M_{throat} = 0.7$ resulting in a 16.2% diffusion rate. The third was designed for approximately an $M_{throat} = 0.6$ with the attendant 10% diffusion rate. The compressor-face Mach number was approximately 0.5 in all design cases.

4.1.2 Aspect Ratio

The aspect ratio, defined as the ratio of major-to-minor axis of the superellipse that defines the throat, was approached from the standpoint of minimizing corner effects at the ends of the major axis and having a diffuser penetration of the outer nacelle surface that would result in a relatively low-drag, boundary-layer diverter between the lip and the nacelle surface.

It was felt that the highest aspect ratio possible would provide the lowest drag installation because the inlet can more closely conform to the nacelle lines. The high-aspect-ratio diffuser was designed with the longest major axis possible without severely compromising the boundary-layer diverter. Since the major axis at the throat is a circular arc, the outer corners of the inlet and diffuser may be pulled away from the nacelle surface by making the center of this arc on the opposite side of the propeller centerline. This results in a larger radius and a flatter arc. This allows the outer corners of the diffuser to penetrate the nacelle surface further aft with the results of a sharper boundary-layer diverter. The aspect ratio of this diffuser was 3.7. The exponents for the superellipse at the throat were 3.2 and 3.2 (fig. 6).

The low-aspect-ratio configuration (aspect ratio 2.1) was the lowest aspect ratio design thought possible with the same diffuser centerline as the high-aspect-ratio duct. The result of having the same centerline while reducing the aspect ratio made the boundary-layer diverter thinner and thinner. The superellipse exponents were 3.2.

The lower diffusion rate duct again maintained the same centerline; however, the throat area was increased to provide the designed diffusion rate. The throat cross-section shape was identical to the high-diffusion rate, aspect ratio 3.7, duct.

4.1.3 Lip Thickness/Contraction Ratio

The requirements for lip thickness and contraction ratio are dependent upon location around the inlet. At the inlet crown line section, the lip can be the thinnest because the local flow angle is dictated by local flow along the spinner surface. At the extreme inlet corner section, the local flow angularity will be effected by both swirl and angle of attack. At the inlet keel section line, both angle of attack and swirl effect the local flow angle. Conventional inlet lips are typically thickest at this point, and this is also the case with the inlets tested here.

The design procedure started with a circle of the appropriate throat area. The lip, with an appropriate distribution on thickness from crown to keel, was applied to the circular throat, then the circle was transformed mathematically to the "bent" ellipse desired at the throat. As a result, the variable lip thickness and contraction ratio were distributed around the superelliptical inlet.

4.1.4 Shaft Fairing

The basic, nonrotating round shaft fairing presents a nominally acceptable fairing since the flow passes over the fairing at approximately a 35-deg angle resulting in an elliptical cross section relative to the flow. Three other shaft fairings were designed with the largest one having a larger maximum thickness than the round one, but a chord equal to the maximum diameter of the compressor-face hub fairing (nonrotating). The two intermediate ones ranged down to the least chord compatible with maintaining nonseparated flows. All shaft fairings had the same maximum thickness.

4.2 TEST PROGRAM

The test program itself was run in a singularly parametric way (only one variable was investigated at a time) so that identified trends were pure.

Boundary-layer investigation rakes were fabricated to make it possible to determine boundary layer thickness and profile shape at locations both inside and outside the diffuser. Of interest were several locations inside the diffuser as well as the boundary layer immediately upstream of the boundary-layer diverter.

4.3 INSTRUMENTATION AND DATA

The primary instrumentation in the model was of two types: static pressure taps and total pressure instrumentation at the compressor face. Static pressure taps were located primarily on the centerline at the crown and keel and secondarily at the intersection of the major axis and the sidewalls. These taps were installed to provide data for flow code verification and to provide details of local flow conditions.

The compressor face total pressure instrumentation was such that the compressor face was mapped with 240 total pressure measurements. This density was designed to provide detailed, specific information on the effect of design variables on the flow entering the engine.

5.0 MODEL AND APPARATUS

5.1 MODEL SCALE

The size of the model was dictated by the desire to use an existing rotating compressor face total pressure rake. This rake was used previously for inlet development testing, and software for data acquisition and reduction was in place. The size of the rotating rake (15-in outer diameter) basically set the model scale when related to the engine-gearbox system used to develop the overall configuration. This relationship produced a scale factor of 0.168 or approximately one-sixth scale.

5.2 15-IN-DIA ROTATING RAKE

The 15-in-dia rotating rake has the capability of being built up with a range of inner diameters so that it could represent the compressor face of a wide variety of engine configurations. Typical utilization of the rake would involve a new centerbody to provide the proper hub-to-tip ratio and new rake arms. Since each of the four arms had 10 total pressure probes, a complete compressor face survey comprised of six steps of the rake produced 240 total pressure data points. The arms were rotated clockwise, looking downstream, by a hydraulic motor fed by 2000 lb/in^2 hydraulic fluid from outside the tunnel (fig. 7 and 8).

The position of the arms was determined from the output of a rotary potentiometer, and the closed-loop rake control system, utilizing the signal from the potentiometer, could be programmed for various rotational steps in the data acquisition process. In this case, the system was programmed for 15-deg steps.

Two additional rake arms were installed, one at 135 deg and the other at 315 deg (looking aft), for dynamic pressure instrumentation. Each of the arms was instrumented with five dynamic pressure transducers (fig. 9).

5.3 EJECTOR

The desire to have airflows through the diffuser system representing takeoff and cruise conditions made it necessary to augment the airflows that could be achieved from natural ram effects, as well as providing takeoff airflow with no external flow. An existing supersonic ejector employing 28 primary nozzles and built to be used with the 15-in-dia rotating rake assembly was employed (fig. 10).

5.4 BASIC FABRICATION TECHNIQUES

Since the airloads on the model were not excessive, the maximum Mach number in the test program was 0.35, the model was fabricated of aluminum and fiber glass/epoxy.

The primary structural frame was of welded and machined aluminum with the outer aerodynamic surfaces of aluminum skin and fiberglass/epoxy layups.

The s-duct diffusers were of molded fiberglass/epoxy construction formed around a male mold of 16-lb tooling foam. The male foam molds were cut on a two-head numerically controlled mill utilizing tapes developed from computer files generated in the duct design process. In this way, elaborate lofting and template cutting were not required. The ducts were made in two halves for attachment to the main support structure of the model. The split-plane between the right and left halves was offset to the right (looking aft) so that a row of static taps could be installed on the crown and keel centerline. This offset parting plane also facilitated partial disassembly to photograph internal flow visualization results.

Various lip configurations were machined of solid aluminum, again utilizing numerically controlled mills, so that no lofting was required. Shaft fairings of solid aluminum were also machined in this manner. A solid aluminum hub fairing (fig. 11) was designed and fabricated.

5.5 INSTRUMENTATION

Model instrumentation, other than the rotating compressor-face rake, was comprised of static pressure taps and boundary layer total pressure rakes. Static pressure taps were installed using stainless steel tubing polished flush with sharp edged holes (fig. 12, 13, and 14).

The boundary-layer rakes were each 1-in high with 20 tubes. They were designed to be easily mounted in any location by introducing a simple hole in the duct wall (fig. 15).

6.0 TEST PROCEDURE

6.1 EJECTOR CALIBRATION

Because the operating characteristics of the multitube supersonic ejector coupled with the s-duct diffuser model were unknown, a static calibration of the entire system was run early in the program. The ejector was run over a complete range of operating primary pressures with the secondary or compressor face weight flow measured by integrating the compressor face rake pressures.

The calibration showed that full takeoff weight flow of approximately 26 lb/s could be obtained with no ram pressure.

6.2 EJECTOR OPERATION WITH TUNNEL FLOW

With tunnel flow, the performance of the ejector was heavily influenced by the effect of ram pressure ratio. With no tunnel flow, the idle airflow of 6 lb/s could be easily obtained. However, as the tunnel Mach number increased, the low value of airflow became impossible to attain. At the maximum tunnel Mach number model internal airflow was above takeoff levels at all times.

To allow testing of lower airflow values, a flat aluminum ring was attached to the end of the ejector diffuser to reduce the exit flow area to the point where both takeoff and cruise airflows could be attained at the higher Mach numbers.

6.3 ANGLES OF ATTACK AND YAW (SWIRL SIMULATION)

The 10- by 10-ft tunnel at the Lewis Research Center can vary model attitude only in pitch. To yaw the model (to simulate swirl), it must be rotated 90 deg on the support sting and then pitched. The pitch mechanism was such that it pitched the model about a virtual center well forward so that the inlet remained near the center of the tunnel at any angle of attack. Pitch or yaw was limited to 15 deg because of the excessive length of the model.

6.4 FLOW VISUALIZATION

Flow visualization was accomplished by opening the diffuser and dotting the interior surface where flow visualization was desired with a mixture of pigment and oil. Internal flow was initiated to the desired weight flow level, and tunnel flow was brought up to the desired Mach number as quickly as possible. Both tunnel and model internal flow was turned off as soon as adequate oil streaks were obtained. The model was then opened up and photographed.

7.0 RESULTS AND DISCUSSION

Since this was a basic parametric investigation, only one variable was changed at a time. As a consequence, each variable will be discussed separately.

7.1 DIFFUSION RATE

At the time of this program, there was no concrete evidence defining the effect of the propeller disk on local flow in the inlet area at angle of attack. What information that was available indicated that the propeller disk attenuated the flow angle; i.e., when the nacelle was pitched to 15 deg, the flow into the inlet only went to, say, 10 deg.

The reduced flow angles that must be accommodated by the inlet system reduces the burden imposed on the inlet/diffuser by changes in flow angle from various flight maneuvers. Inlet lips may be sharper and throat Mach numbers higher.

Design throat Mach number for the high-diffusion rate ducts (16% diffusion rate) was 0.70. For the low-diffusion rate duct (10% diffusion rate), the design throat Mach number was 0.64. These conditions were derived from cruise engine airflow and airplane cruise Mach number.

Figure 16 (a through e) shows the compressor face total pressure recovery as a function of corrected airflow through the compressor face. For the case of angle of attack, the data shows a definite trend toward higher pressure recovery for lower diffusion rates. In other words, higher throat Mach numbers penalize pressure recovery performance. At these low forward speeds, the acceleration around the lip is greater, and the higher diffusion rate would result in an increase in secondary flow effects.

Figure 17 (a through f) shows the crown and keel Mach number distributions as well as the compressor face total pressure contours. The Mach numbers for the 16% diffusion duct and the contour plots indicate slightly worse profiles at the compressor face. Compressor face distortion for the diffusion rate comparison is shown in Figure 24.

7.2 ASPECT RATIO

Aspect ratio is defined as the ratio of the minor to major axes of the superellipse defining the throat of the inlet/diffuser system. The high-aspect-ratio diffuser has a ratio of 3.7 and the low of 2.1. The primary advantages of the low-aspect-ratio configuration are that it allows a sharper boundary-layer diverter, and the inlet experiences less corner flow subject to the effect of swirl or yaw.

Figure 19 (a through i) shows compressor face total pressure recovery as a function of corrected airflow. At zero angle of attack and Mach numbers up to 0.2, the high-aspect-ratio configuration has an incrementally higher total pressure recovery of approximately 0.1%. As the angle of attack and Mach number increases, the pressure recovery of the low-aspect-ratio configuration becomes high.

Examination of Figures 20 (a through i) and 21 (a through i), which depict wall Mach number distributions and compressor face contour plots, show that the higher aspect ratio diffuser consistently had lower wall Mach numbers down the keel with Mach numbers on the leeward, windward, and crown sides similar to those of the low-aspect-ratio configuration. The corresponding contour maps show the higher aspect ratio diffuser to have larger areas of locally lower total pressure recovery, compared to the low-aspect-ratio duct, at zero angle of attack and zero Mach number, as well as Mach number above 0.2. These contour map trends compare favorably to the trends in evidence on the pressure recovery plots.

7.3 LIP THICKNESS

The thickness of the lip, forward of the throat, determines the contraction ratio of the inlet. The flowfield in the area of the inner inlet lip, that is that part of the inlet nearest the propeller spinner surface, will experience small variations in local flow angle with airplane maneuver because of the effects of the cowling and spinner surface. The lower inlet lip, that part farthest from the spinner, will experience the greatest variation in local flow angle because angle of attack and swirl angle are relatively unattenuated in that area. The lip on that part of the inlet farthest from the vertical plane of symmetry experiences primarily crosswind effects. The basis of lip and cowl shape is shown in Figure 22, and a photograph of all the lips is shown in Figure 23.

With these flow angularity effects, the inlet lips were designed with thickness, or contraction ratio, to accommodate them. However, the thinnest inlet lip was designed with a constant contraction ratio around its periphery in hopes that it would provide an end point in design. Lip internal flow visualization is shown in Figures 24 and 25.

The design procedure was to set up the desired distribution of lip thickness around a circular inlet of the required throat area, then mathematically transform the throat from a circle to a superellipse. All throat superellipses had exponents of 3.2. Since the lip thickness varied around the circular inlet, the centerline of the circular throat and circular highlight were not coincident. A schematic of this geometry and contraction ratio details prior to the transformation into a superellipse is shown in Figure 22.

The total pressure recovery as a function of corrected airflow plots shown in Figure 26 (a through i) indicates a strong fall off in pressure recovery with air flow. Wall Mach number distributions and compressor face contour plots are contained in Figure 27 (a through i). For the thin and thick lips, forward speed has a negligible effect on recovery. For the very thin lip, the zero forward speed case indicates severe lip separation resulting in deterioration in total pressure recovery. Once freestream Mach number was brought up to the M=0.20 level, the performance of the very thin lip was basically the same as the thin and thick lips. The zero forward speed compressor face distortion map, for takeoff airflow, graphically illustrates this separation effect (see fig. 27a). Also shown in this figure are the wall Mach number comparisons for the three lips. The compressor face map comparison indicates that the crown and sidewalls are similar for all three lips, but for the very thin lip, the keel indicates complete separation propagating to the compressor face. For all the forward speed cases, the total pressure ratio curves, as well as the compressor face maps, are similar indicating that the thin lip would be the better configuration. The compressor face total pressure distortion for lip configurations is shown in Figure 28.

7.4 SHAFT FAIRING

The basic design philosophy for the shaft fairing was to minimize friction and profile drag, while ensuring that separation did not occur around the shaft or fairing. It must be kept in mind that the flow over the shaft fairing was at approximately 35 deg to the shaft centerline, resulting in a smaller effective thickness ratio than the classical one based on thickness divided by chord. The basic circular shaft, then, actually presented an elliptical section to the diffuser flow. Basic shaft fairing cross sections are shown in Figure 29, and a photograph of fairings is shown in Figure 30.

The thickness of all of the shaft fairings was set by the diameter of the round shaft and an allowance for the thickness of the structure of the fairing placed around it. The wetted area and separation characteristics varied with the chord of the fairings. Typical flow over the shaft fairing is shown in Figures 31 and 32, and internal duct flow showing the effect of cumulative diffusion is shown in Figures 33 and 34.

The largest fairing, referred to as large on the plots, was designed with the trailing edge coincident with the maximum radius of the compressor-face hub fairing. The large fairing had a thickness to chord ratio of 32%, which would present an 18.4% thick profile with the flow traversing the fairing at 35 deg to the shaft centerline.

The small fairing, whose leading and trailing edges fell short of the maximum radius of the compressor-face hub fairing, was 47% thick normal to the shaft centerline, but was 27.1% with the flow at 35 deg.

The round shaft fairing, with the flow at 35 deg, would present the flow with an elliptical cross section of 57.3% thickness ratio (see fig. 29).

In Figures 35 (a through f) is shown the compressor face total pressure recovery as a function of corrected airflow for various freestream Mach numbers, angles of attack, and yaw. All of these data were taken with a 16.2% diffusion rate, 3.7 aspect ratio, thin lip configuration. These data show that the large fairing has consistently the highest total pressure recovery. The differences between the highest and lowest total pressure recoveries for all of the conditions tested was on the order of 0.1% or less. This indicates that the configuration of the shaft fairing over fairly large limits does not have a first-order effect.

Figures 36 (a through g) and 37 (a through g) show the wall Mach number distributions for crown, keel, windward and leeward walls, and compressor face total pressure contour maps for the three shaft fairing configurations at various corrected airflows and freestream Mach numbers.

The wall Mach number distributions show little or no variation with shaft fairing configuration. Predictable variations, in wall Mach independent of configuration, occur as a function of freestream Mach number or corrected airflow. Angle of attack or yaw did not have an appreciable effect on wall Mach number distributions.

The compressor face total pressure maps provide more insight into what is actually taking place in the flow around the shaft fairings. The wake behind the round shaft fairing (or elliptical cross section relative to the flow) indicates that separation behind the fairing impacts the compressor face map in the top of the annulus and was the primary contributor to the lower total pressure recovery experienced by that configuration. The upper annulus part of the maps, for both small and large shaft fairings, reflects the different wake characteristics of the two fairing configurations. The large shaft fairing appears not to have separated, and the "stem" at the top of the map shows typical wake characteristics from normal boundary layer growth on the fairing. The "stem" on the maps for the small shaft fairing indicates that some separation occurred further forward on the aft surfaces of the fairing, but the flow in the wake has accelerated back toward the overall compressor face Mach number. The trailing edge of the large fairing is closer to the compressor face, and the wake has not had a long enough distance to decay.

As the freestream Mach number increased, the wake characteristics behind the large fairing remained relatively unchanged. However, the "stem" behind the small fairing decreased in width and disappeared. Of interest is the thickening of the boundary layer on the hub fairing just at the base of the "stem." This was interaction of the separated wake from the fairing with the boundary layer on the hub fairing.

The two bulges at the top of the annulus were apparently the result of secondary flow effects which were considered quite strong in diffuser configurations such as these. Compressor face total pressure distortion, as a function of shaft fairing configuration, is shown in Figure 38.

7.5 BOUNDARY LAYER

The boundary-layer profiles, coupled with flow visualization photographs, graphically illustrate details of the flow, particularly in the regions around the shaft fairing. Boundary-layer profiles are given in Figures 39 (a through h) and 40 (a through d).

The boundary-layer profiles for the aft most rake position (X/L=0.703) show a flat vertical profile indicating, at least locally, separated flow. The flow visualization photographs show fairly large separation bubbles on either side of the shaft fairing toward the trailing edge. This phenomena was apparent early on in the program and was considered the source of the "bulges" in the upper two quadrants of the compressor face maps.

The boundary-layer profiles forward of the separation bubbles indicate fully developed turbulent boundary layers.

The cause of the separation bubbles was considered to be the combined diffusion. In other words, the local sum of overall duct diffusion and that associated with that part of the shaft fairing aft of the point of maximum fairing thickness. Since the "bulges" appear on nearly all of the compressor face maps, it may be necessary to locally contour the walls to relieve the local diffusion rate in these areas. Eliminating these "bulges" should have an appreciable impact on total pressure recovery and compressor face distortion.

8.0 CONCLUSIONS

Based on the results of the overall program, it may be concluded that:

(1) The analytical design codes, as adapted for the complex geometry of turboprop inlets, are suitable for use.
(2) The 10% diffusion rate configuration had slightly better performance than the 16.2% configuration, suggesting that conventional, lower, diffusion rates are a preferable choice.
(3) The lower aspect ratio cross-section configuration had marginally superior performance, particularly with respect to compressor face distortion.
(4) The three lip configurations tested all provided acceptable performance at Mach numbers above 0.2. Below this value the thinnest lip separated with attendant loss in total pressure recovery and increase in distortion. The intermediate thickness lip was deemed the better of the three.
(5) Of the three shaft fairing configurations tested, all presented a faired surface to the flow since the flow crossed the shaft at approximately a 35-deg angle. This resulted in even the round shaft presenting an elliptical section to the flow. Test results indicated that the smallest of the two airfoil shaped fairings was superior because of minimal wake, small wetted area, and the least aggregate duct diffusion.

The adapted design codes provided configurations that resulted in acceptable performance in terms of distortion and total pressure recovery. Further configuration optimization may be achieved, without code modification, by utilizing established trends to refine design inputs.

ORIGINAL PAGE IS
OF POOR QUALITY

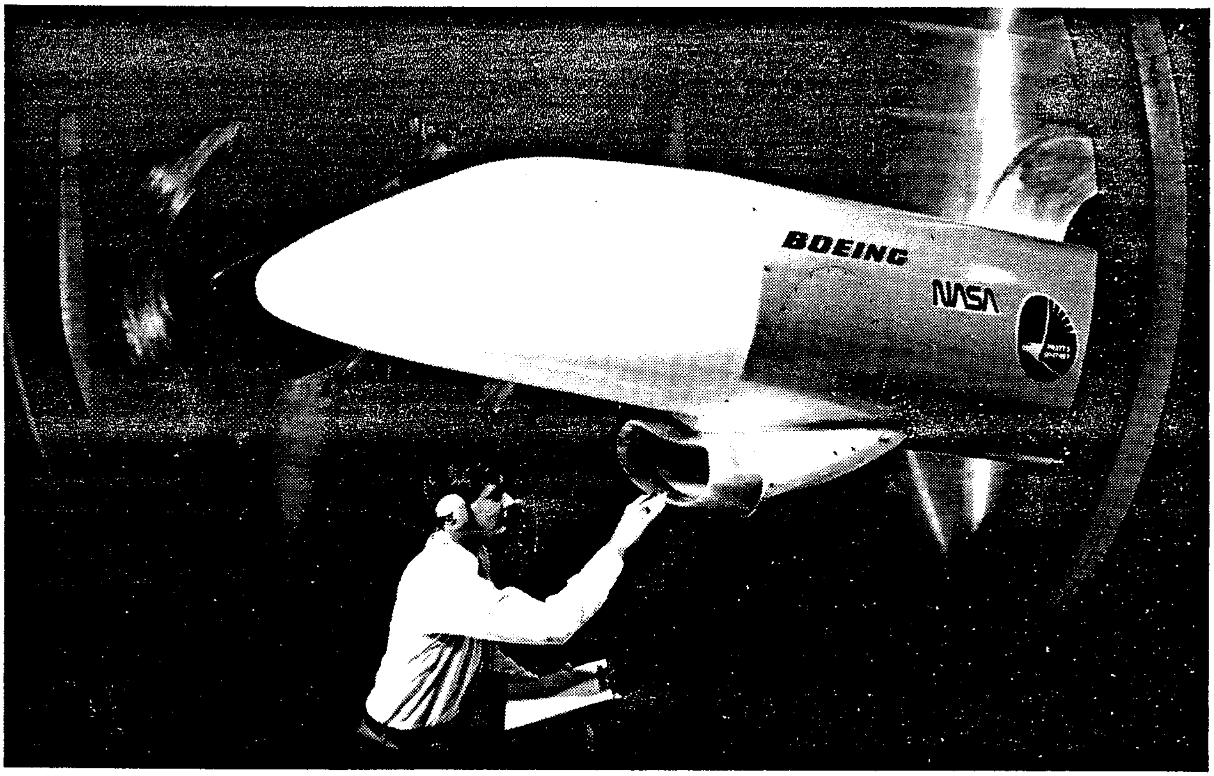

Figure 1. Model Installed in NASA/Le 10- X 10-ft Tunnel

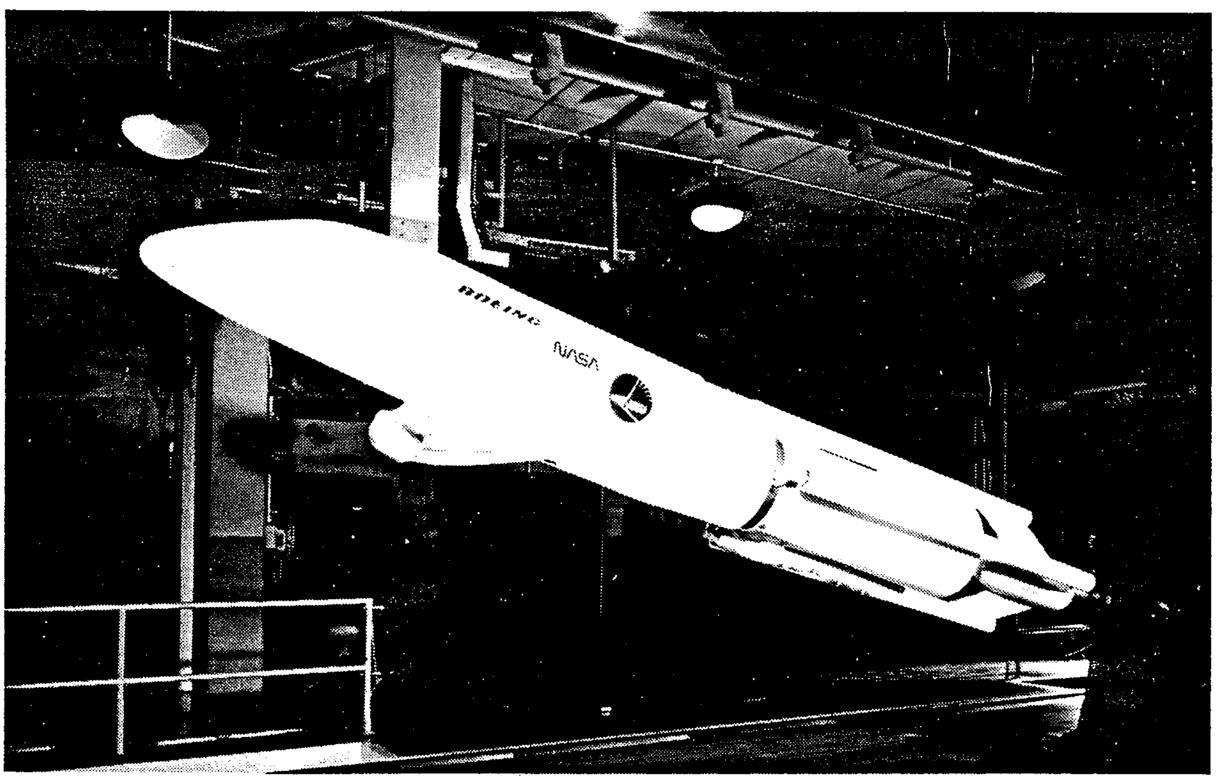

Figure 2. Complete Model in Build-Up Area—NASA/Le 10- X 10-ft Tunnel

PRECEDING PAGE BLANK NOT FILMED

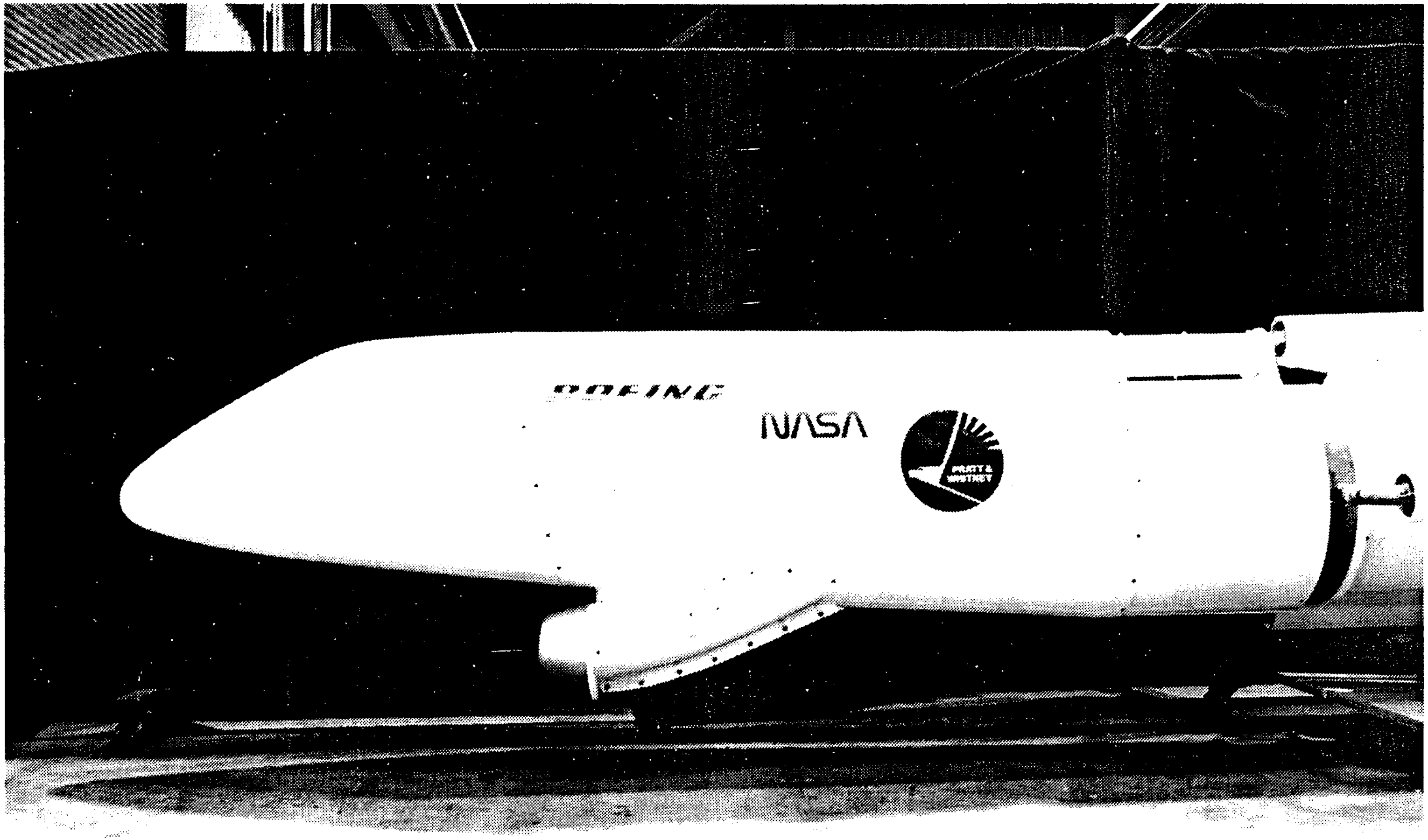

ORIGINAL PAGE IS
OF POOR QUALITY

Figure 3. Side View of Model

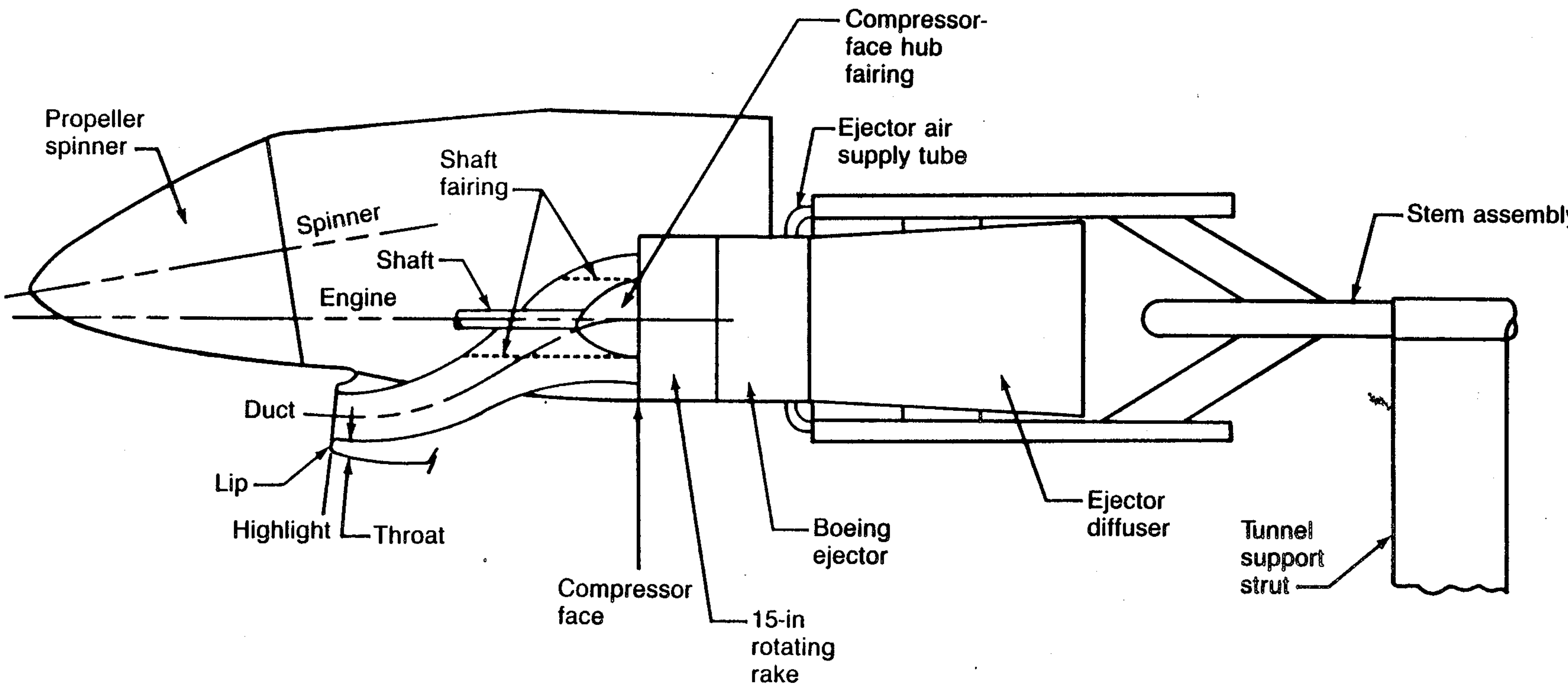

Figure 4. S-Duct Model Schematic

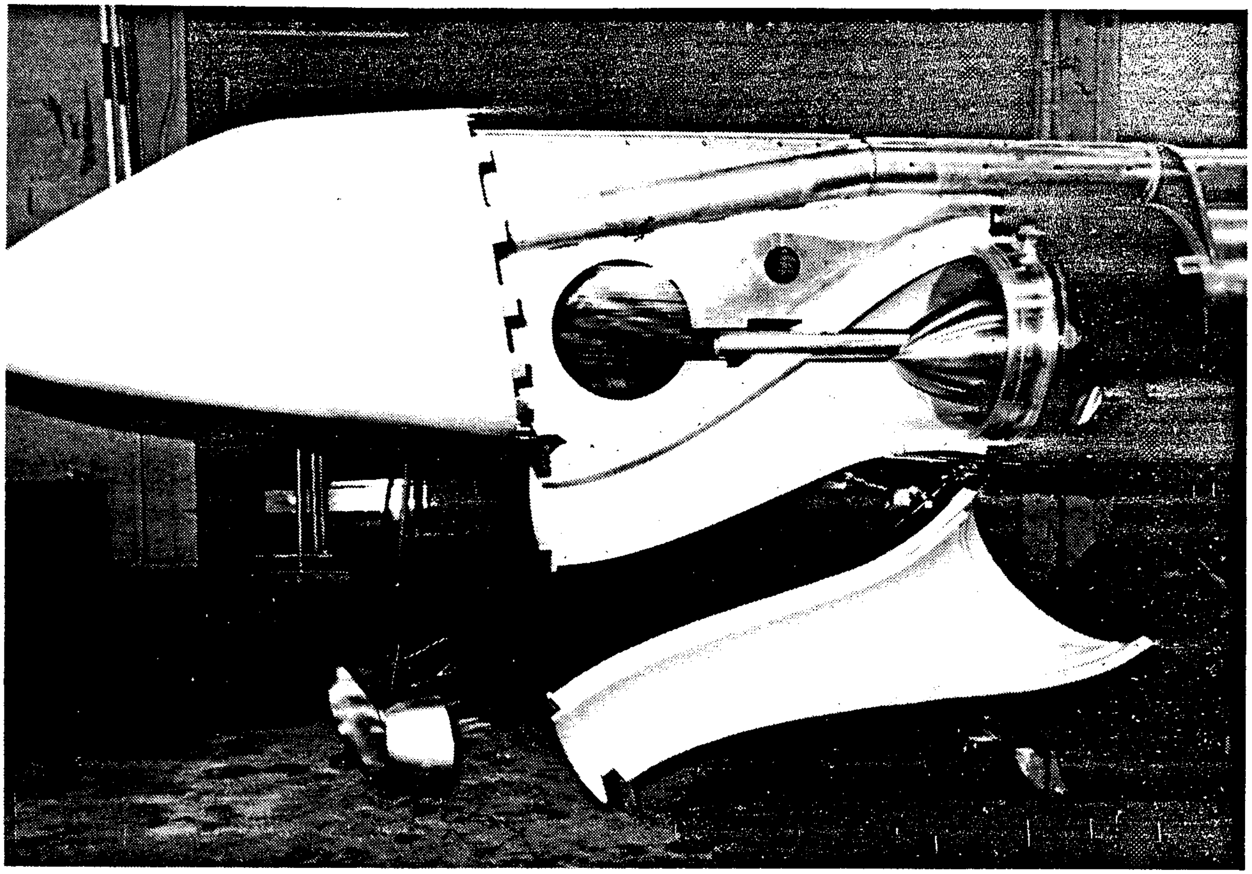

Figure 5. Side View of Model With Cowling, Duct Half, and Lip Removed

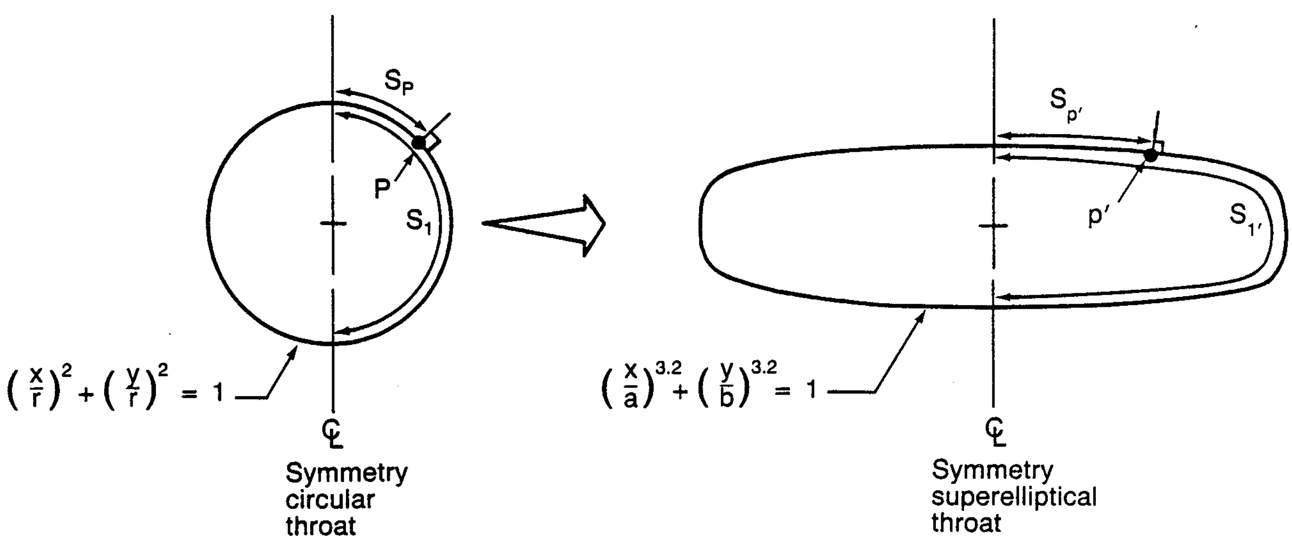

Figure 6. Throat Geometry Development

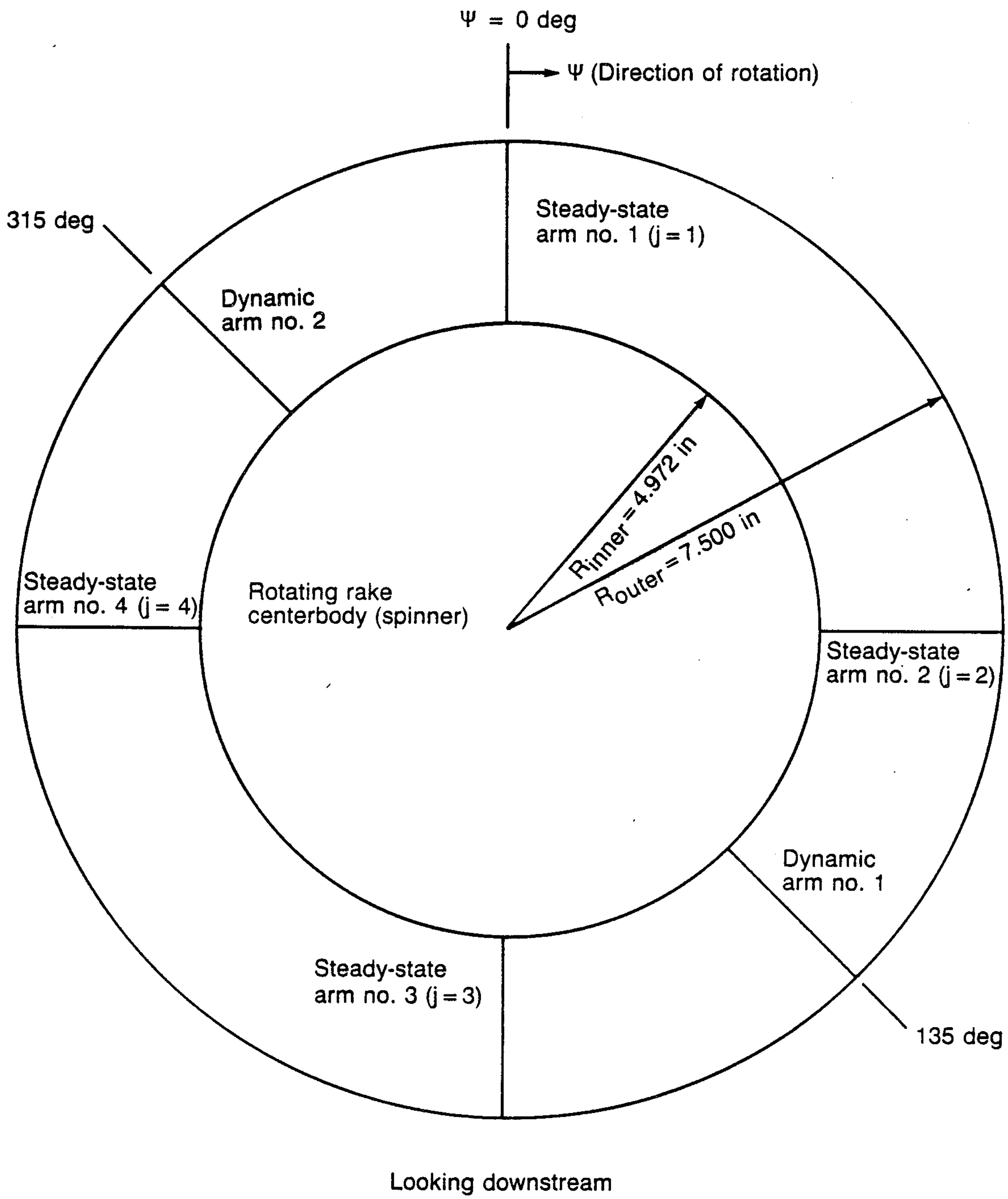

Figure 7. Turboprop Core-Inlet Test Compressor-Face Rotating Rake

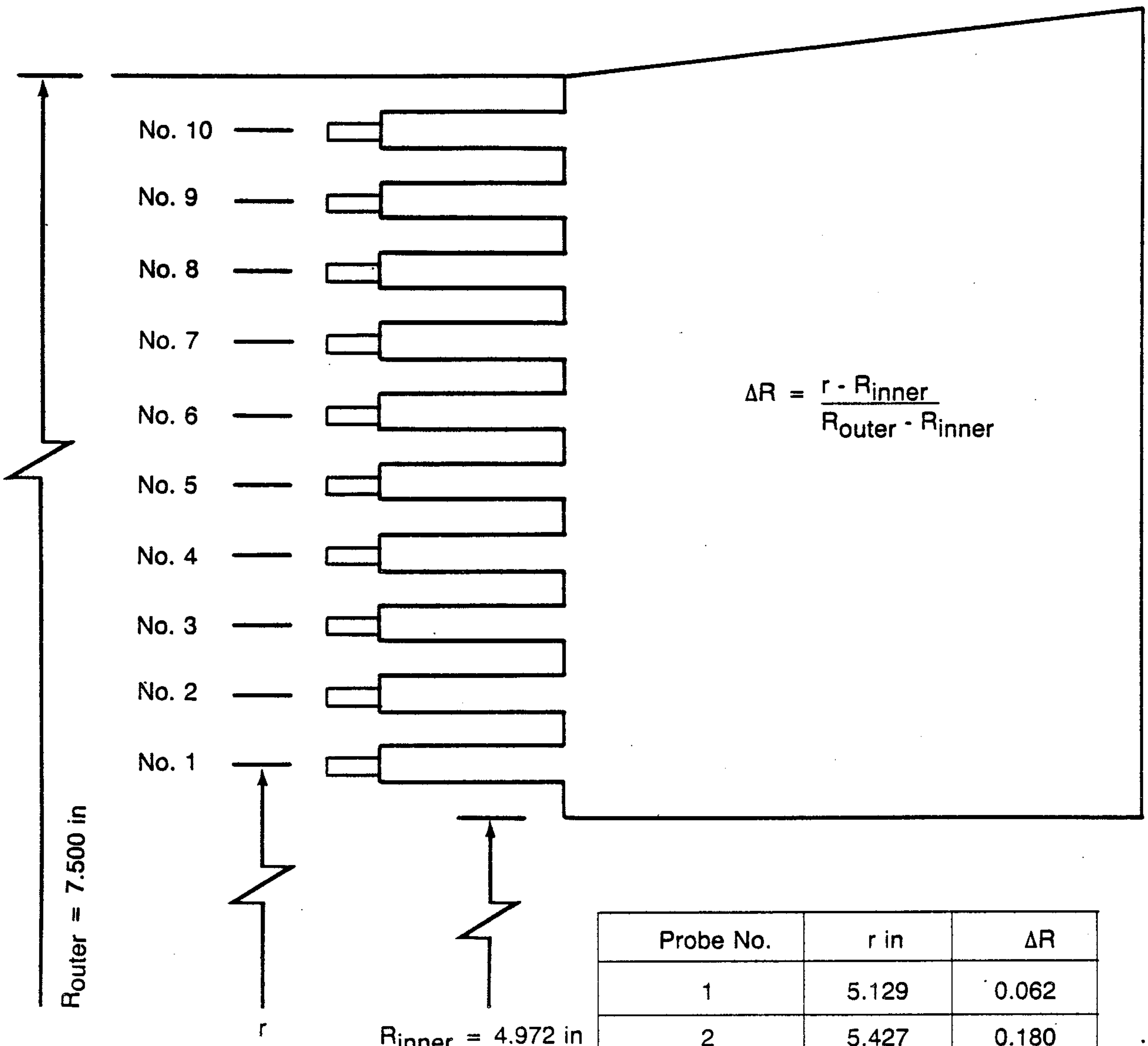

Probe No.	r in	ΔR
1	5.129	0.062
2	5.427	0.180
3	5.710	0.292
4	5.980	0.399
5	6.238	0.501
6	6.486	0.599
7	6.725	0.693
8	6.955	0.784
9	7.178	0.872
10	7.395	0.958

Figure 8. Steady-State Compressor-Face Rake Arm

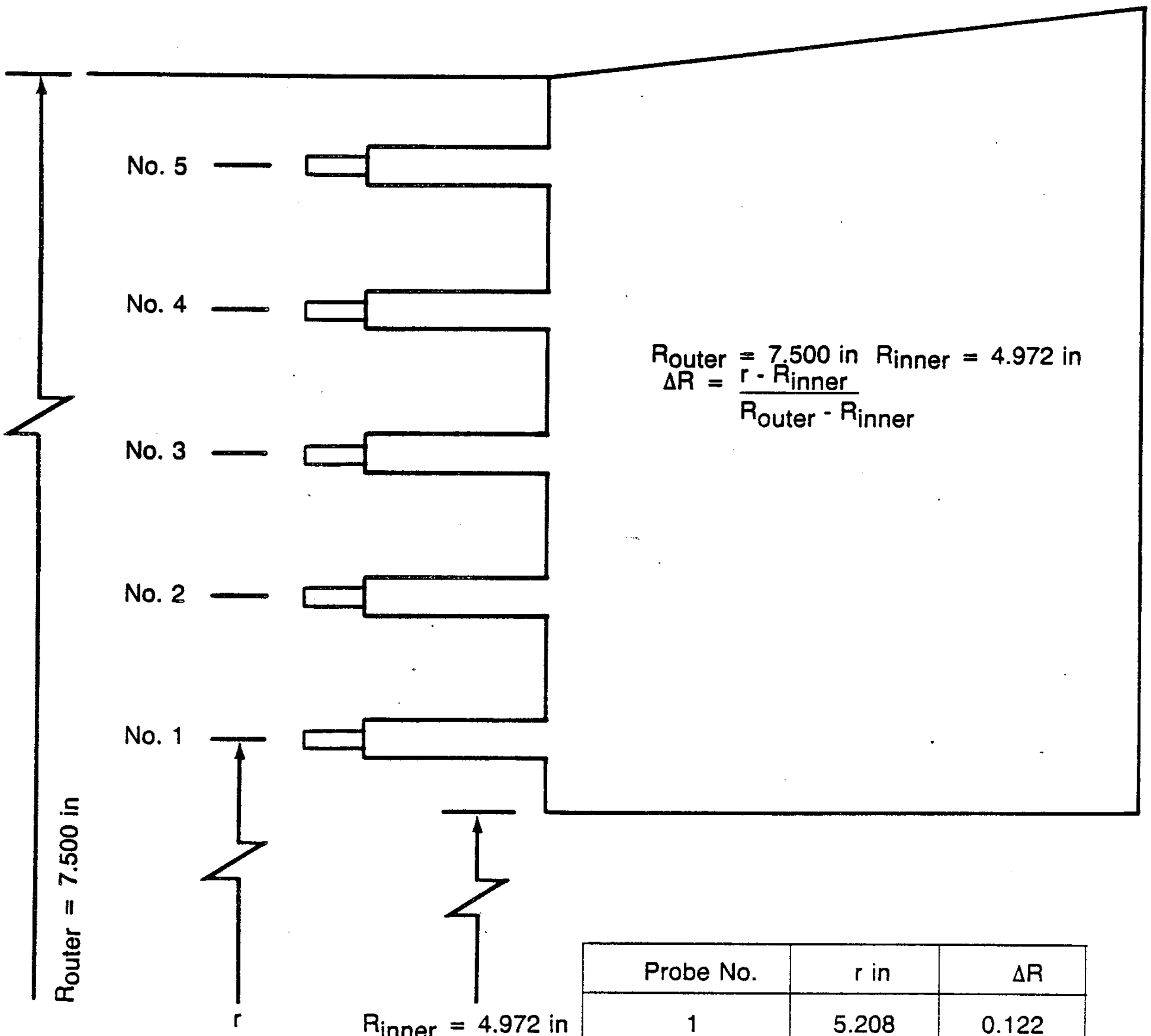

Probe No.	r in	ΔR
1	5.208	0.122
2	5.847	0.346
3	6.364	0.550
4	6.841	0.739
5	7.288	0.916

All Probes Are Centered in Equal Areas

Figure 9. Compressor-Face Rake Dynamic Pressure Arms (RMS)

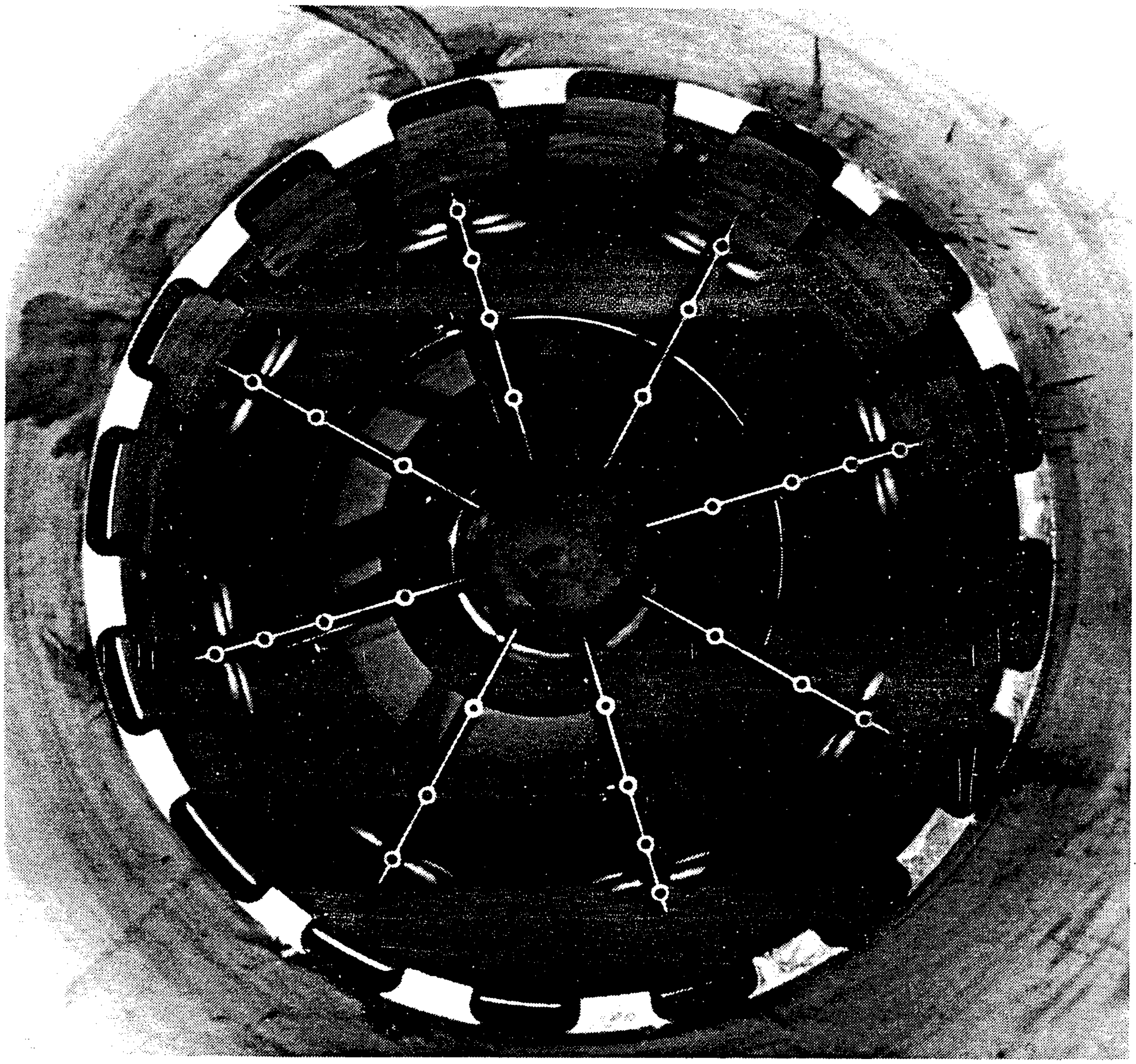

Figure 10. Supersonic Ejector Primary Nozzles—Looking Upstream

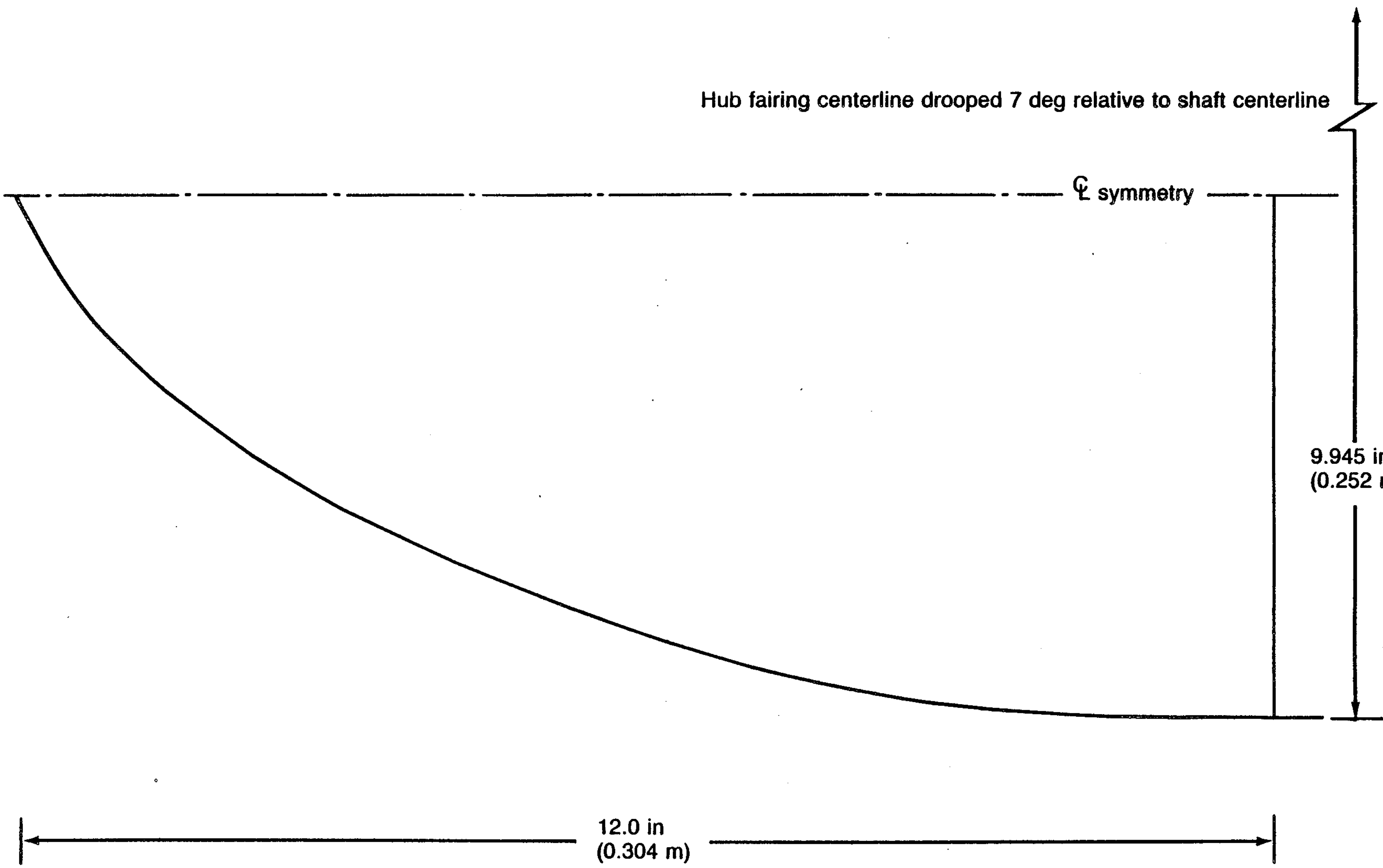

Figure 11. Compressor-Face Hub Fairing Contour

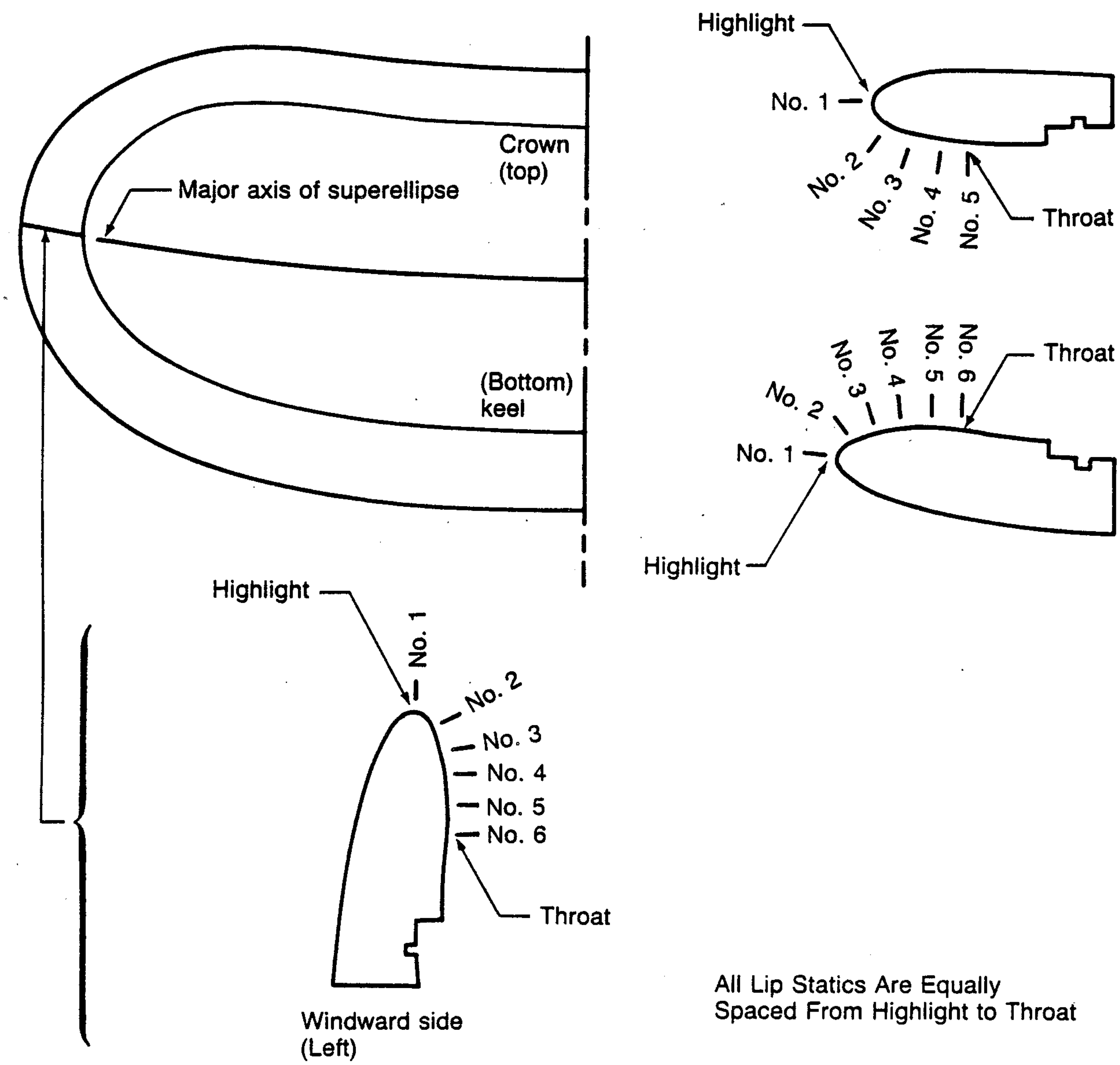

Figure 12. Lip Static Pressure Instrumentation

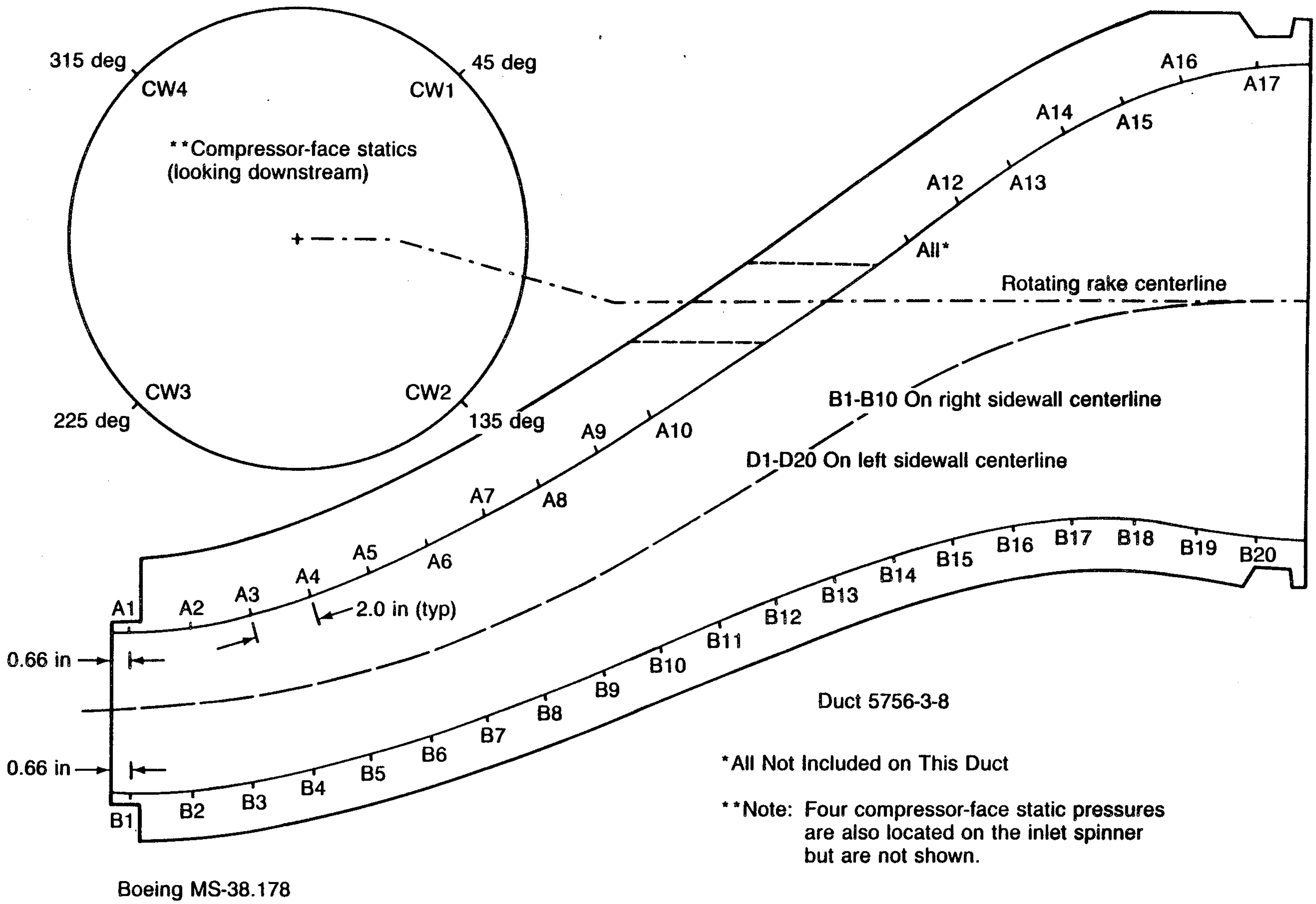

Figure 13. Turboprop Inlet-Duct Static Pressure Instrumentation— 10% Diffusion Duct

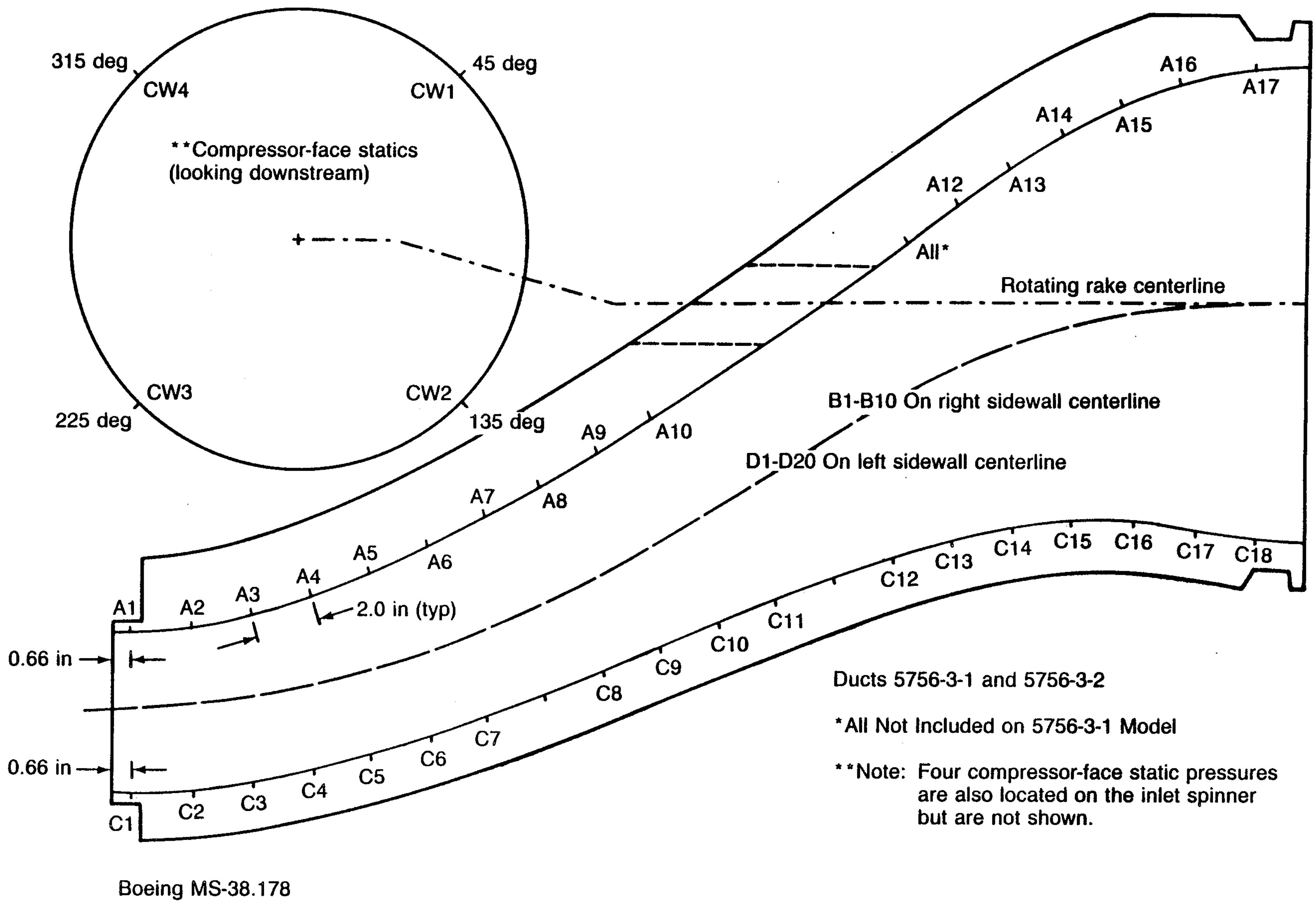

Figure 14. Turboprop Inlet-Duct Static Pressure Instrumentation—16.2% Diffusion Duct

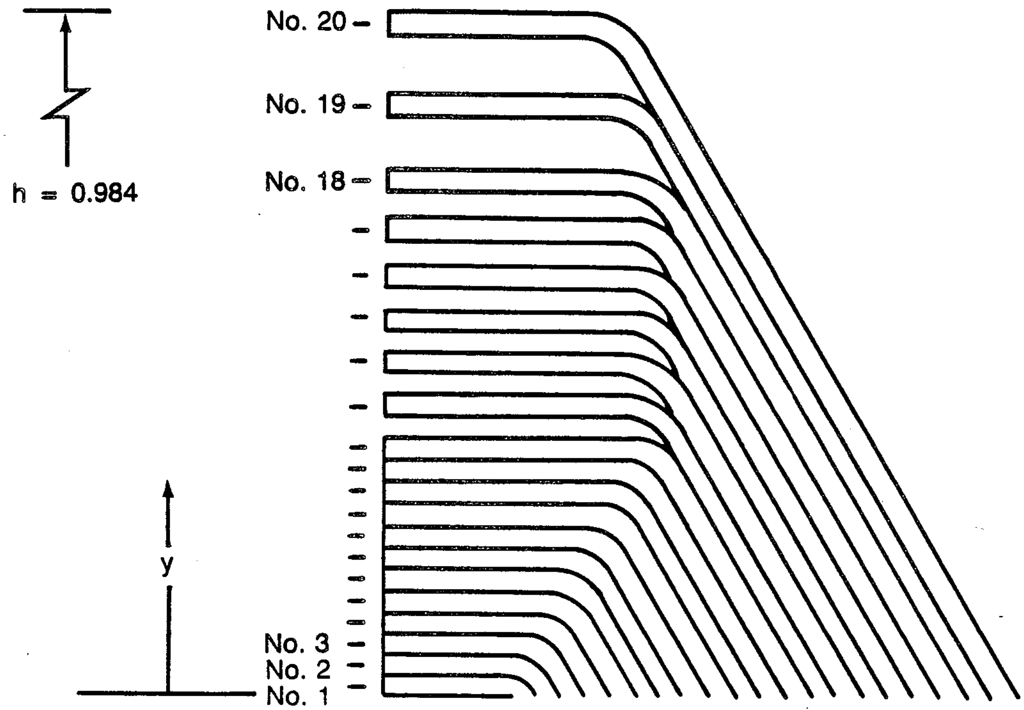

Probe No.	y/h	Probe No.	y/h
1	0.016	11	0.341
2	0.049	12	0.374
3	0.081	13	0.439
4	0.114	14	0.504
5	0.146	15	0.569
6	0.179	16	0.634
7	0.211	17	0.699
8	0.244	18	0.764
9	0.276	19	0.882
10	0.309	20	1.000

Figure 15. Boundary-Layer Rake

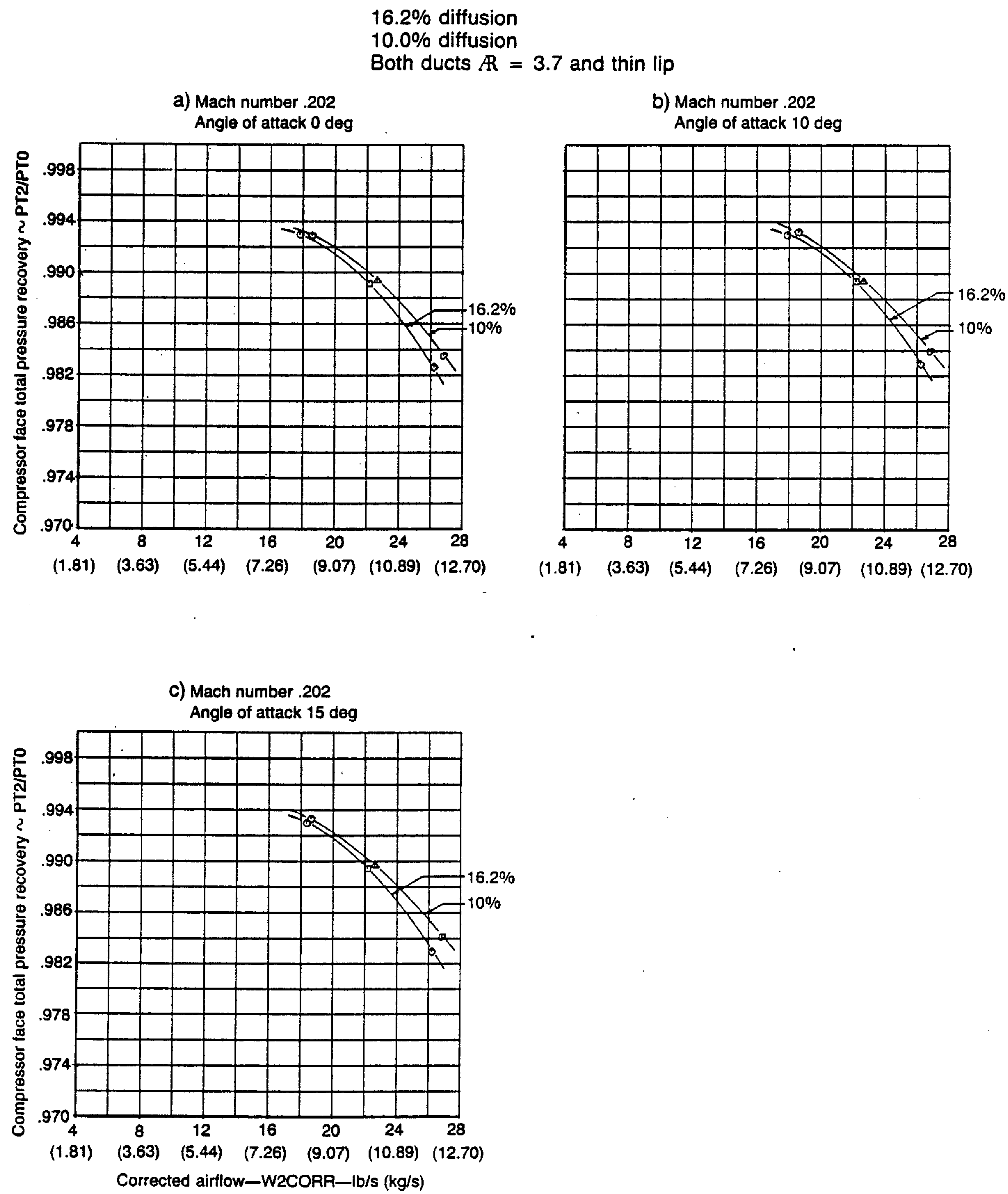

Figure 16. Duct Diffusion Comparison—Pressure Recovery for 16.2% and 10% Diffusers With 3.7-Aspect-Ratio Duct and Thin Lip

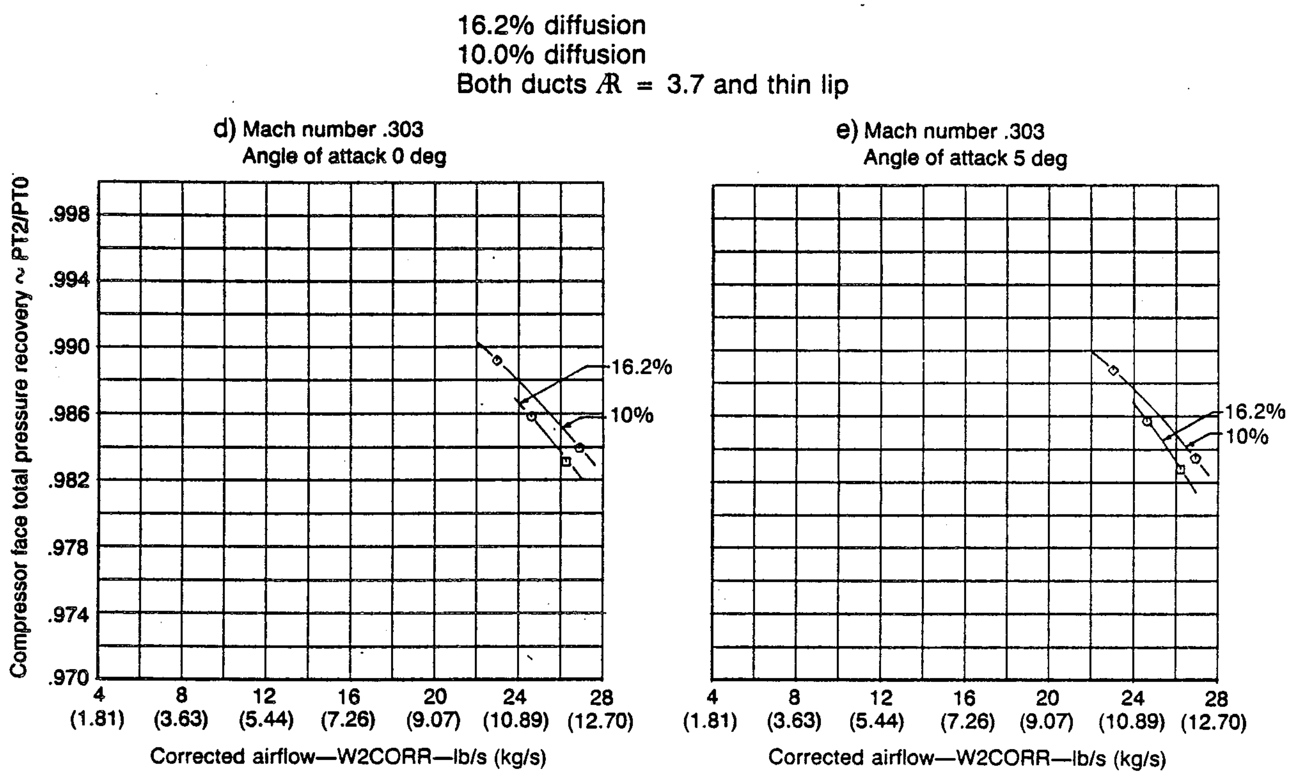

Figure 16. Duct Diffusion Comparison—Pressure Recovery for 16.2% and 10% Diffusers With 3.7-Aspect-Ratio Duct and Thin Lip (Concluded)

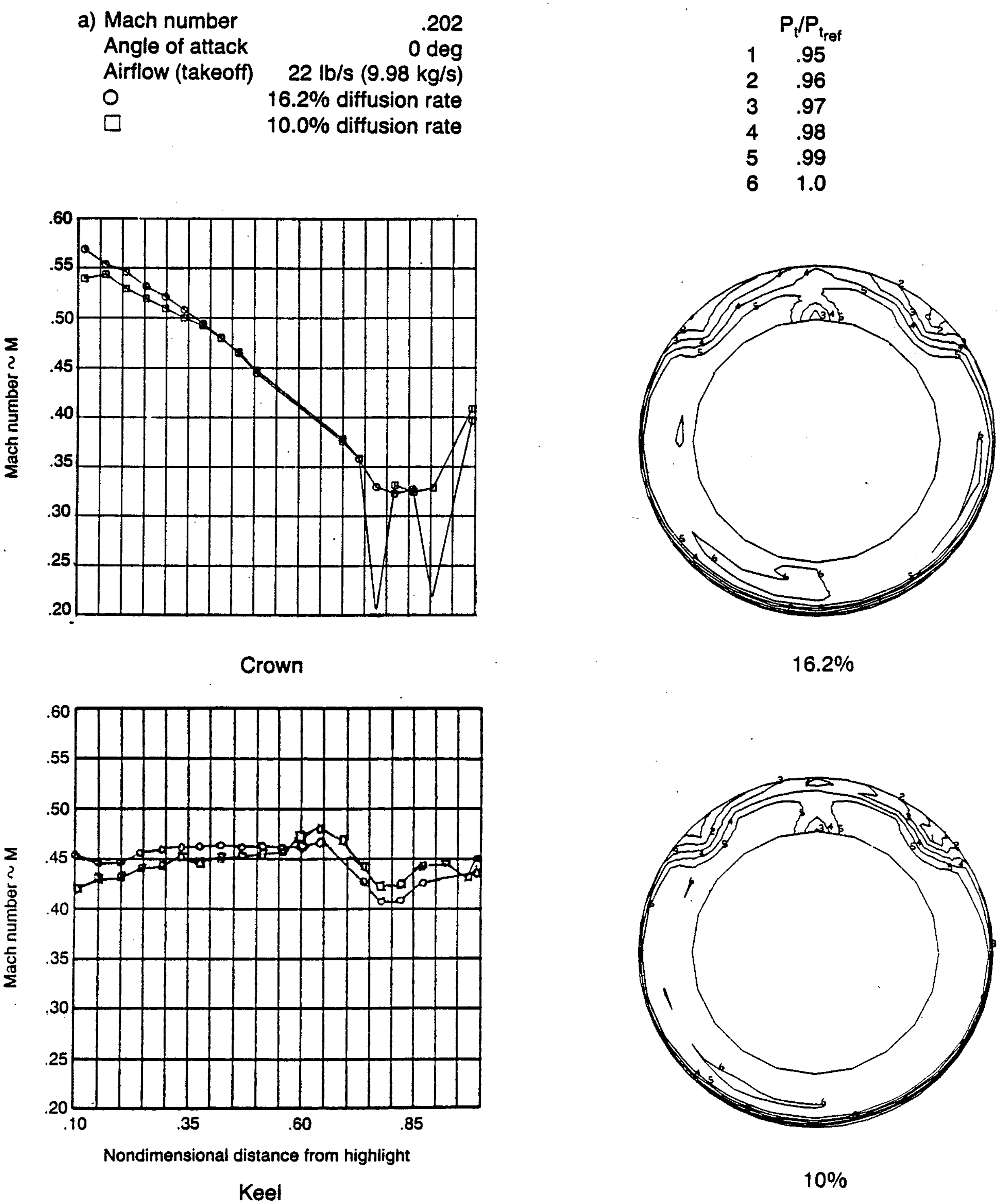

Figure 17. Duct Diffusion Comparison—Duct Surface Mach Number and Compressor Face Pressures for 16.2% and 10% Diffusers With 3.7-Aspect-Ratio Duct and Thin Lip

b) Mach number .202
Angle of attack 10 deg
Airflow (takeoff) 22 lb/s (9.98 kg/s)
○ 16.2% diffusion rate
□ 10.0% diffusion rate

	$P_t/P_{t_{ref}}$
1	.95
2	.96
3	.97
4	.98
5	.99
6	1.0

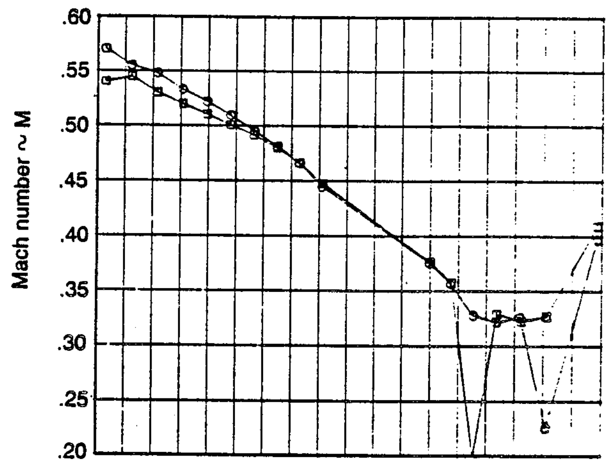

Crown

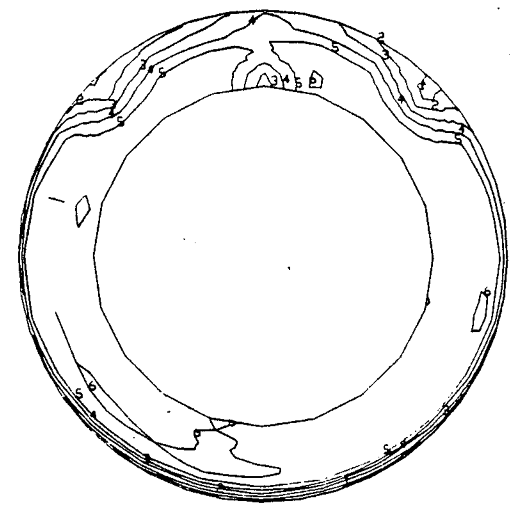

16.2%

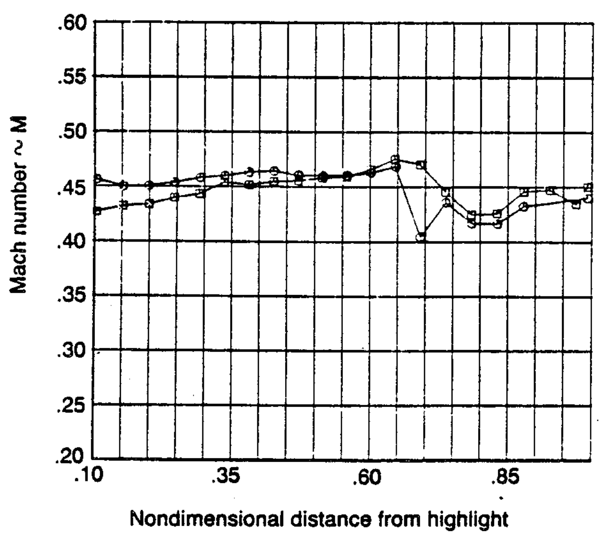

Keel

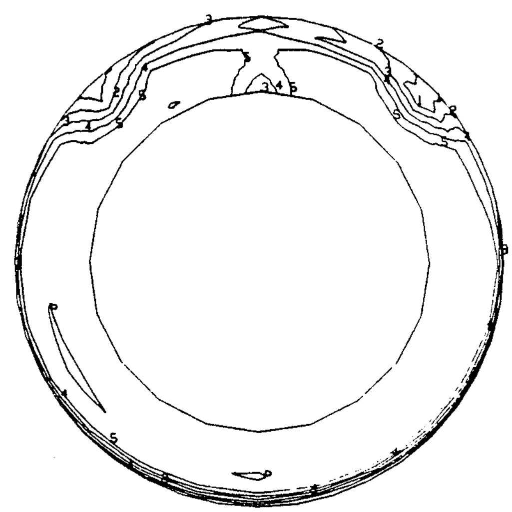

10%

Figure 17. Duct Diffusion Comparison—Duct Surface Mach Number and Compressor Face Pressures for 16.2% and 10% Diffusers With 3.7-Aspect-Ratio Duct and Thin Lip (Continued)

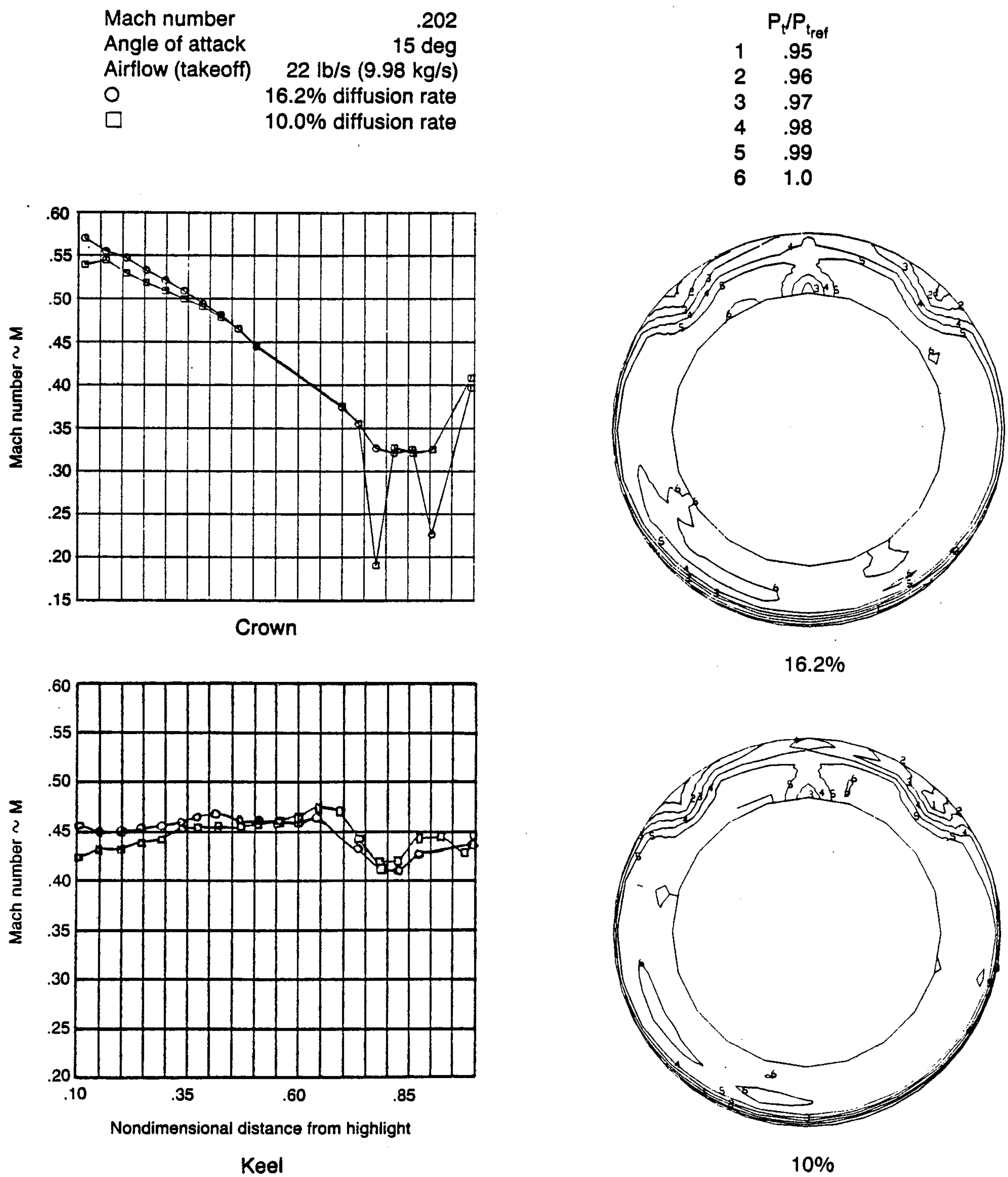

Figure 17. Duct Diffusion Comparison—Duct Surface Mach Number and Compressor Face Pressures for 16.2% and 10% Diffusers With 3.7-Aspect-Ratio Duct and Thin Lip (Continued)

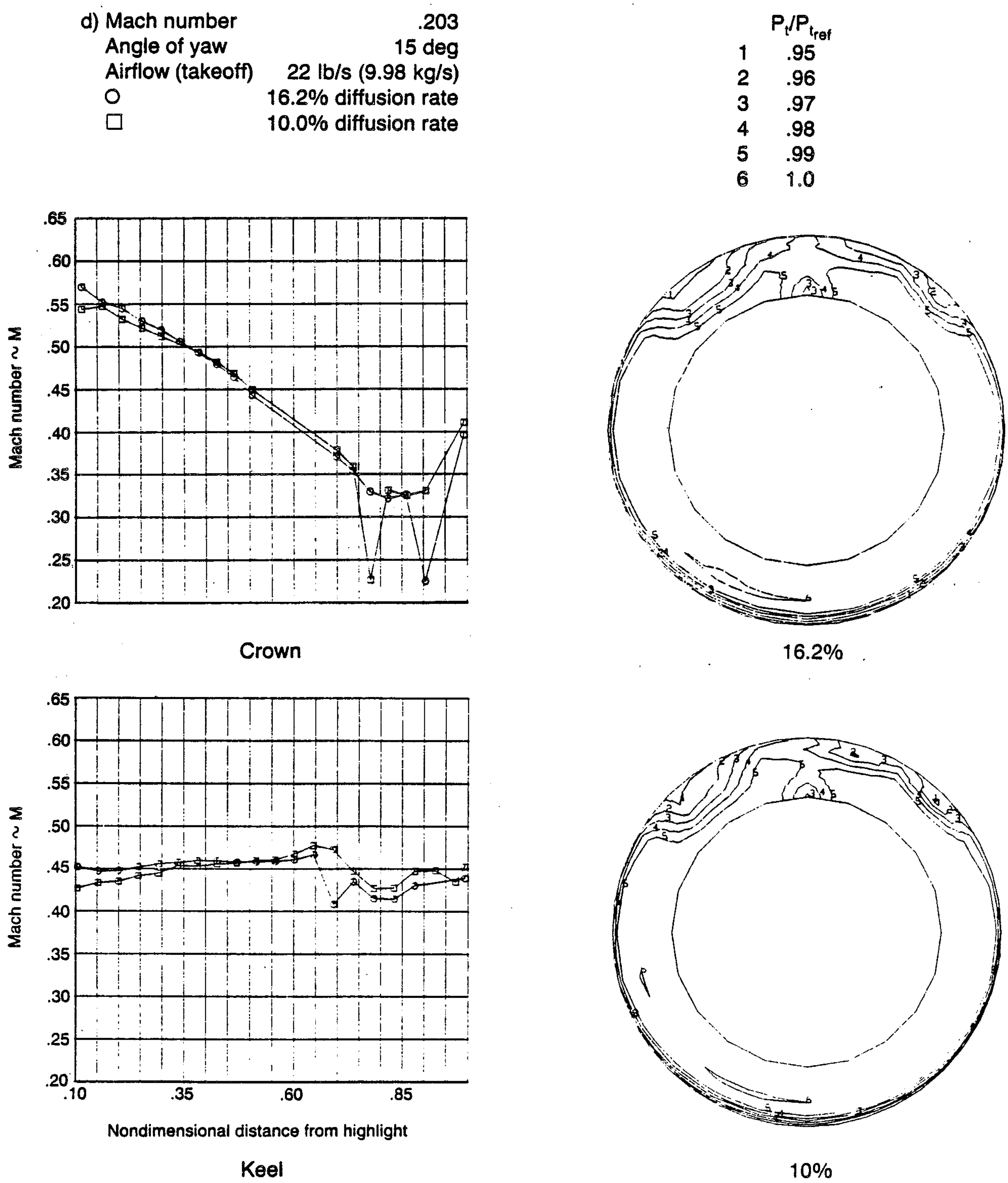

Figure 17. Duct Diffusion Comparison—Duct Surface Mach Number and Compressor Face Pressures for 16.2% and 10% Diffusers With 3.7-Aspect-Ratio Duct and Thin Lip (Continued)

e) Mach number .303
Angle of attack 0 deg
Airflow (cruise) 26 lb/s (11.79 kg/s)
○ 16.2% diffusion rate
□ 10.0% diffusion rate

	$P_t/P_{t_{ref}}$
1	.95
2	.96
3	.97
4	.98
5	.99
6	1.0

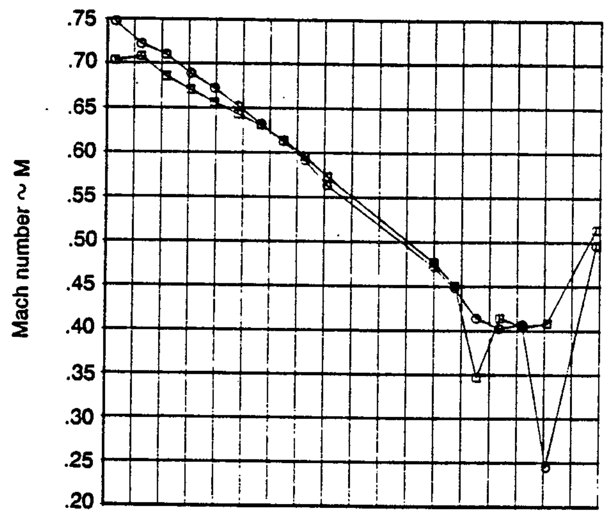

Crown

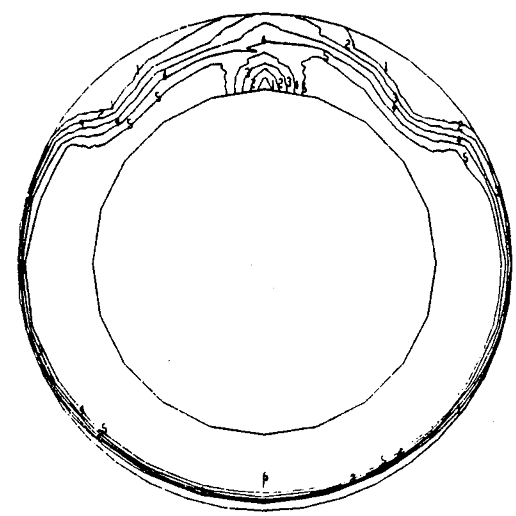

16.2%

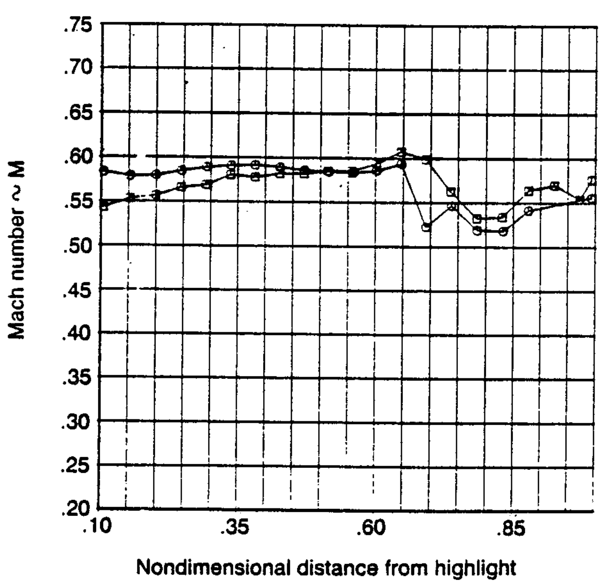

Keel

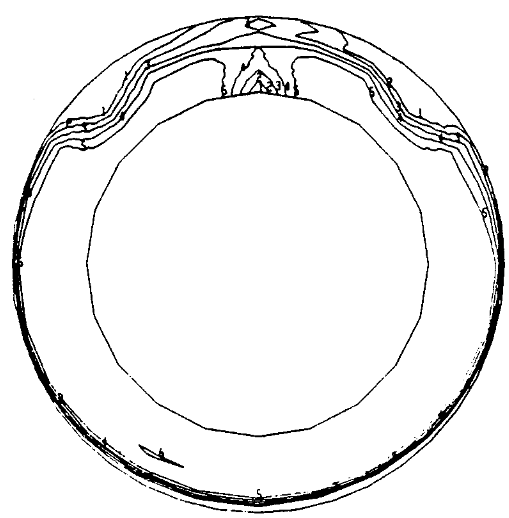

10%

Figure 17. Duct Diffusion Comparison—Duct Surface Mach Number and Compressor Face Pressures for 16.2% and 10% Diffusers With 3.7-Aspect-Ratio Duct and Thin Lip (Continued)

f) Mach number .303
Angle of attack 5 deg
Airflow (cruise) 26 lb/s (11.79 kg/s)
○ 16.2% diffusion rate
□ 10.0% diffusion rate

	$P_t/P_{t_{ref}}$
1	.95
2	.96
3	.97
4	.98
5	.99
6	1.0

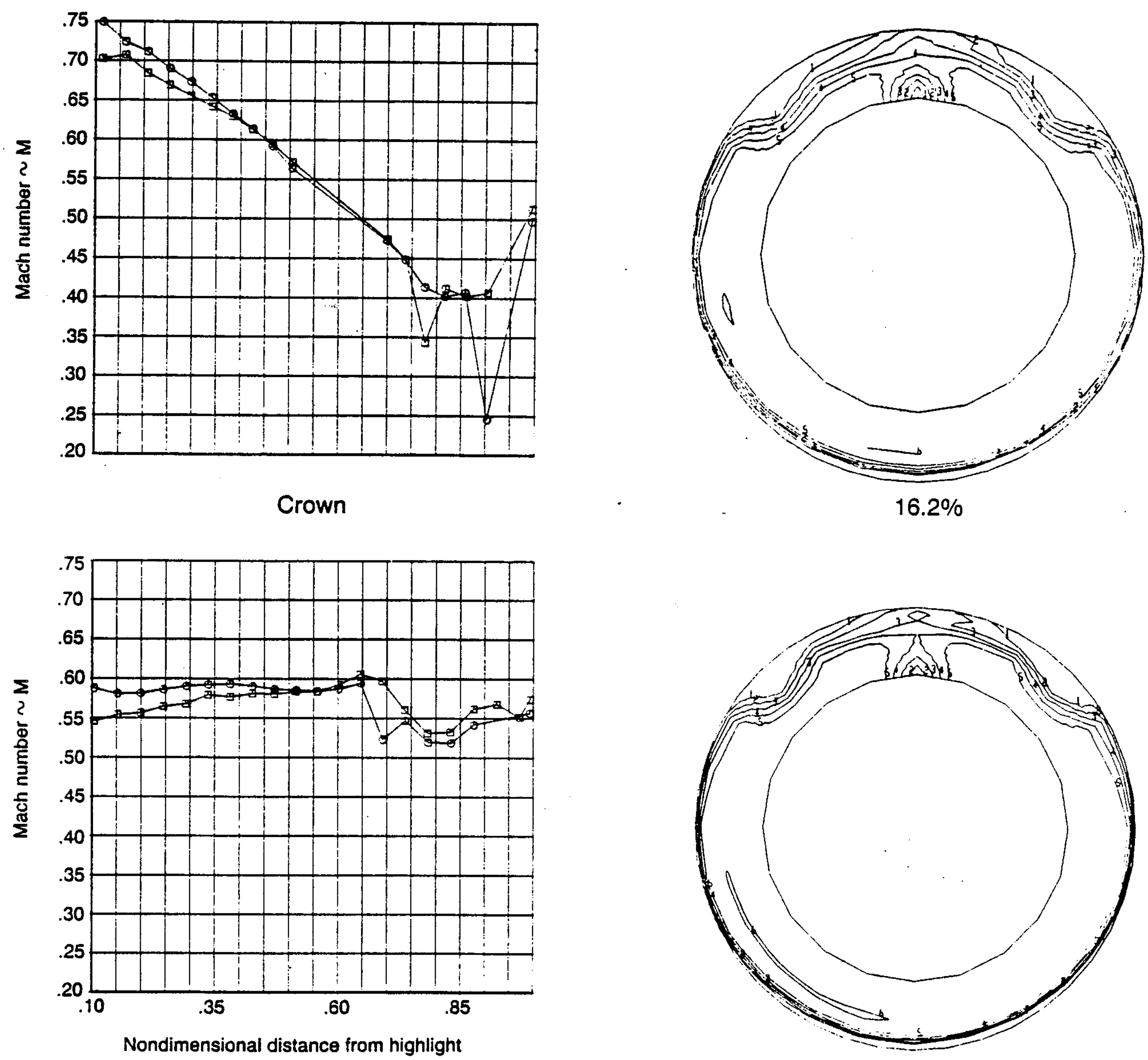

Figure 17. Duct Diffusion Comparison—Duct Surface Mach Number and Compressor Face Pressures for 16.2% and 10% Diffusers With 3.7-Aspect-Ratio Duct and Thin Lip (Concluded)

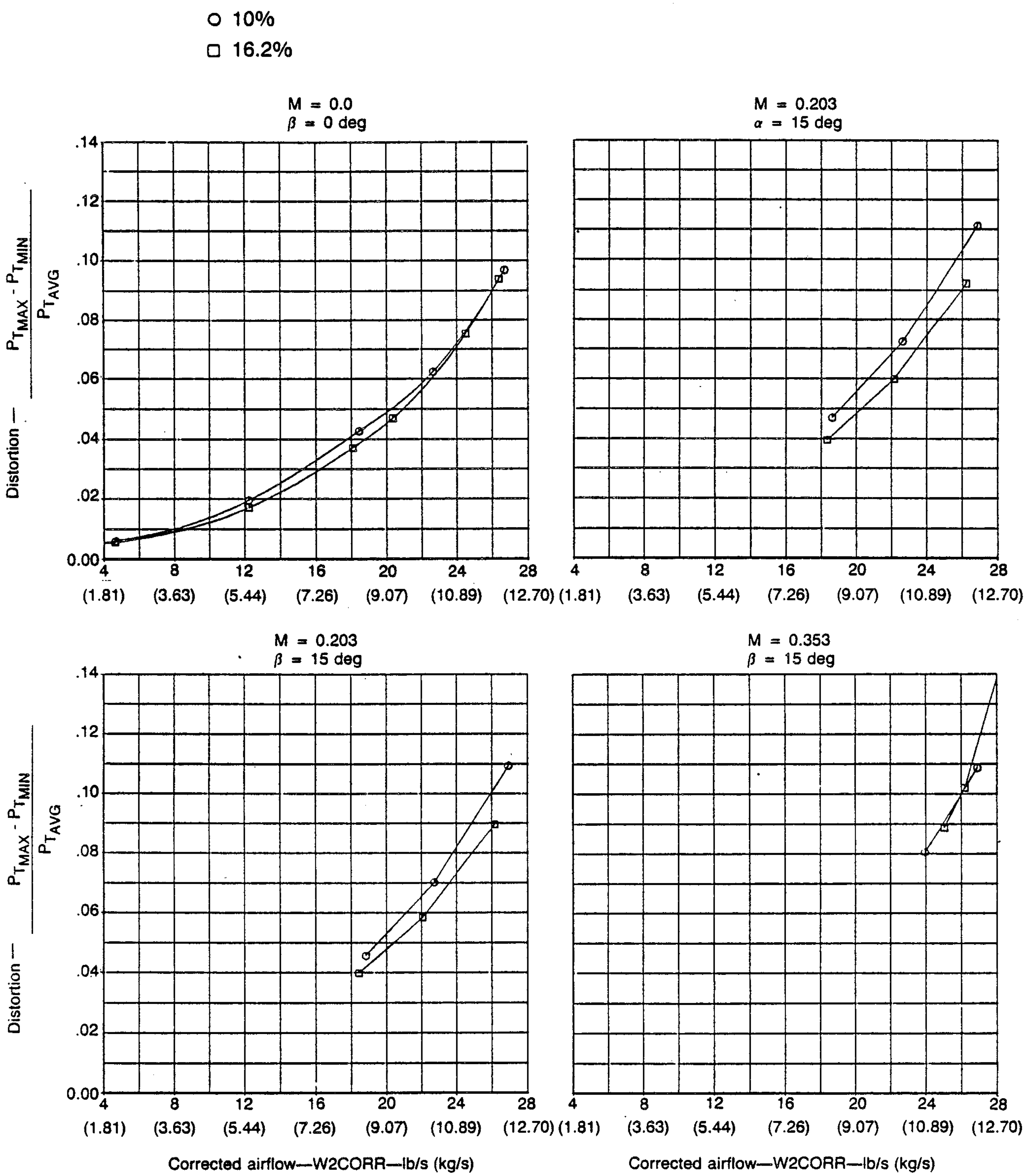

Figure 18. Compressor Face Distortion Comparison for 16.2% and 10% Diffusers

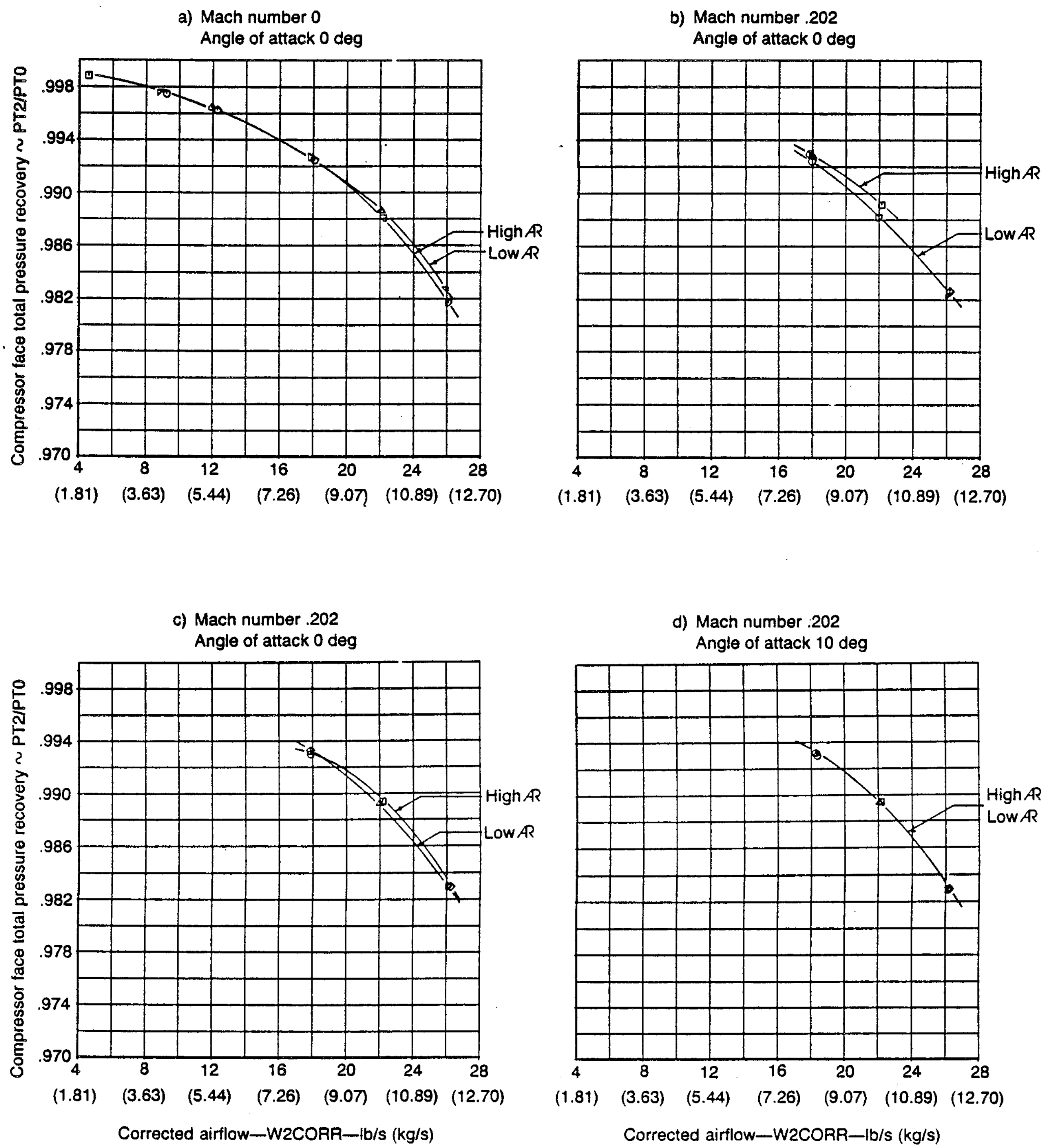

Figure 19. Duct Aspect Ratio Comparison—Compressor Face Pressure Recovery for 2.1- and 3.7-Aspect-Ratio Ducts With 16.2% Diffuser and Thin Lip

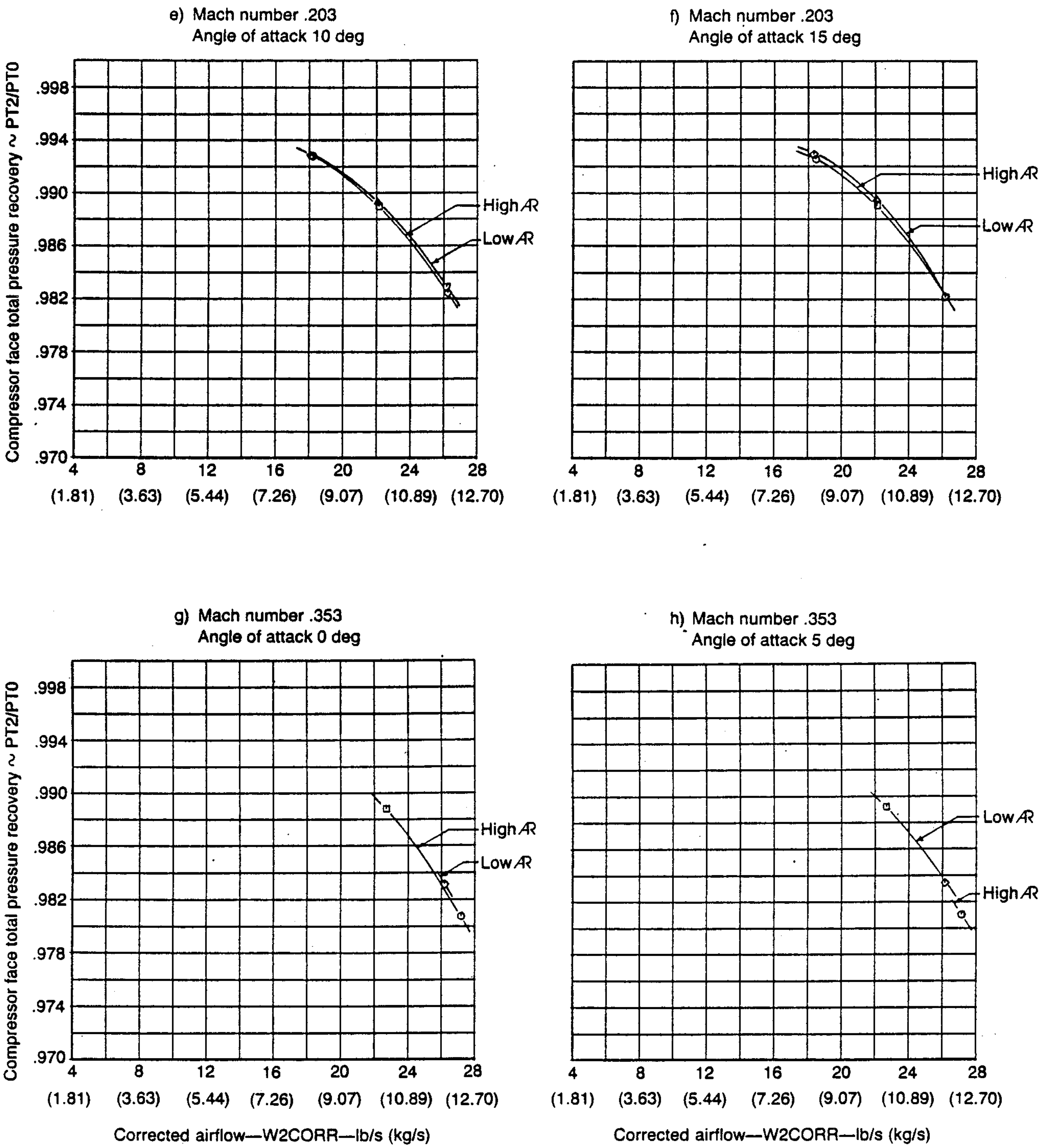

Figure 19. Duct Aspect Ratio Comparison—Compressor Face Pressure Recovery for 2.1- and 3.7-Aspect-Ratio Ducts With 16.2% Diffuser and Thin Lip (Continued)

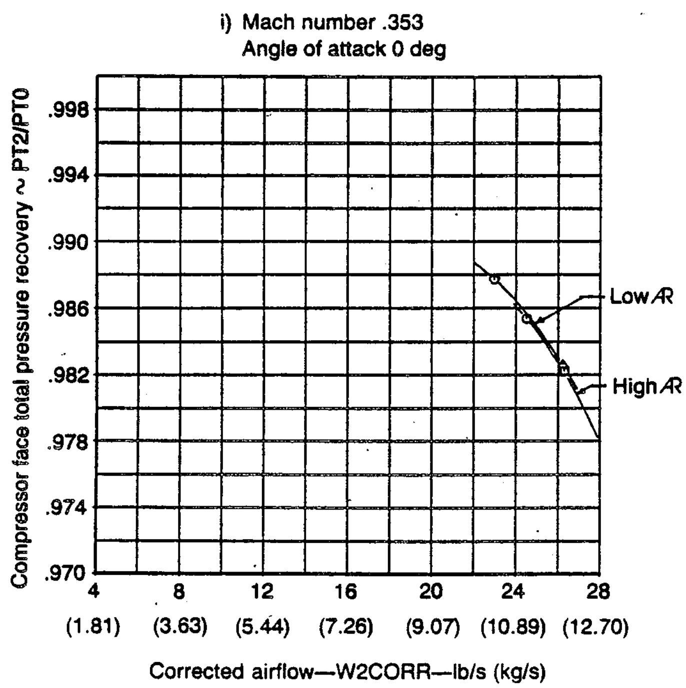

Figure 19. Duct Aspect Ratio Comparison—Compressor Face Pressure Recovery for 2.1- and 3.7-Aspect-Ratio Ducts With 16.2% Diffuser and Thin Lip (Concluded)

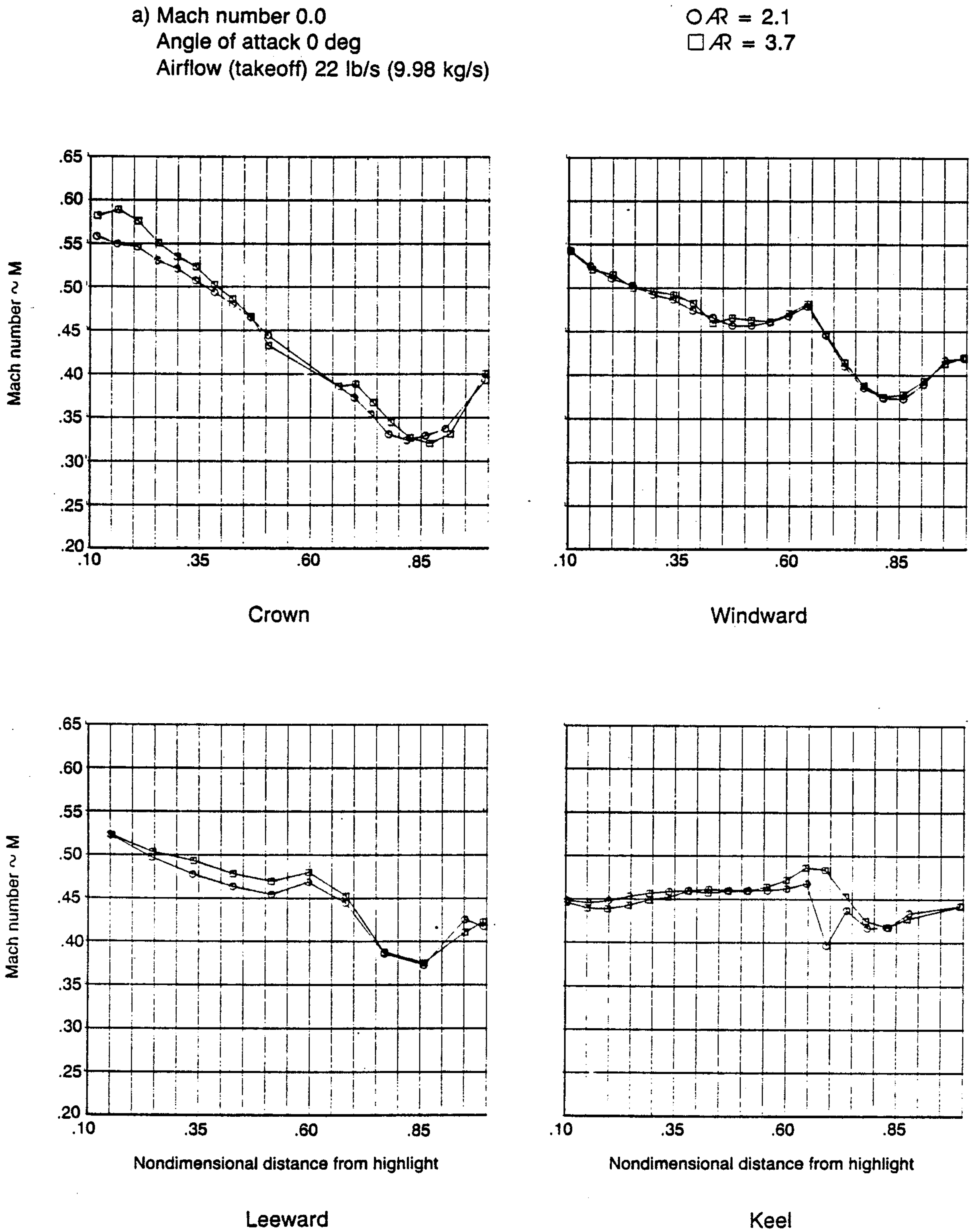

Figure 20. Duct Aspect Ratio Comparison—Duct Surface Mach Number for 2.1- and 3.7-Aspect-Ratio Ducts With 16.2% Diffuser and Thin Lip

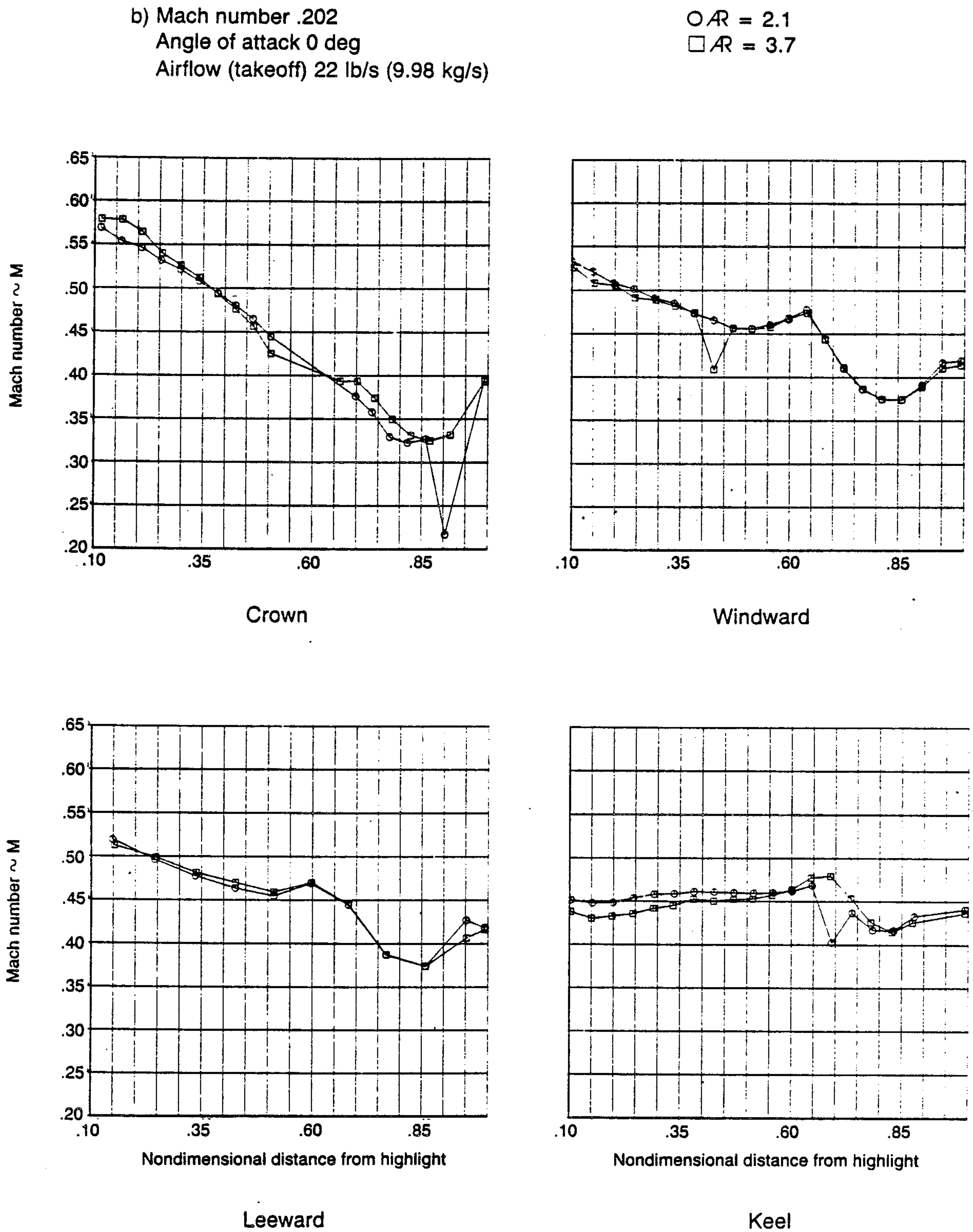

Figure 20. Duct Aspect Ratio Comparison—Duct Surface Mach Number for 2.1- and 3.7-Aspect-Ratio Ducts With 16.2% Diffuser and Thin Lip (Continued)

c) Mach number .202
Angle of attack 10 deg
Airflow (takeoff) 22 lb/s (9.98 kg/s)

○ Æ = 2.1
□ Æ = 3.7

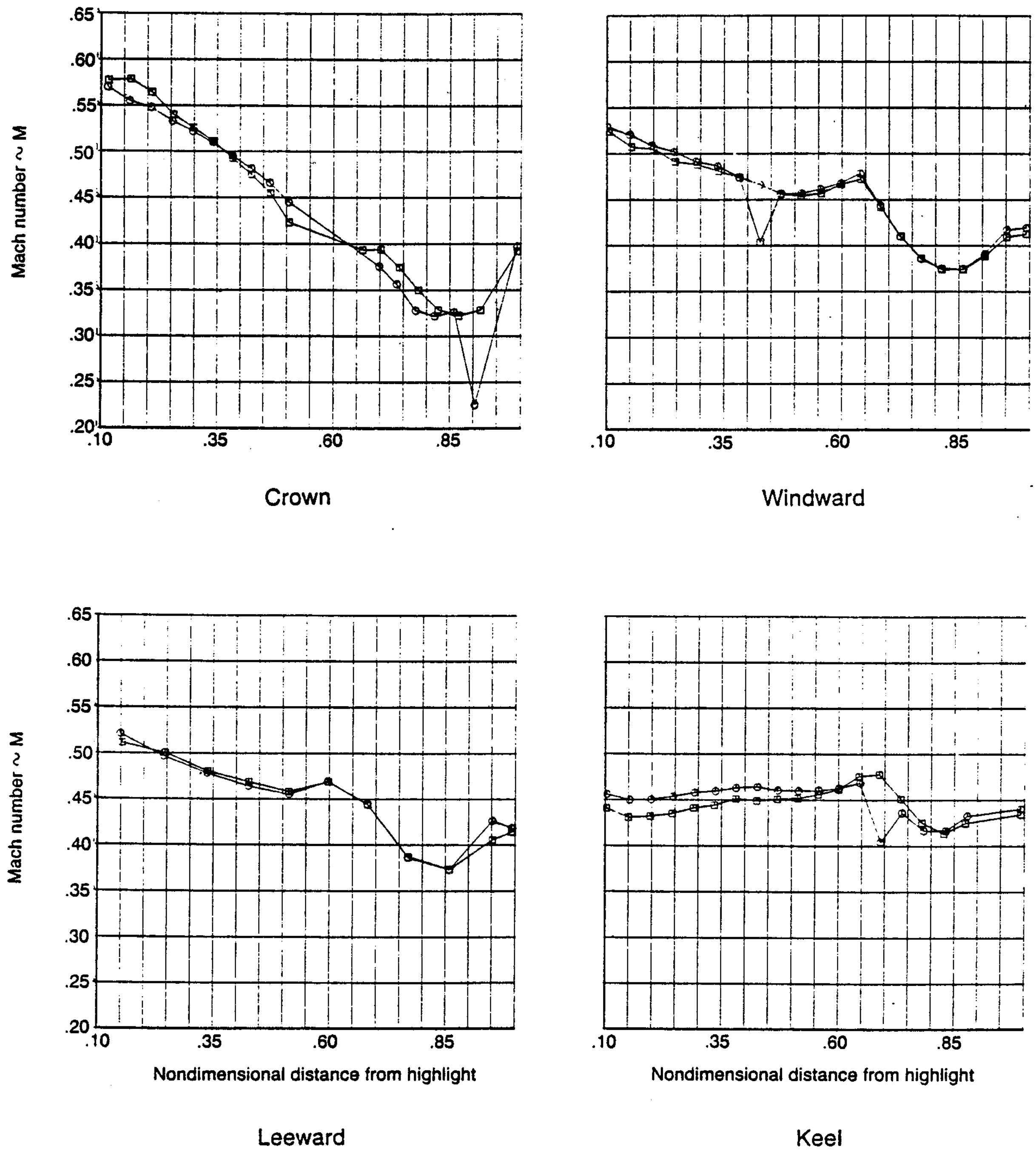

Figure 20. Duct Aspect Ratio Comparison—Duct Surface Mach Number for 2.1- and 3.7-Aspect-Ratio Ducts With 16.2% Diffuser and Thin Lip (Continued)

d) Mach number .202
Angle of attack 15 deg
Airflow (takeoff) 22 lb/s (9.98 kg/s)

○ Æ = 2.1
□ Æ = 3.7

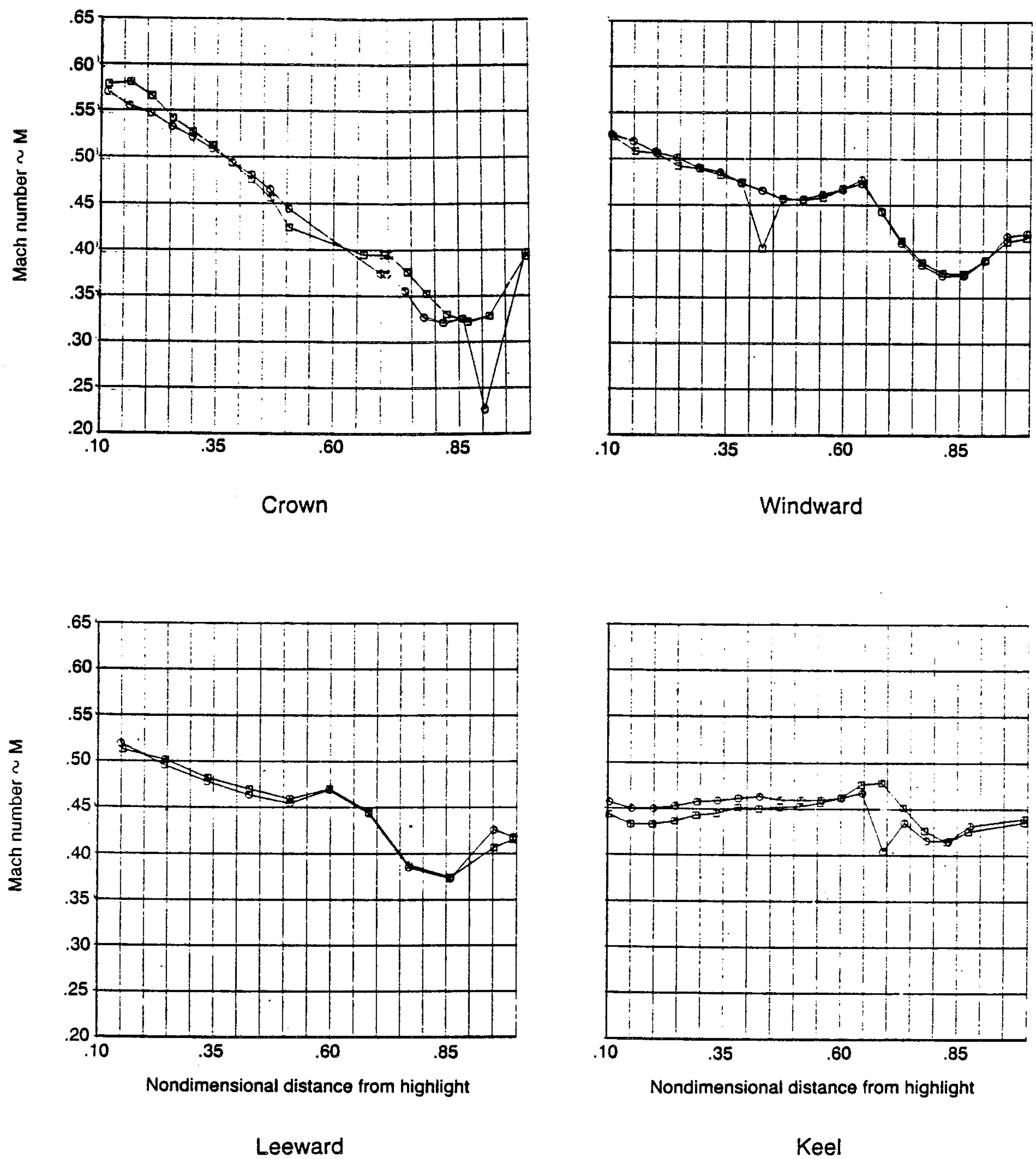

Figure 20. Duct Aspect Ratio Comparison—Duct Surface Mach Number for 2.1- and 3.7-Aspect-Ratio Ducts With 16.2% Diffuser and Thin Lip (Continued)

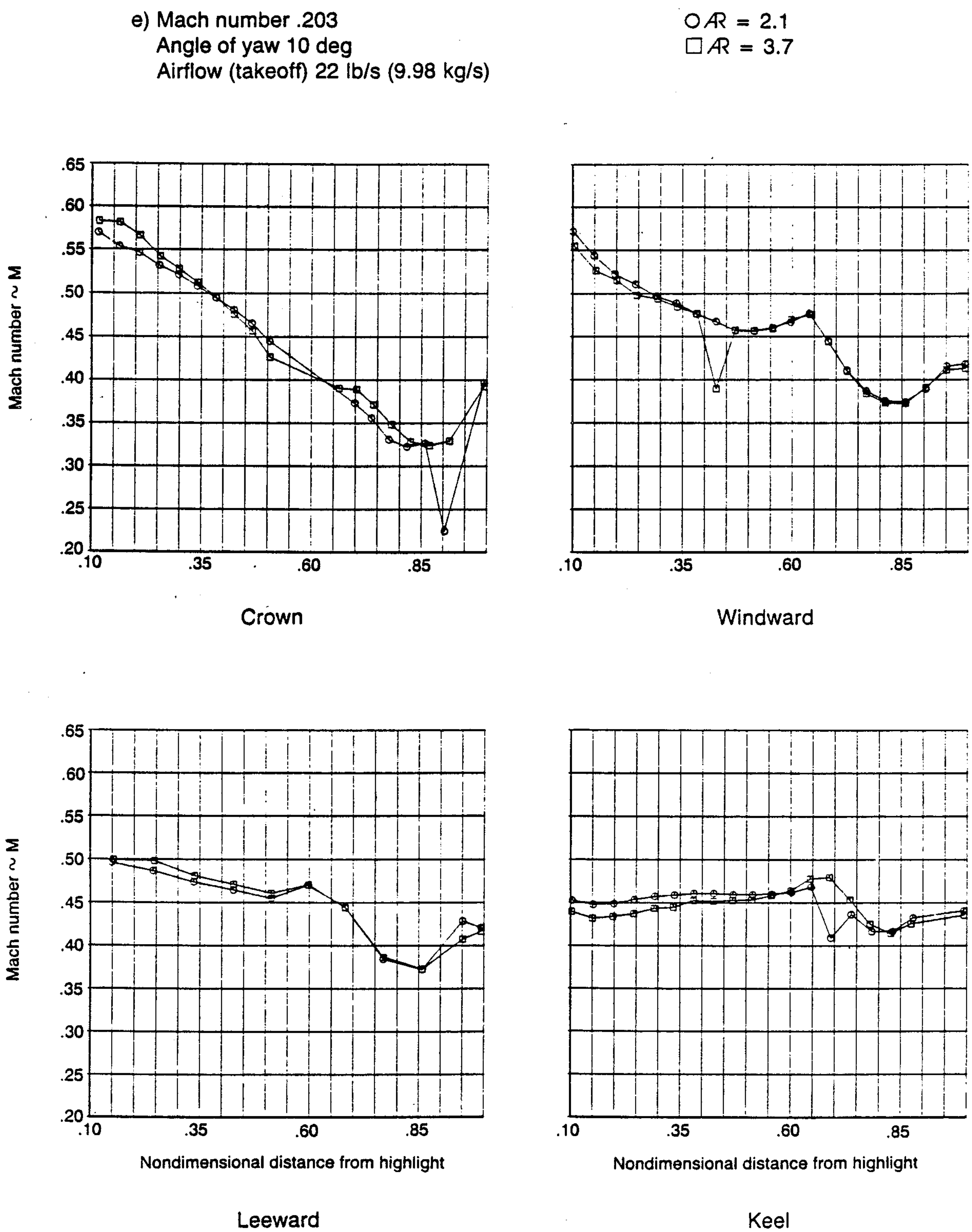

Figure 20. Duct Aspect Ratio Comparison—Duct Surface Mach Number for 2.1- and 3.7-Aspect-Ratio Ducts With 16.2% Diffuser and Thin Lip (Continued)

f) Mach number .203
Angle of yaw 15 deg
Airflow (takeoff) 22 lb/s (9.98 kg/s)

○ AR = 2.1
□ AR = 3.7

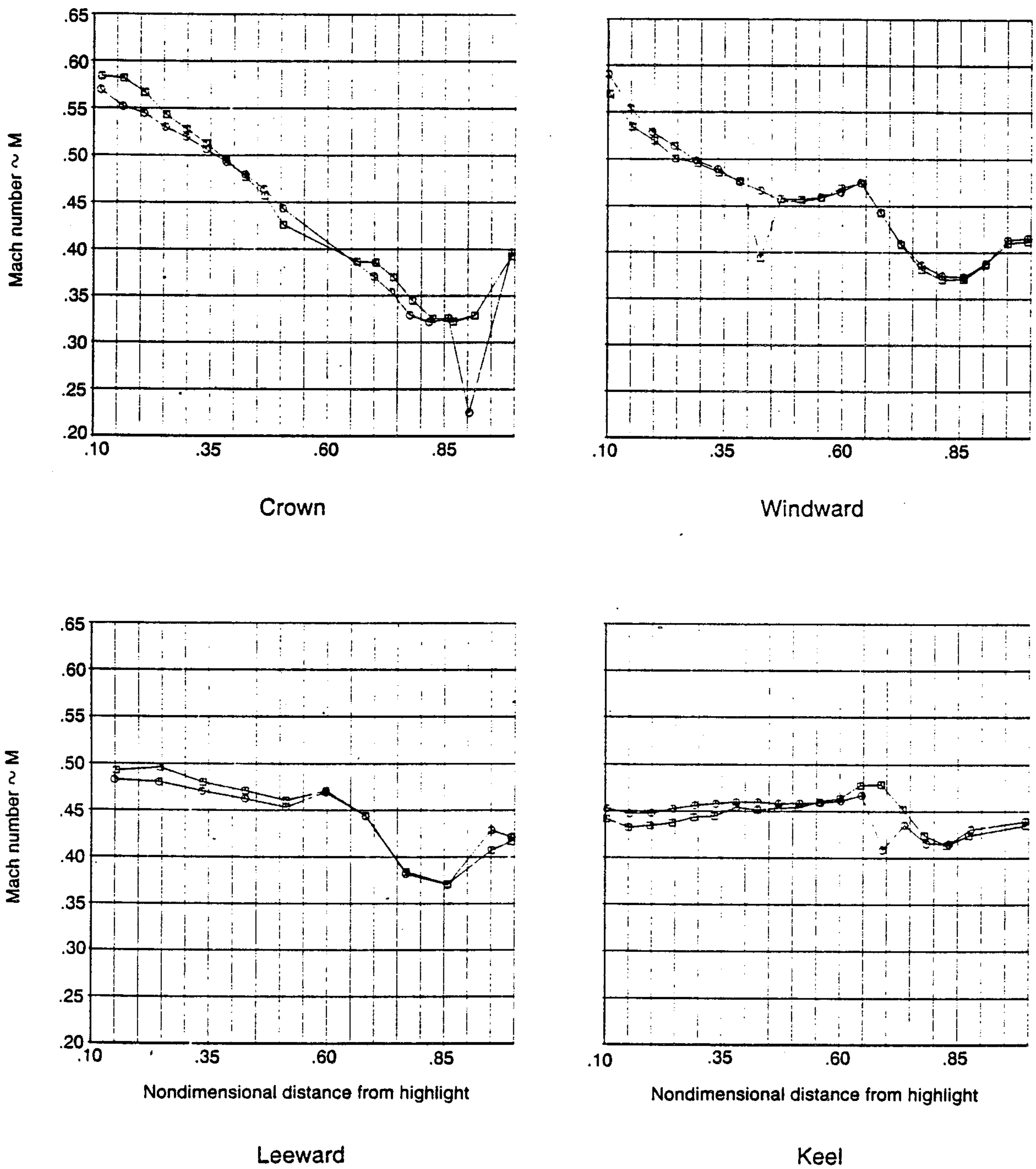

Figure 20. Duct Aspect Ratio Comparison—Duct Surface Mach Number for 2.1- and 3.7-Aspect-Ratio Ducts With 16.2% Diffuser and Thin Lip (Continued)

g) Mach number .353
Angle of attack 0 deg
Airflow (cruise) ○ 27 lb/s (12.25 kg/s)
□ 26 lb/s (11.79 kg/s)

○ AR = 2.1
□ AR = 3.7

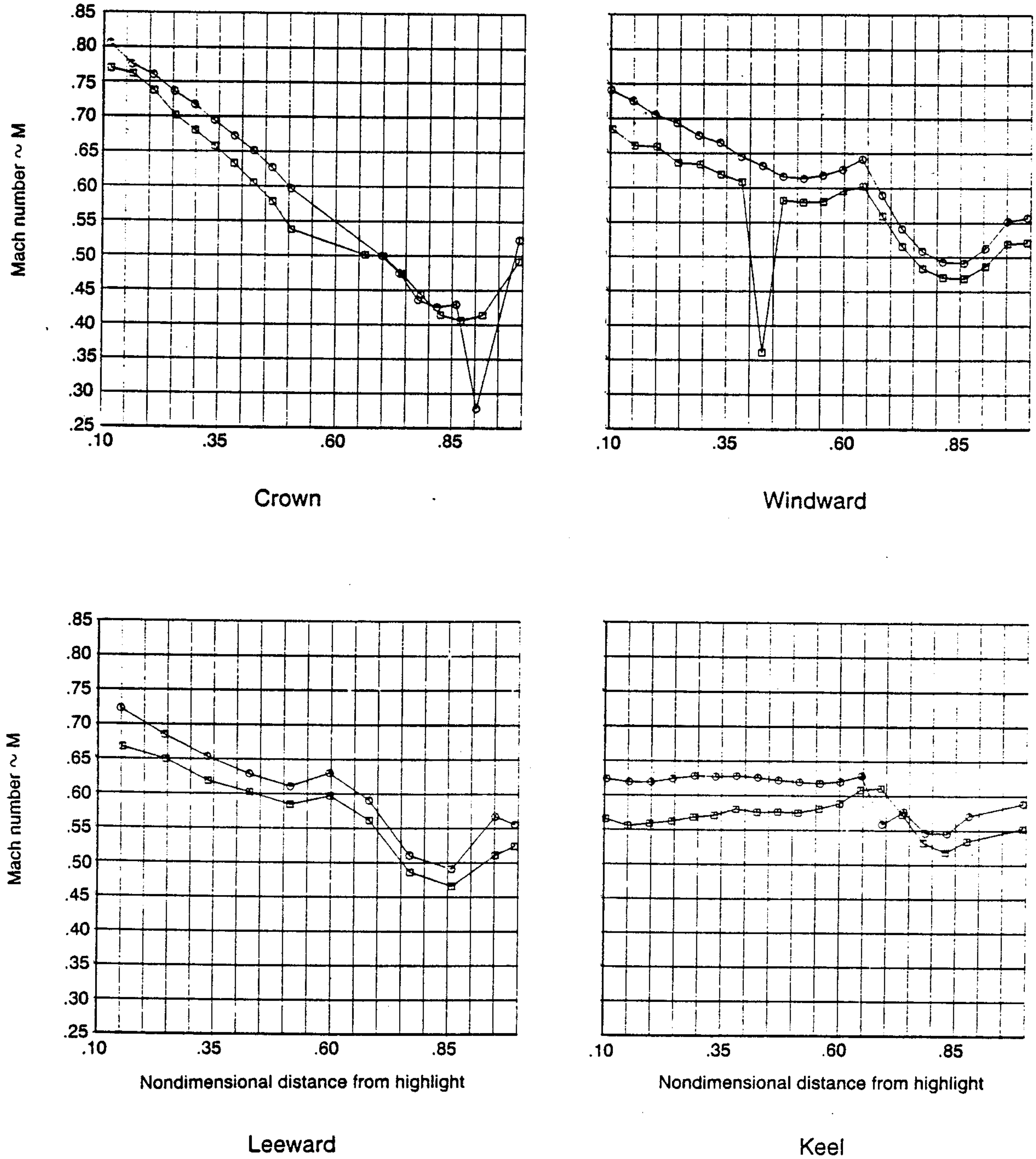

Figure 20. Duct Aspect Ratio Comparison—Duct Surface Mach Number for 2.1- and 3.7-Aspect-Ratio Ducts With 16.2% Diffuser and Thin Lip (Continued)

h) Mach number .353
Angle of attack 5 deg
Airflow (cruise) ○ 27 lb/s (12.25 kg/s)
□ 26 lb/s (11.79 kg/s)

○AR = 2.1
□AR = 3.7

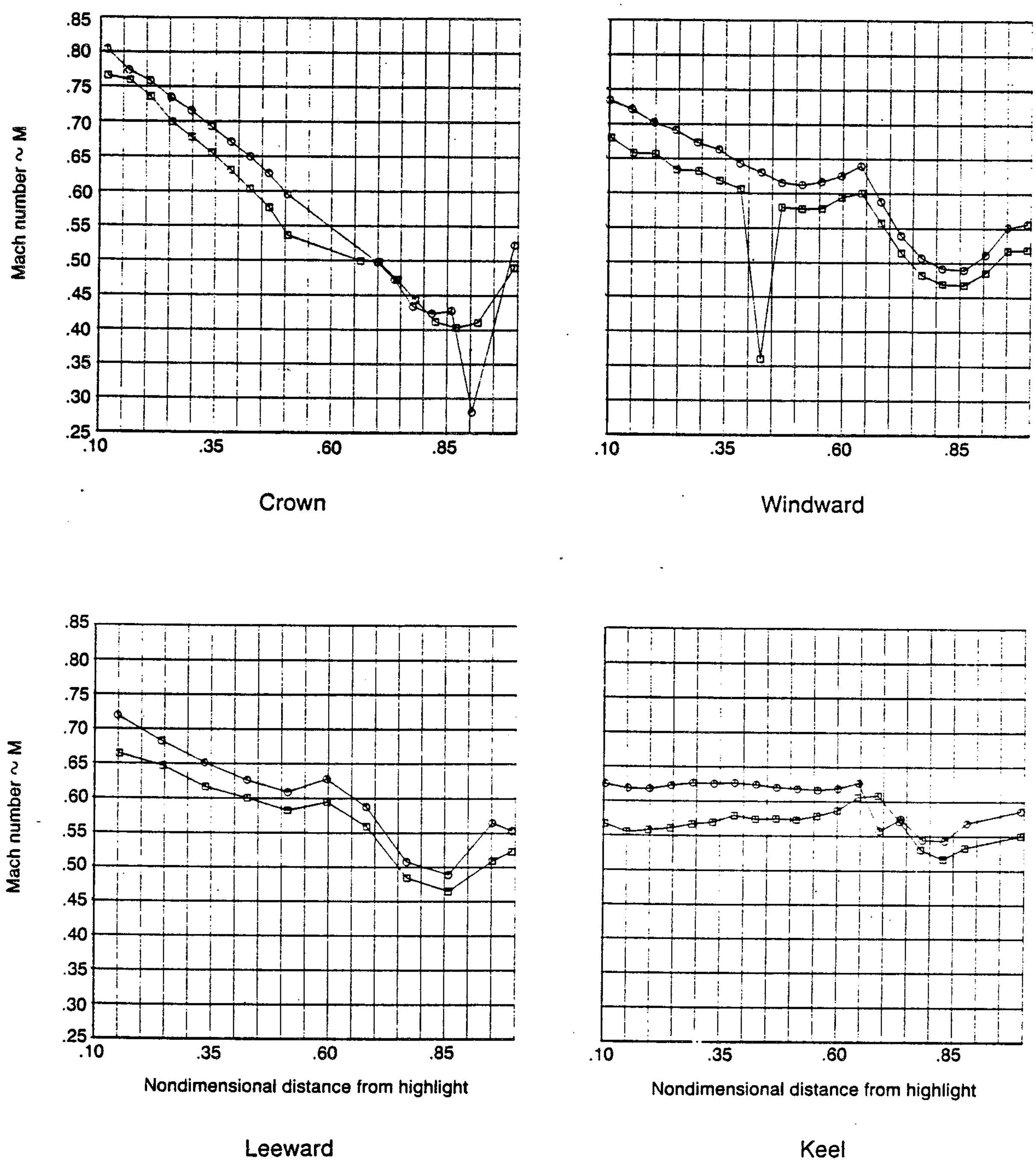

Figure 20. Duct Aspect Ratio Comparison—Duct Surface Mach Number for 2.1- and 3.7-Aspect-Ratio Ducts With 16.2% Diffuser and Thin Lip (Continued)

i) Mach number .355
Angle of yaw 5 deg
Airflow (takeoff) 26 lb/s (11.79 kg/s)

○ AR = 2.1
□ AR = 3.7

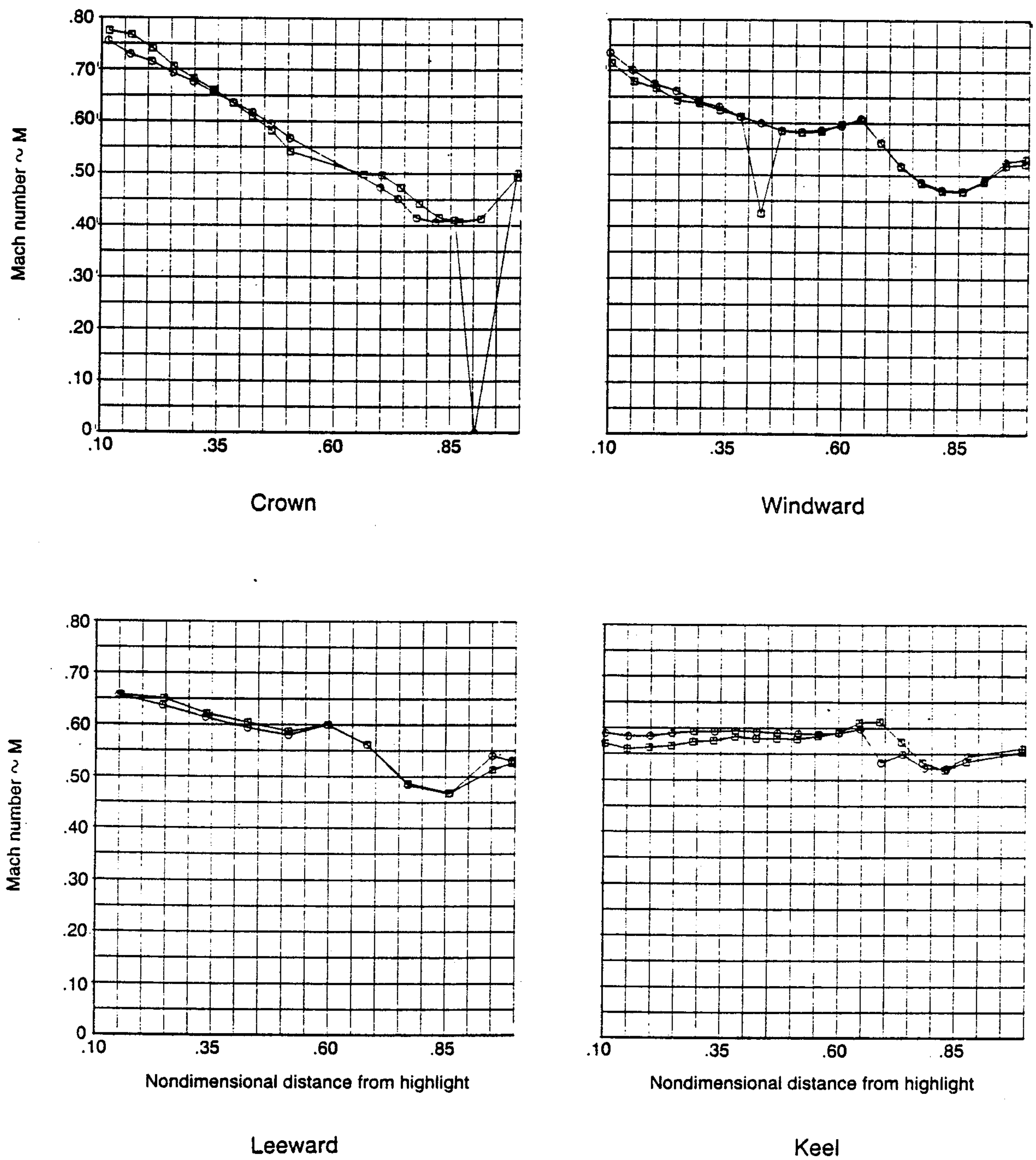

Figure 20. Duct Aspect Ratio Comparison—Duct Surface Mach Number for 2.1- and 3.7-Aspect-Ratio Ducts With 16.2% Diffuser and Thin Lip (Concluded)

a) Mach number 0.0
Angle of attack 0 deg
Airflow (takeoff) 22 lb/s (9.98 kg/s)

	$P_t/P_{t_{ref}}$
1	.95
2	.96
3	.97
4	.98
5	.99
6	1.0

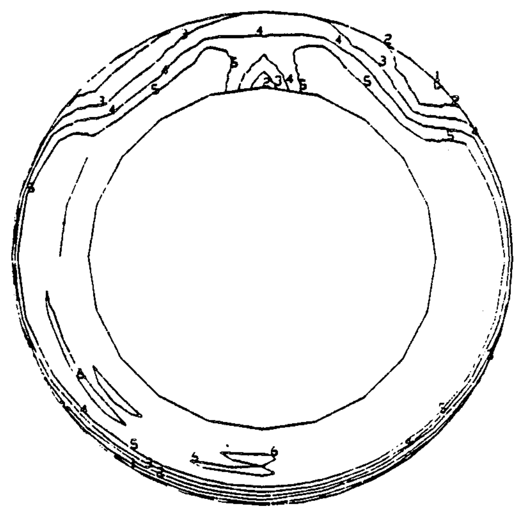

$AR = 2.1$

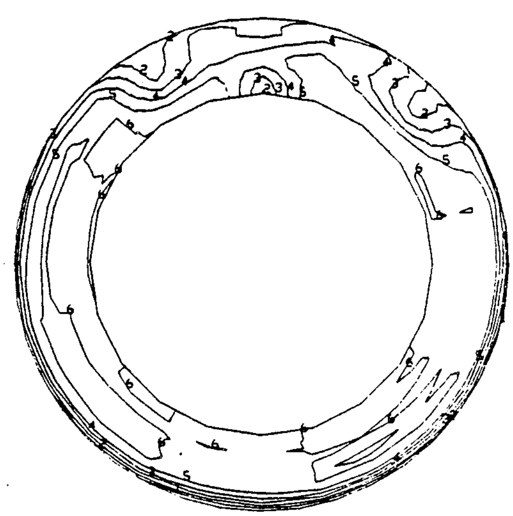

$AR = 3.7$

Figure 21. Duct Aspect Ratio Comparison—Compressor Face Pressures for 2.1- and 3.7-Aspect-Ratio Ducts With 16.2% Diffuser and Thin Lip

b) Mach number .202
Angle of attack 0 deg
Airflow (takeoff) 22 lb/s (9.98 kg/s)

	$P_t/P_{t_{ref}}$
1	.95
2	.96
3	.97
4	.98
5	.99
6	1.0

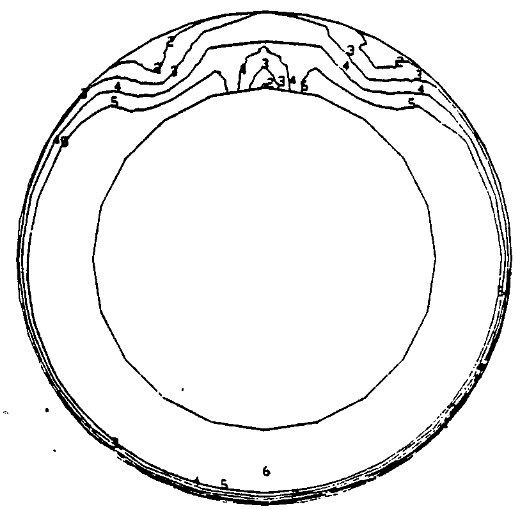

$AR = 2.1$

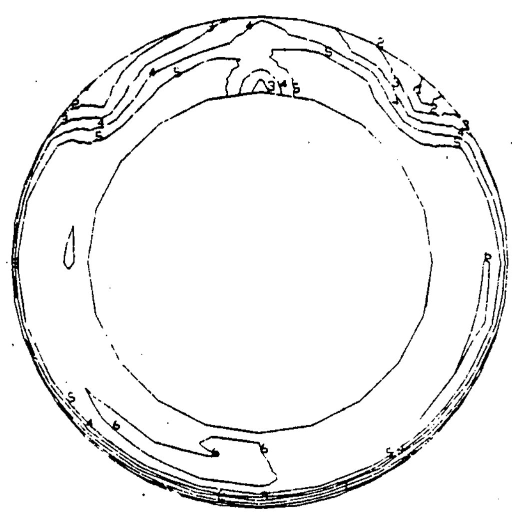

$AR = 3.7$

Figure 21. Duct Aspect Ratio Comparison—Compressor Face Pressures for 2.1- and 3.7-Aspect-Ratio Ducts With 16.2% Diffuser and Thin Lip (Continued)

c) Mach number .202
Angle of attack 10 deg
Airflow (takeoff) 22 lb/s (9.98 kg/s)

	$P_t/P_{t_{ref}}$
1	.95
2	.96
3	.97
4	.98
5	.99
6	1.0

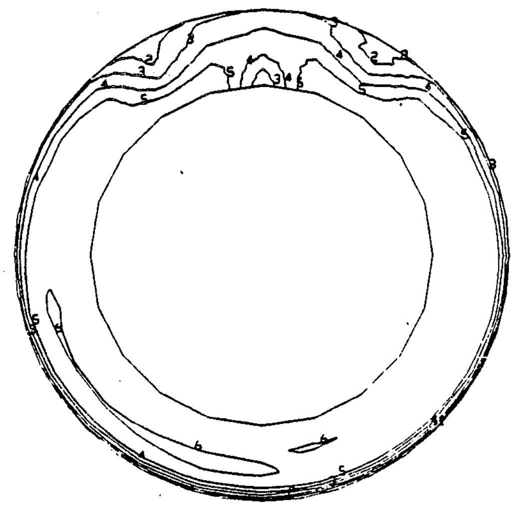

$AR = 2.1$

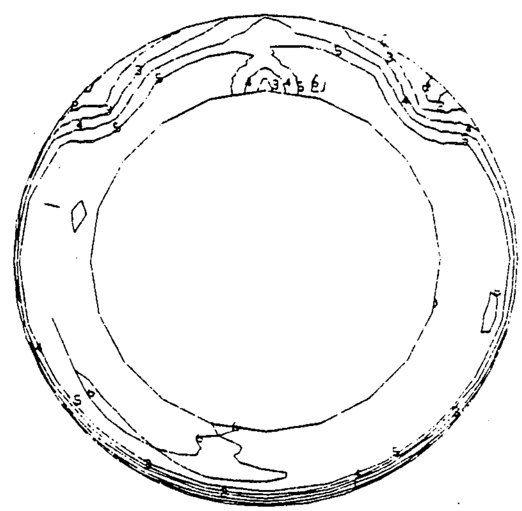

$AR = 3.7$

Figure 21. Duct Aspect Ratio Comparison—Compressor Face Pressures for 2.1- and 3.7-Aspect-Ratio Ducts With 16.2% Diffuser and Thin Lip (Continued)

d) Mach number .202
Angle of attack 15 deg
Airflow (takeoff) 22 lb/s (9.98 kg/s)

	$P_t/P_{t_{ref}}$
1	.95
2	.96
3	.97
4	.98
5	.99
6	1.0

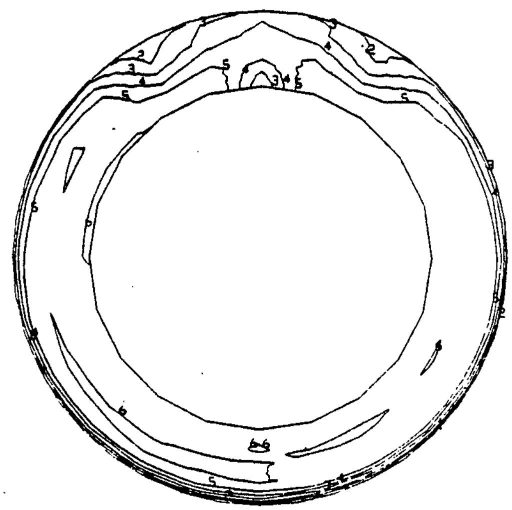

$AR = 2.1$

$AR = 3.7$

Figure 21. Duct Aspect Ratio Comparison—Compressor Face Pressures for 2.1- and 3.7-Aspect-Ratio Ducts With 16.2% Diffuser and Thin Lip (Continued)

e) Mach number .203
Angle of attack 10 deg
Airflow (takeoff) 22 lb/s (9.98 kg/s)

	$P_t/P_{t_{ref}}$
1	.95
2	.96
3	.97
4	.98
5	.99
6	1.0

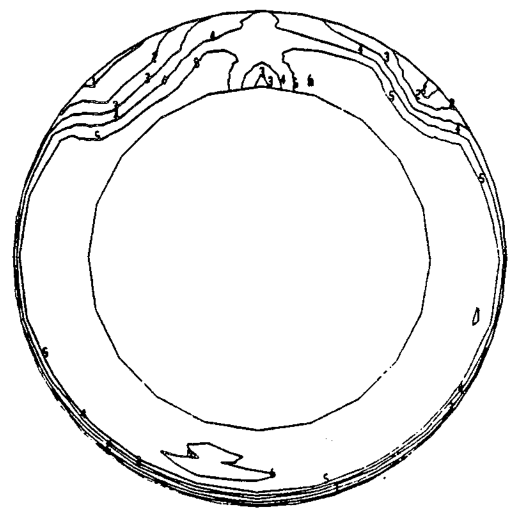

$AR = 2.1$

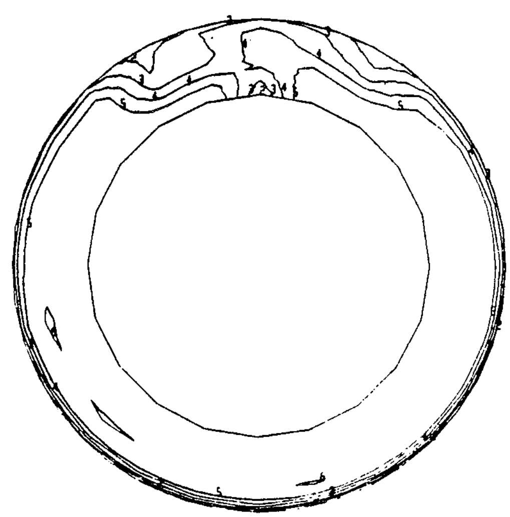

$AR = 3.7$

Figure 21. Duct Aspect Ratio Comparison—Compressor Face Pressures for 2.1- and 3.7-Aspect-Ratio Ducts With 16.2% Diffuser and Thin Lip (Continued)

f) Mach number .203
Angle of yaw 15 deg
Airflow (takeoff) 22 lb/s (9.98 kg/s)

	$P_t/P_{t_{ref}}$
1	.95
2	.96
3	.97
4	.98
5	.99
6	1.0

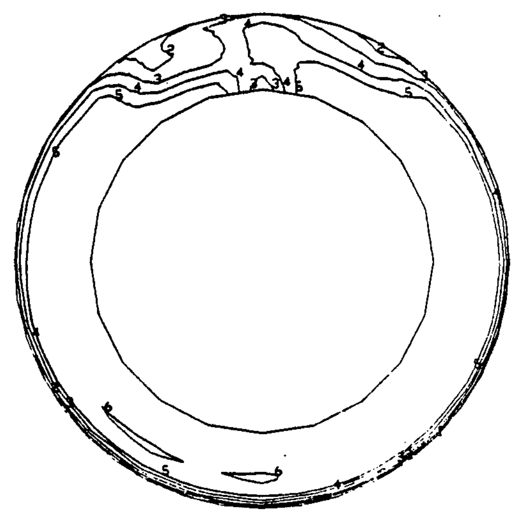

$AR = 2.1$

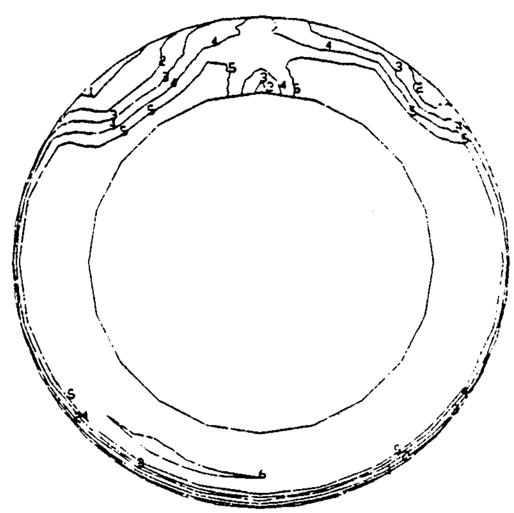

$AR = 3.7$

Figure 21. Duct Aspect Ratio Comparison—Compressor Face Pressures for 2.1- and 3.7-Aspect-Ratio Ducts With 16.2% Diffuser and Thin Lip (Continued)

g) Mach number .353
Angle of attack 0 deg
Airflow (cruise) 27 lb/s (12.25 kg/s), Æ = 2.1
26 lb/s (11.79 kg/s) Æ = 3.7

	$P_t/P_{t_{ref}}$
1	.95
2	.96
3	.97
4	.98
5	.99
6	1.0

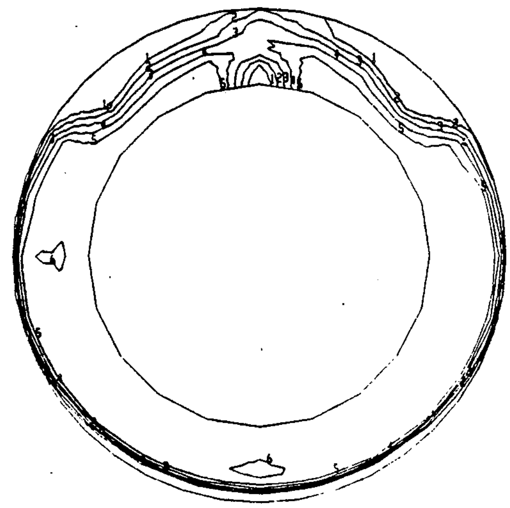

Æ = 2.1

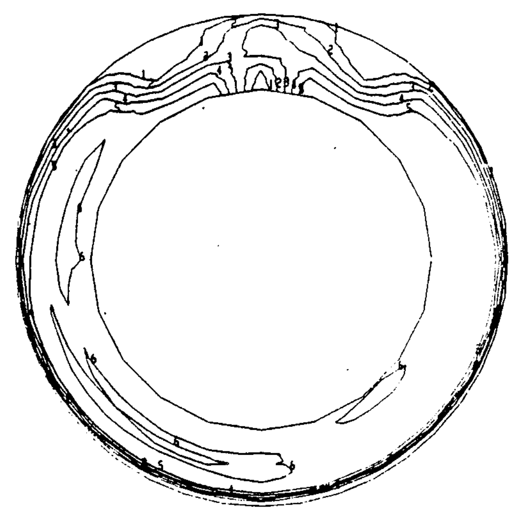

Æ = 3.7

Figure 21. Duct Aspect Ratio Comparison—Compressor Face Pressures for 2.1- and 3.7-Aspect-Ratio Ducts With 16.2% Diffuser and Thin Lip (Continued)

h) Mach number .353
Angle of attack 5 deg
Airflow (cruise) 27 lb/s (12.25 kg/s), AR = 2.1
26 lb/s (11.79 kg/s) AR = 3.7

	$P_t/P_{t_{ref}}$
1	.95
2	.96
3	.97
4	.98
5	.99
6	1.0

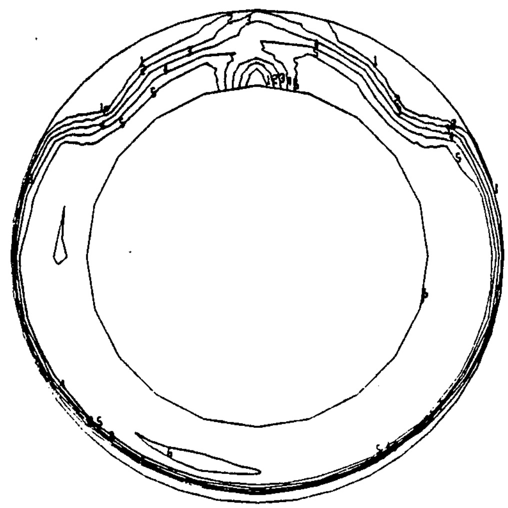

AR = 2.1

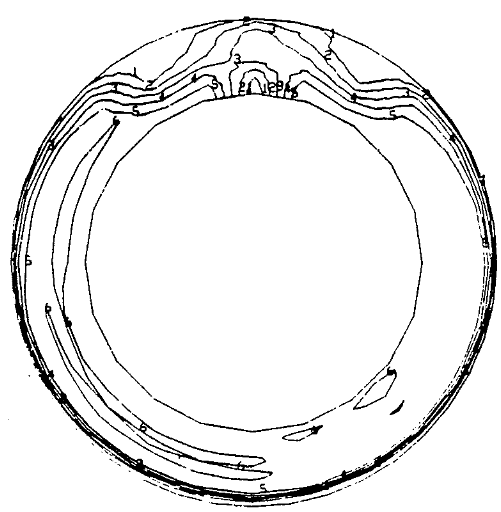

AR = 3.7

Figure 21. Duct Aspect Ratio Comparison—Compressor Face Pressures for 2.1- and 3.7-Aspect-Ratio Ducts With 16.2% Diffuser and Thin Lip (Continued)

i) Mach number .355
Angle of attack 5 deg
Airflow (takeoff) 26 lb/s (11.79 kg/s)

	$P_t/P_{t_{ref}}$
1	.95
2	.96
3	.97
4	.98
5	.99
6	1.0

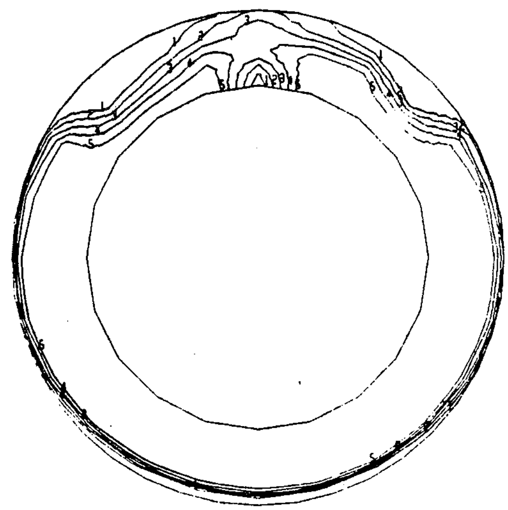

AR = 2.1

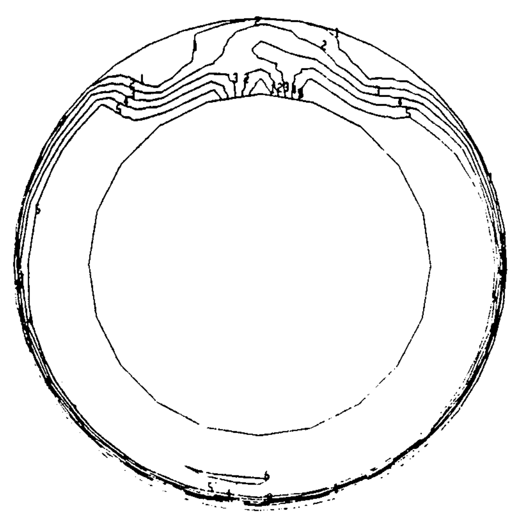

AR = 3.7

Figure 21. Duct Aspect Ratio Comparison—Compressor Face Pressures for 2.1- and 3.7-Aspect-Ratio Ducts With 16.2% Diffuser and Thin Lip (Concluded)

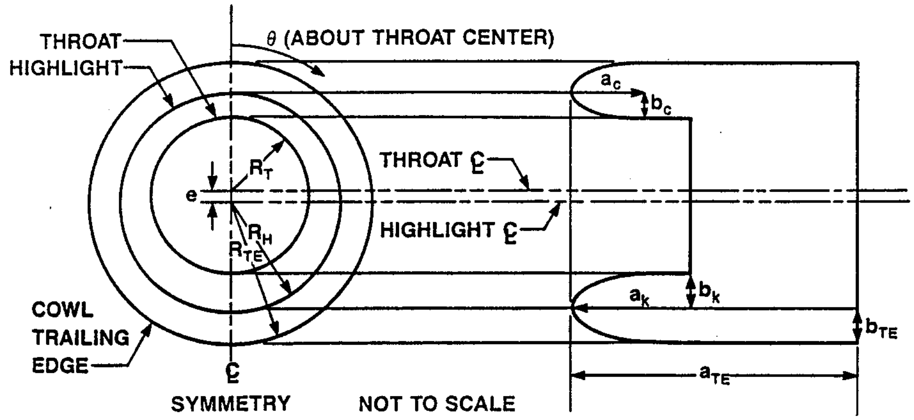

LIP AND COWL SURFACE CONTOUR EQUATION

$$\left(\frac{x}{a}\right)^n + \left(\frac{y}{b}\right)^m = 1.0$$

LIP	CONTRACTION RATIO CROWN	CONTRACTION RATIO KEEL
VERY THIN	1.213	1.213
THIN	1.246	1.280
FAT	1.246	1.380

SURFACE	θ	n	m
THROAT TO HIGHLIGHT	0 TO 45	2.8	2.0
	45 TO 90	VARIES LINEARLY	
	90	2.4	2.0
	90 TO 135	VARIES LINEARLY	
	135 TO 180	2.0	2.0
HIGHLIGHT TO COWL TRAILING EDGE	0 TO 180	1.7	1.7

Figure 22. Basis of S-Duct Lip and Cowl Shape Definition

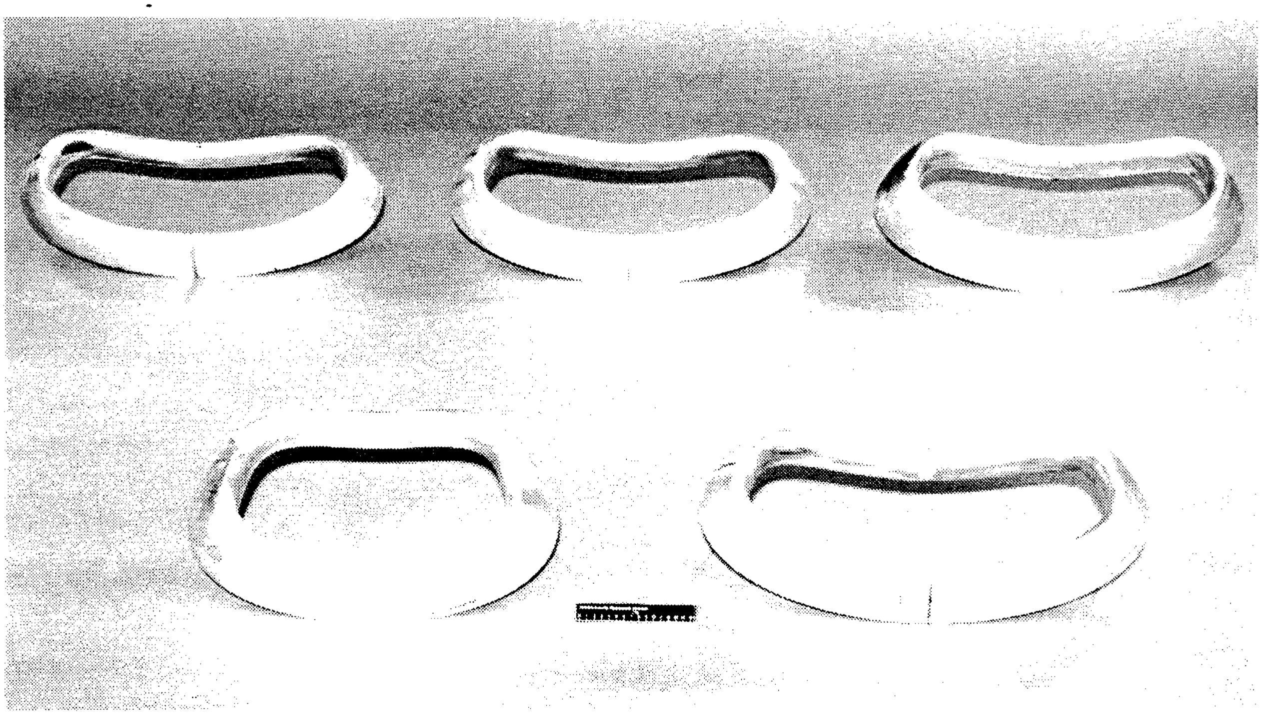

Figure 23. High- and Low-Aspect-Ratio Very Thin, Thin, and Thick Lips

Figure 24. Lip Internal Flow Visualization Showing Separation Behind Very Thin Lip

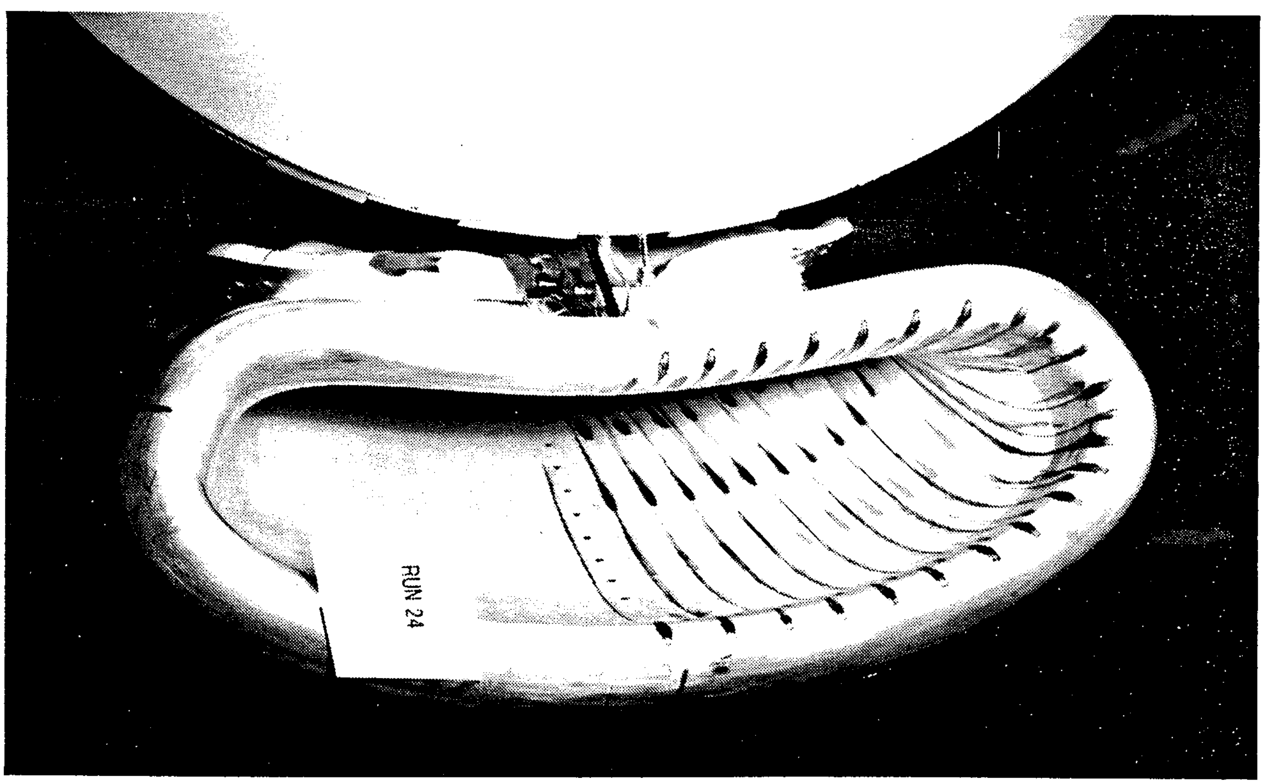

Figure 25. Lip Internal Flow Visualization Showing Unseparated Flow Behind Thin Lip

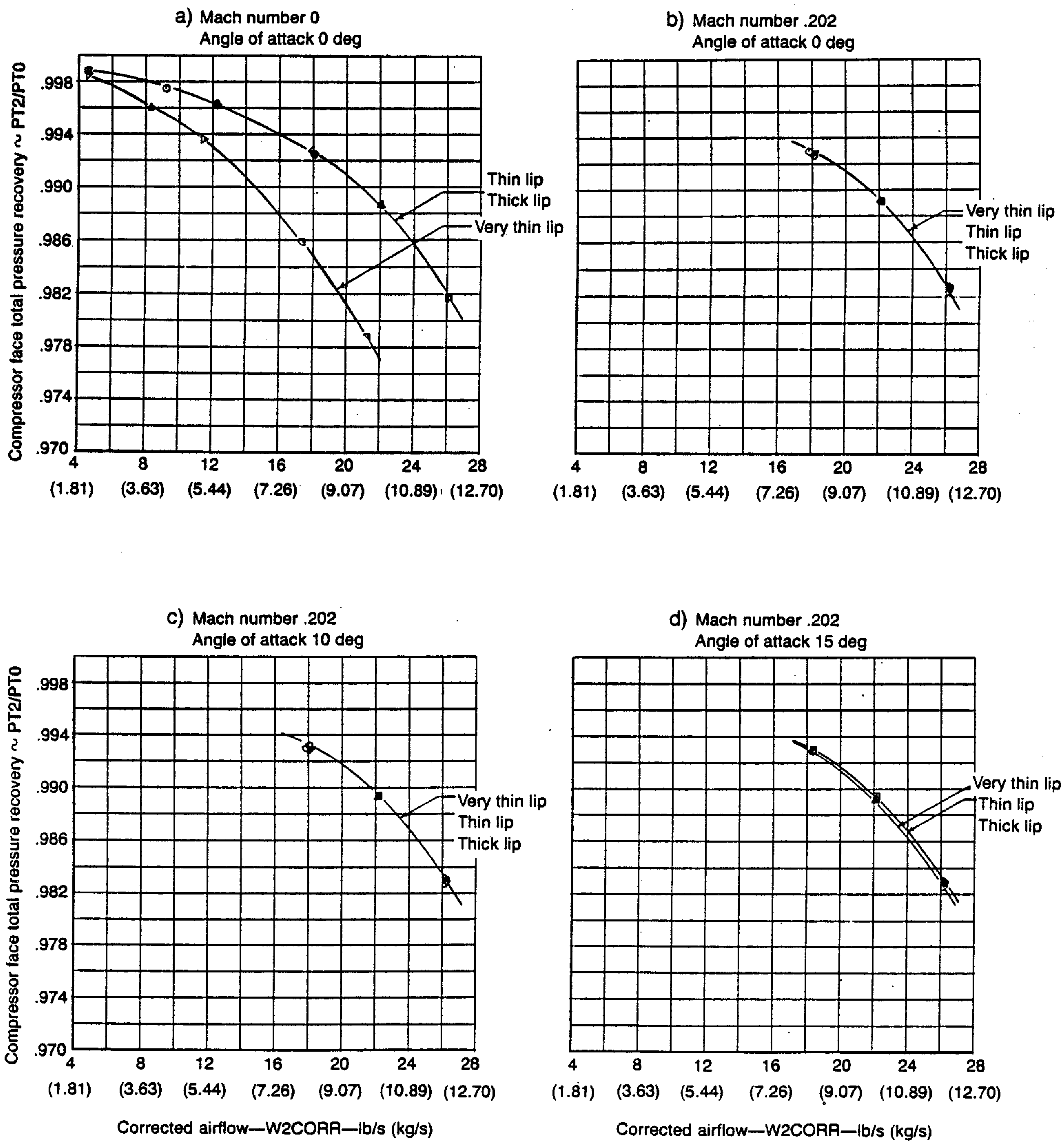

Figure 26. Lip Thickness Comparison—Compressor Face Pressure Recovery for Very Thin, Thin, and Thick Lips With 16.2% Diffuser and 3.7-Aspect-Ratio Duct

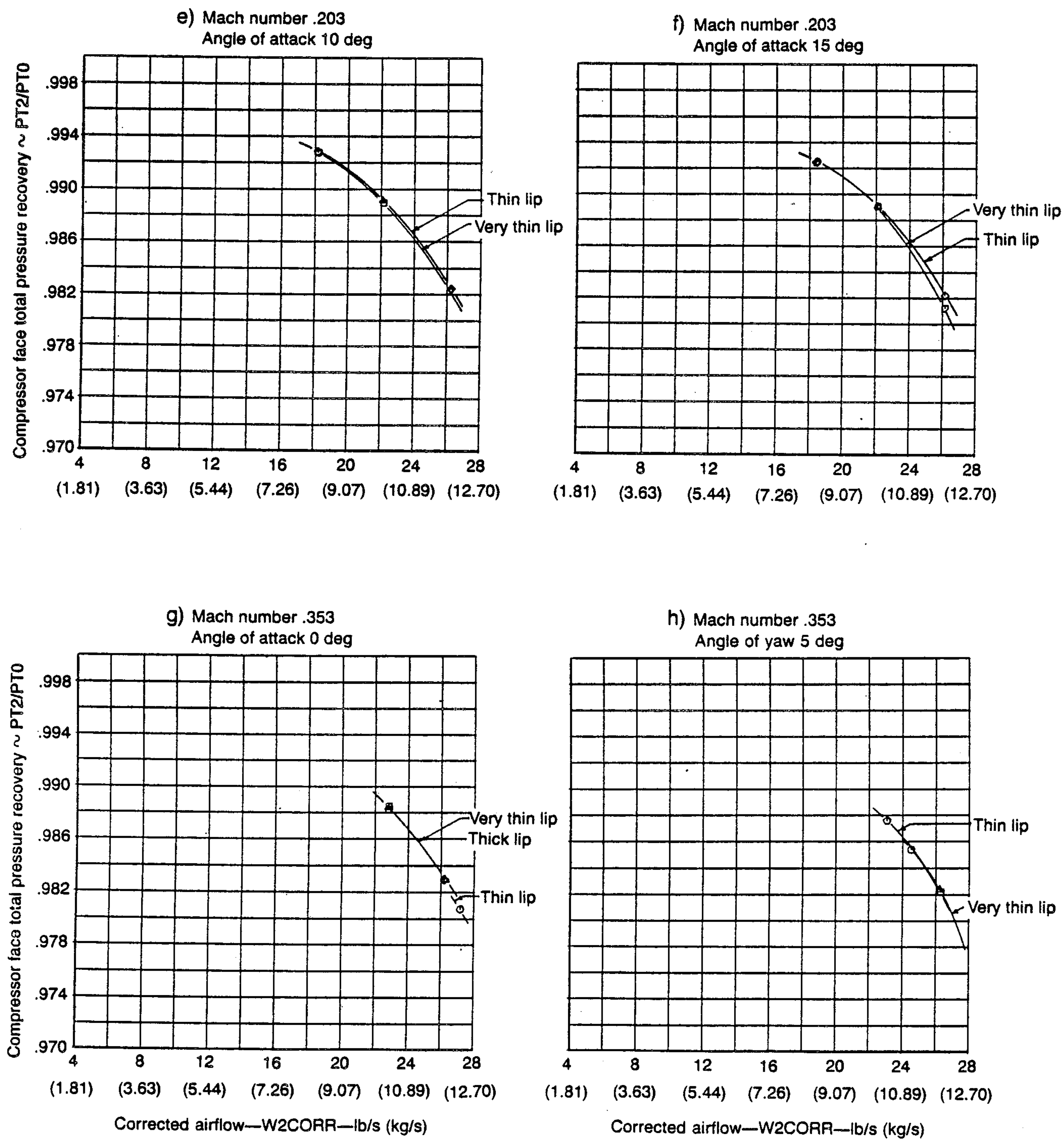

Figure 26. Lip Thickness Comparison—Compressor Face Pressure Recovery for Very Thin, Thin, and Thick Lips With 16.2% Diffuser and 3.7-Aspect-Ratio Duct (Continued)

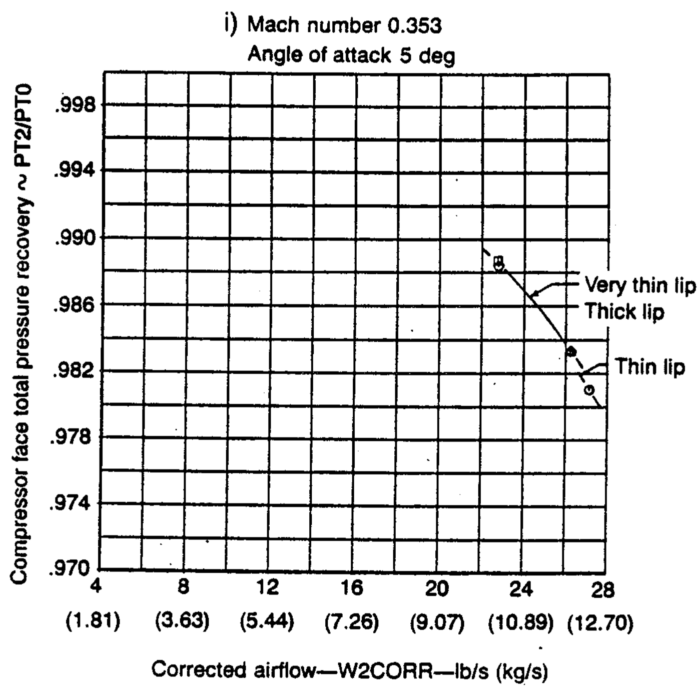

Figure 26. Lip Thickness Comparison—Compressor Face Pressure Recovery for Very Thin, Thin, and Thick Lips With 16.2% Diffuser and 3.7-Aspect-Ratio Duct (Concluded)

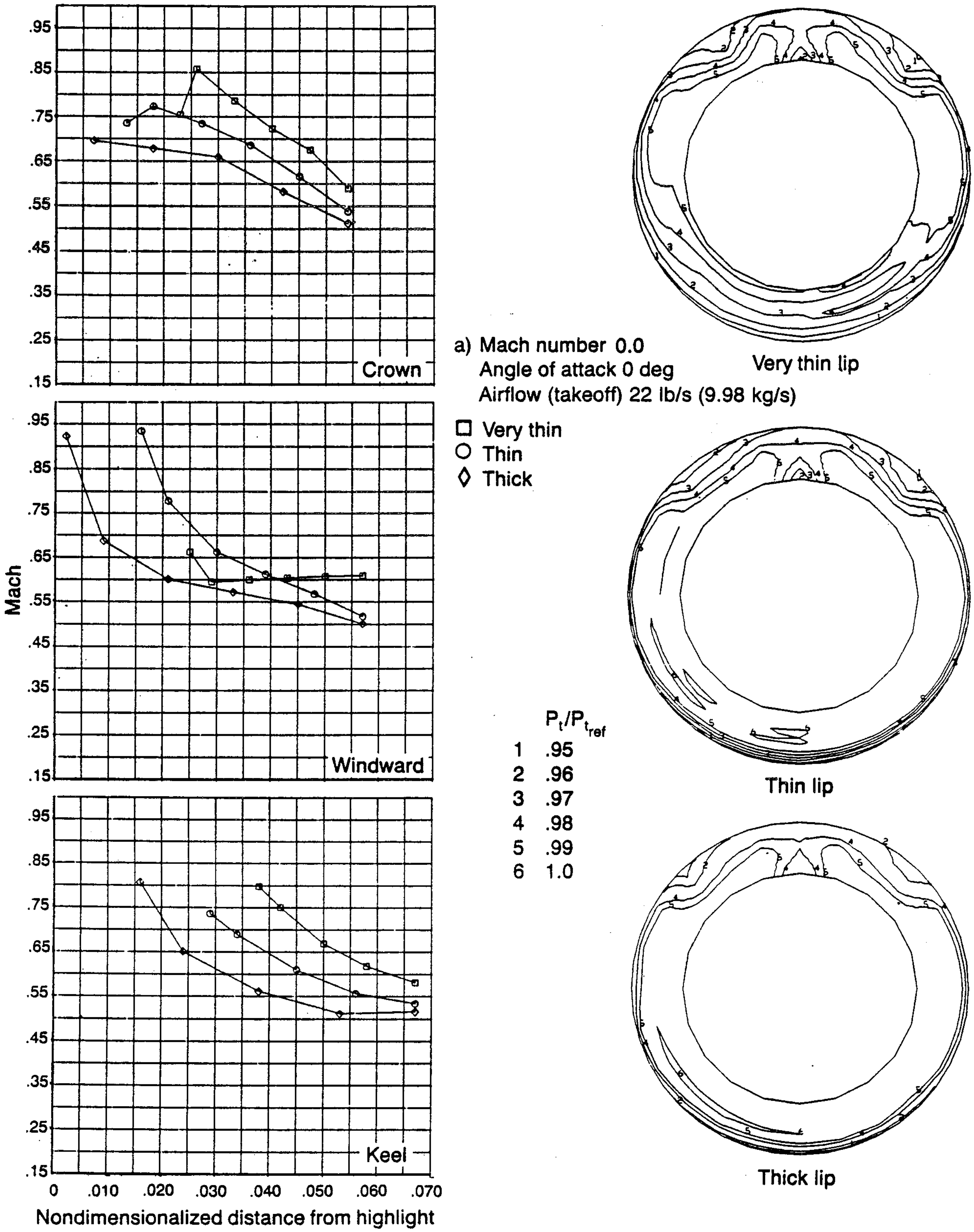

Figure 27. Lip Thickness Comparison—Duct Surface Mach Number and Compressor Face Pressures for Very Thin, Thin, and Thick Lips With 16.2% Diffuser and 3.7-Aspect-Ratio Duct

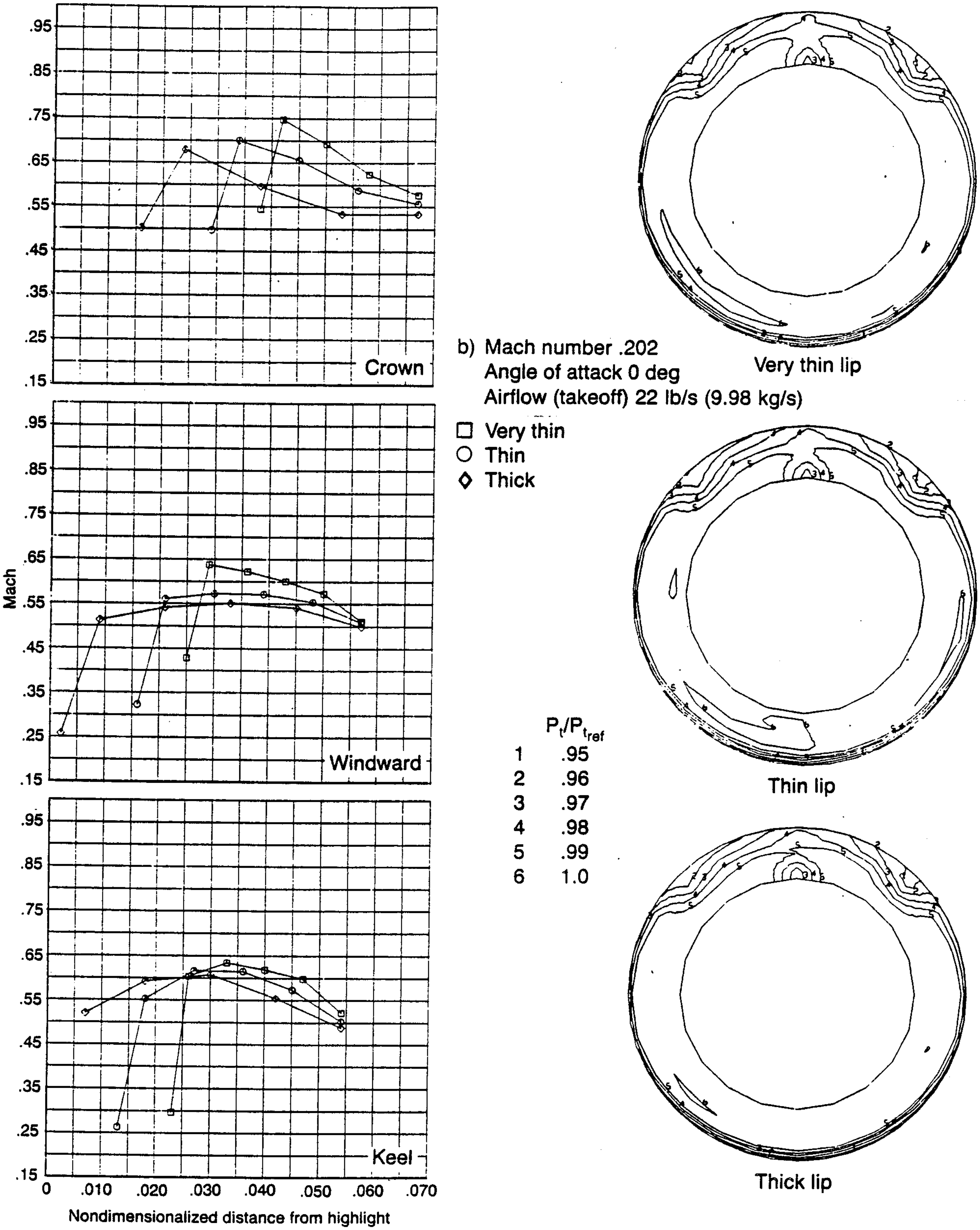

Figure 27. Lip Thickness Comparison—Duct Surface Mach Number and Compressor Face Pressures for Very Thin, Thin, and Thick Lips With 16.2% Diffuser and 3.7-Aspect-Ratio Duct (Continued)

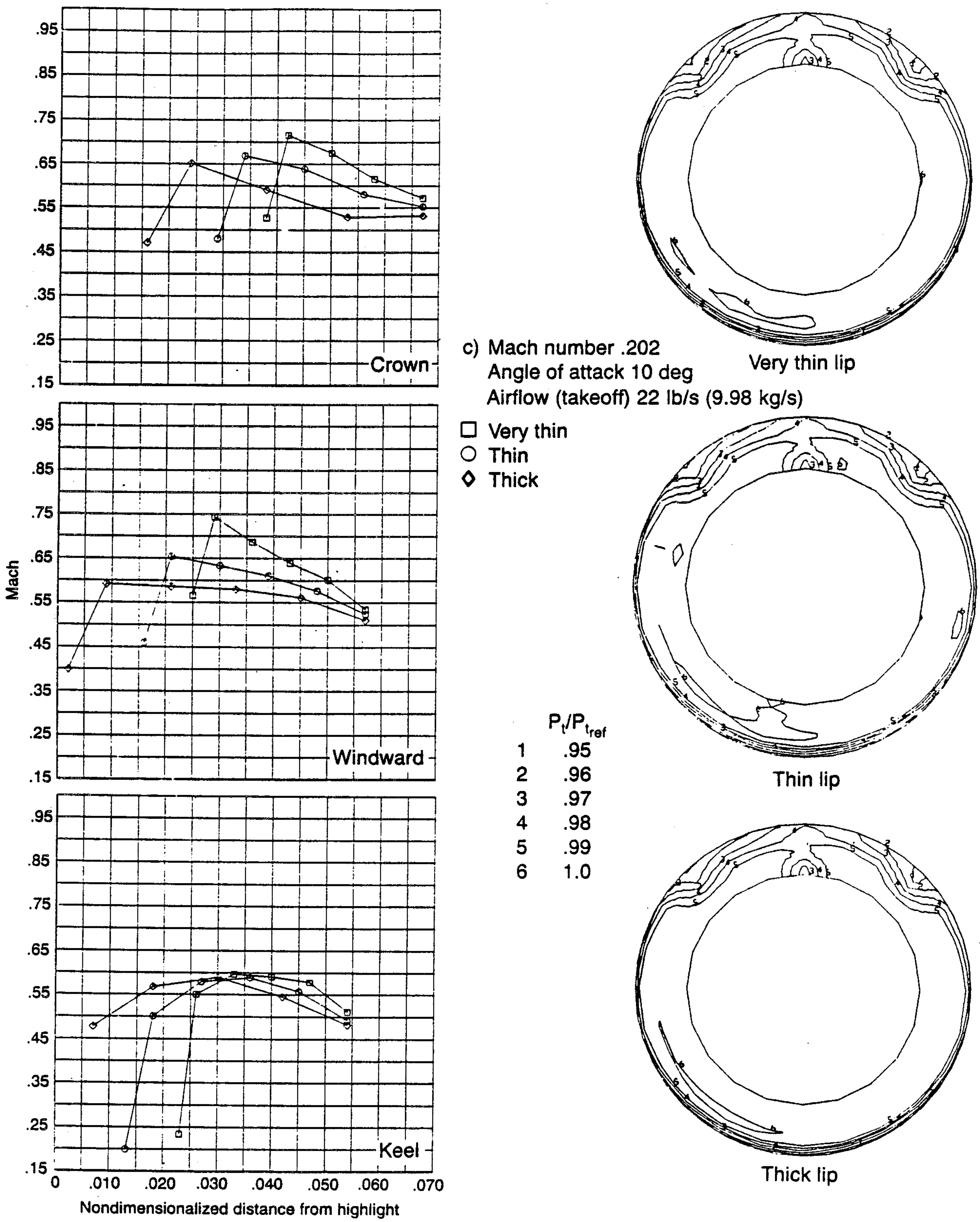

Figure 27. Lip Thickness Comparison—Duct Surface Mach Number and Compressor Face Pressures for Very Thin, Thin, and Thick Lips With 16.2% Diffuser and 3.7-Aspect-Ratio Duct (Continued)

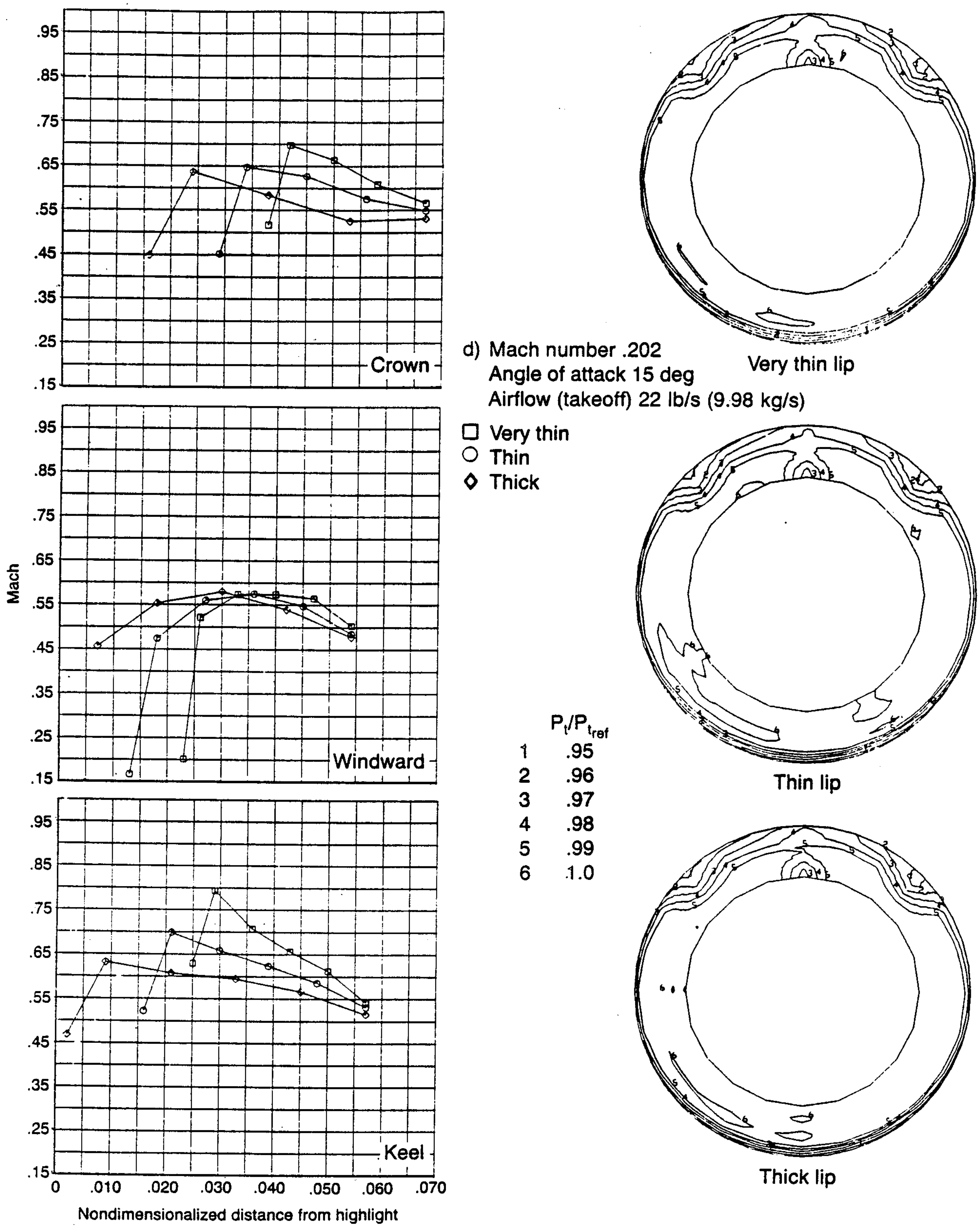

Figure 27. Lip Thickness Comparison—Duct Surface Mach Number and Compressor Face Pressures for Very Thin, Thin, and Thick Lips With 16.2% Diffuser and 3.7-Aspect-Ratio Duct (Continued)

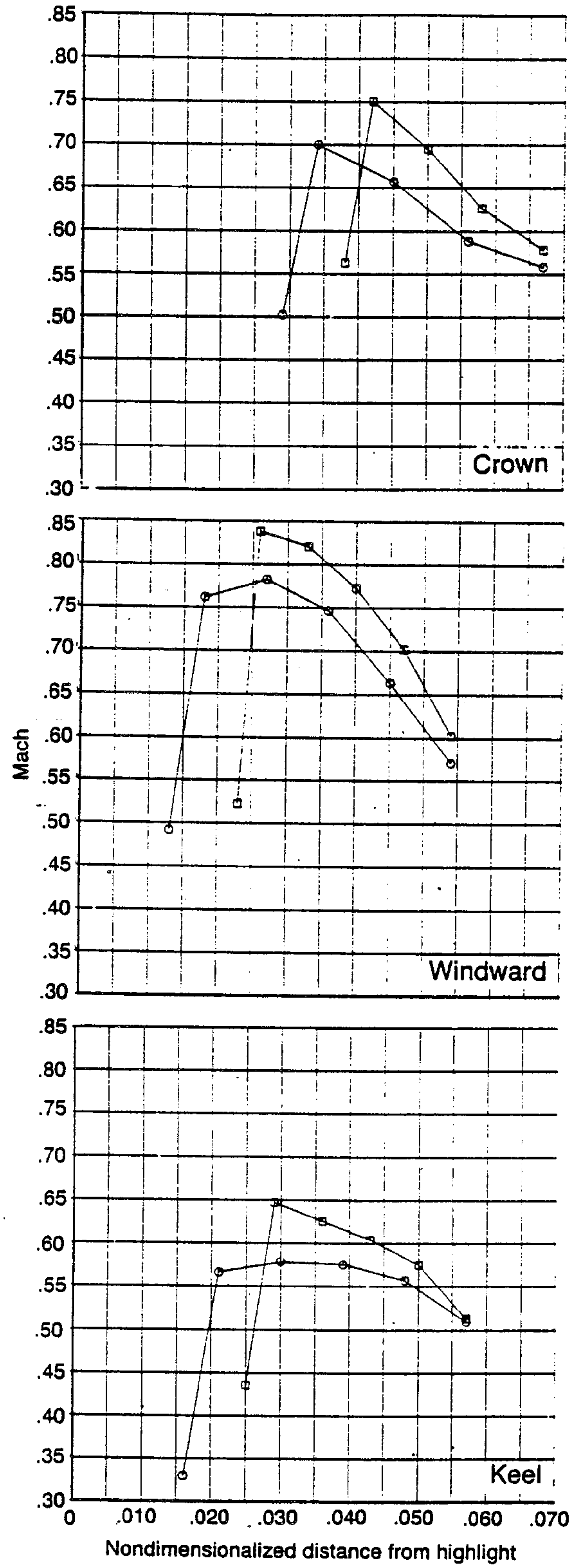

e) Mach number .203
Angle of yaw 10 deg
Airflow (takeoff) 22 lb/s (9.98 kg/s)

□ Very thin
○ Thin

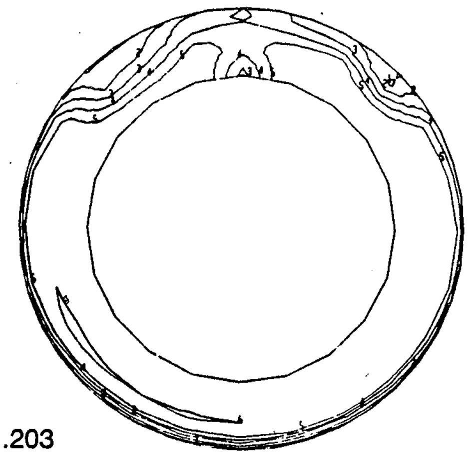

Very thin lip

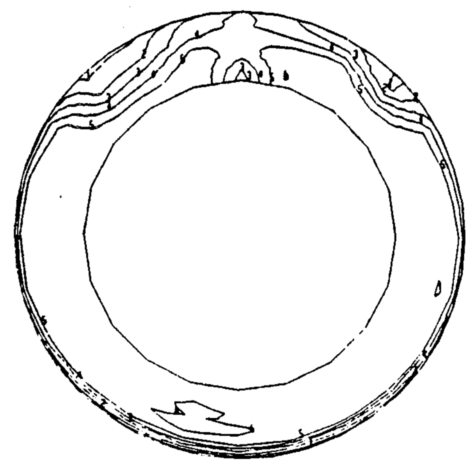

Thin lip

	$P_t/P_{t_{ref}}$
1	.95
2	.96
3	.97
4	.98
5	.99
6	1.0

Figure 27. Lip Thickness Comparison—Duct Surface Mach Number and Compressor Face Pressures for Very Thin, Thin, and Thick Lips With 16.2% Diffuser and 3.7-Aspect-Ratio Duct (Continued)

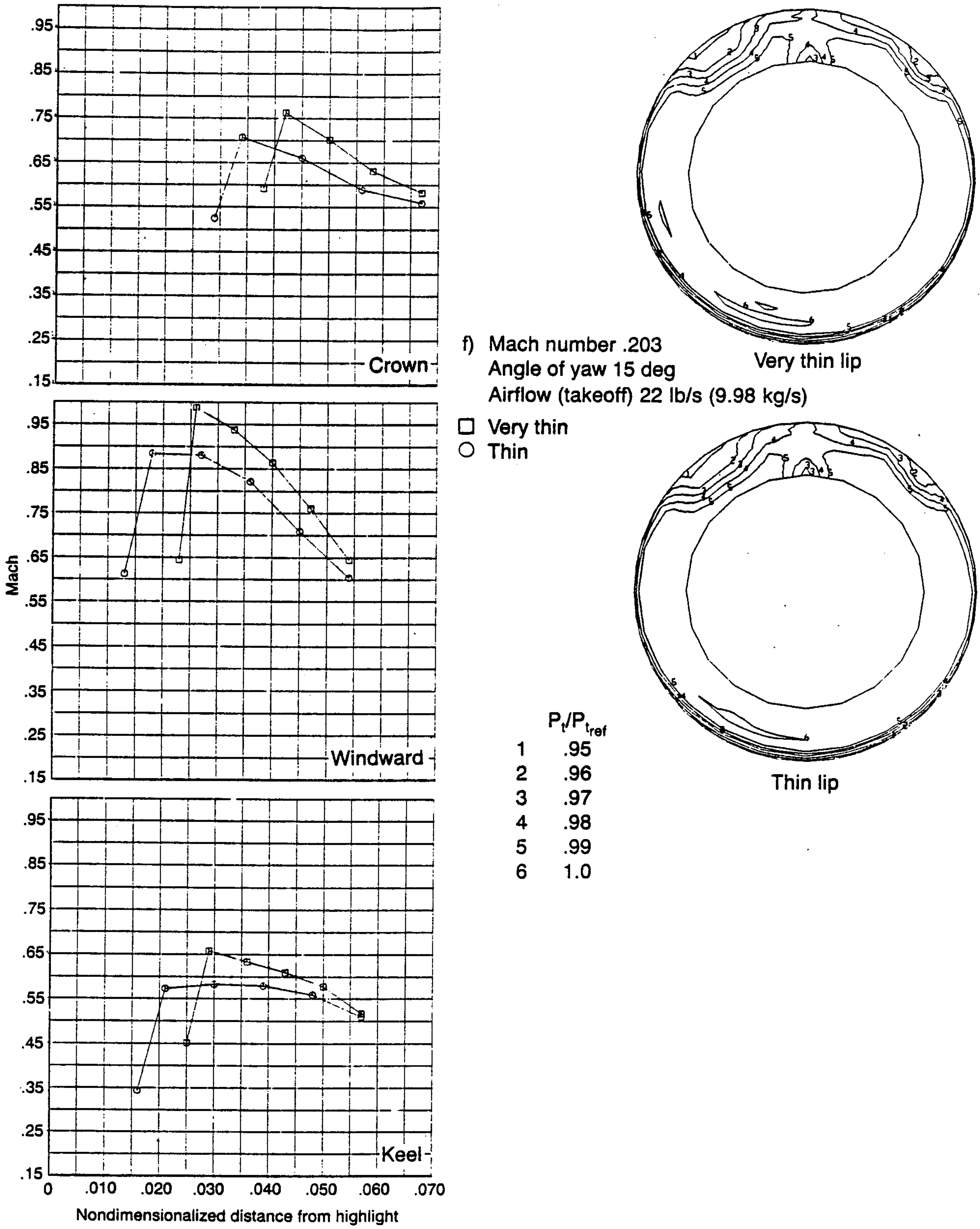

Figure 27. Lip Thickness Comparison—Duct Surface Mach Number and Compressor Face Pressures for Very Thin, Thin, and Thick Lips With 16.2% Diffuser and 3.7-Aspect-Ratio Duct (Continued)

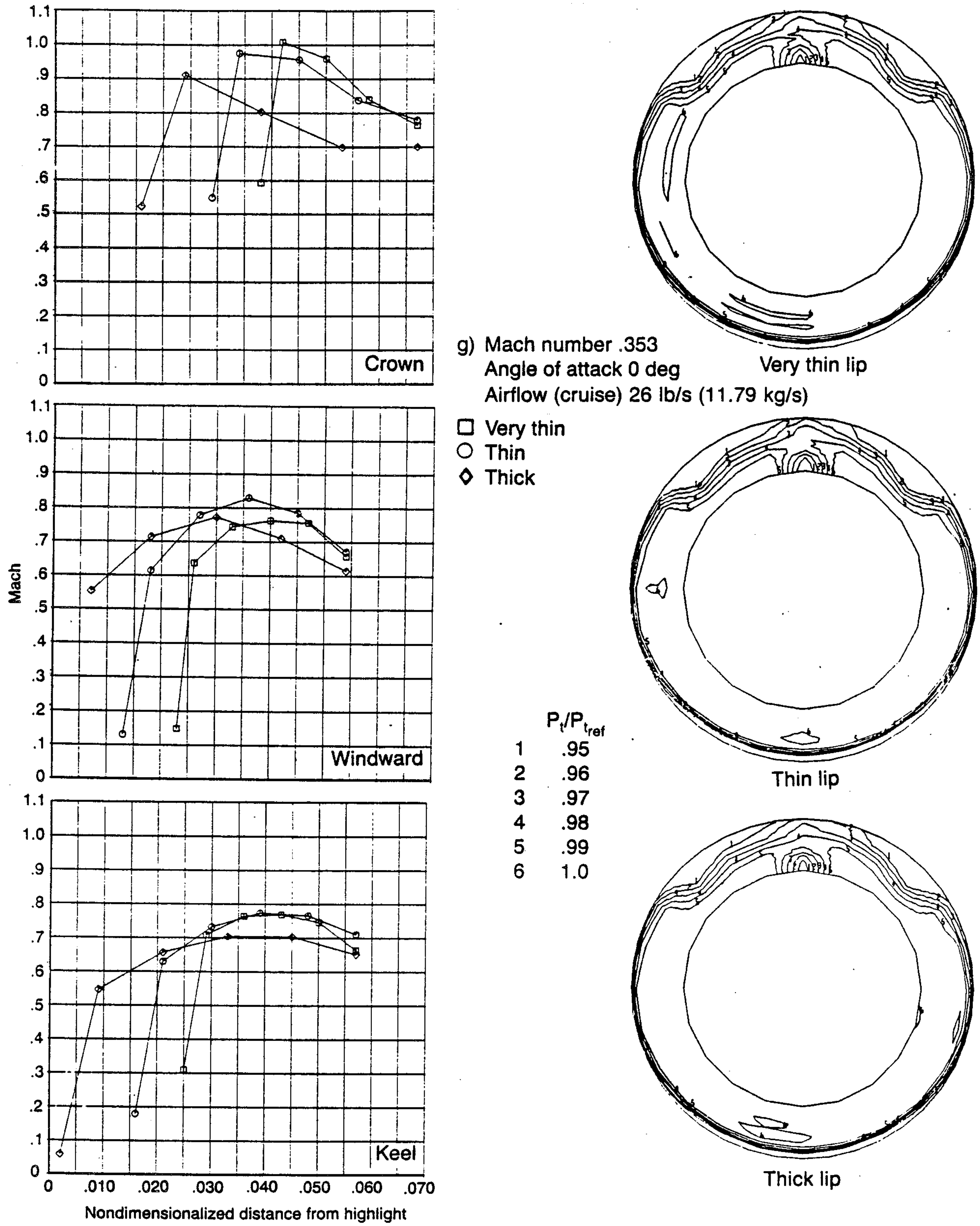

Figure 27. Lip Thickness Comparison—Duct Surface Mach Number and Compressor Face Pressures for Very Thin, Thin, and Thick Lips With 16.2% Diffuser and 3.7-Aspect-Ratio Duct (Continued)

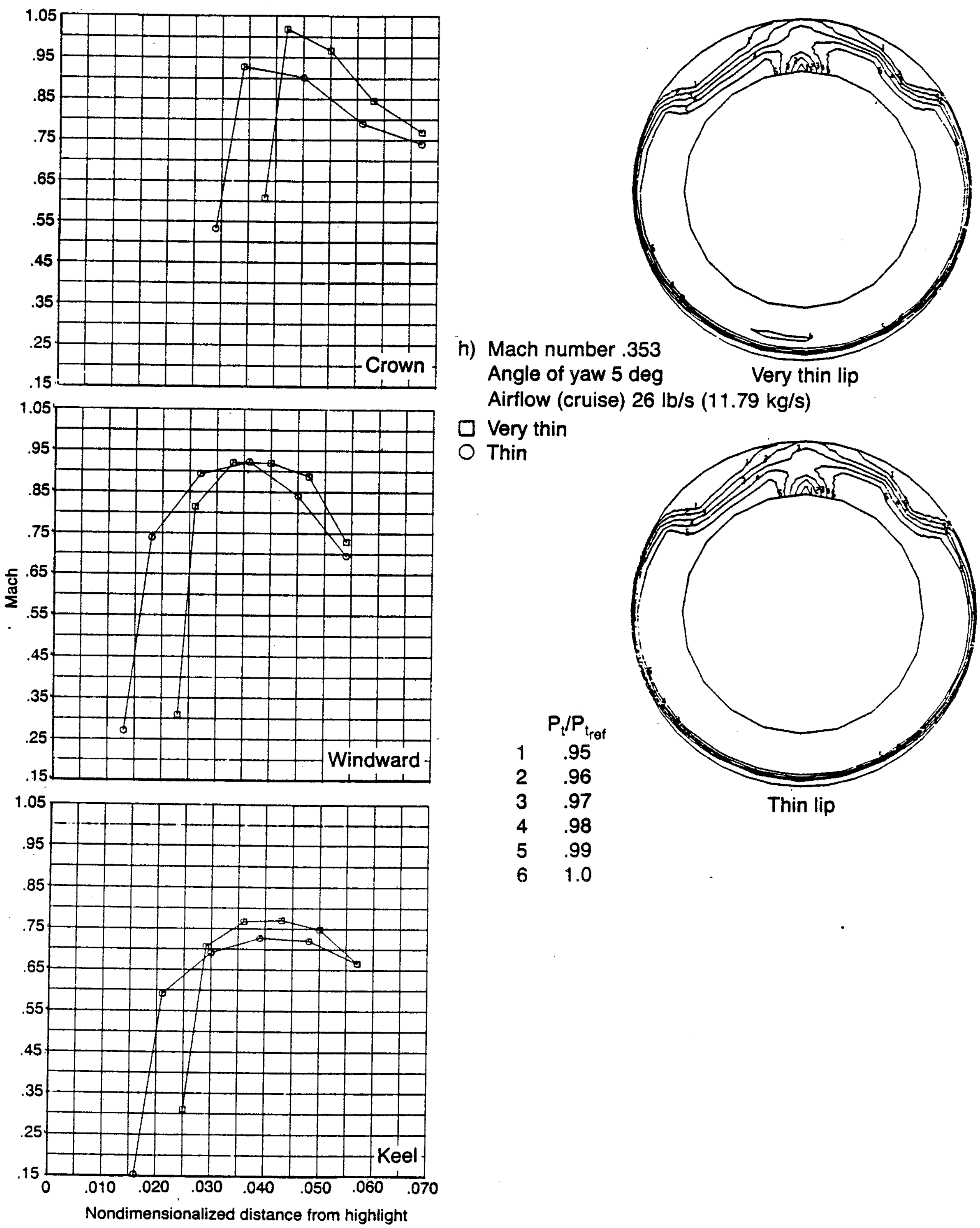

Figure 27. Lip Thickness Comparison—Duct Surface Mach Number and Compressor Face Pressures for Very Thin, Thin, and Thick Lips With 16.2% Diffuser and 3.7-Aspect-Ratio Duct (Continued)

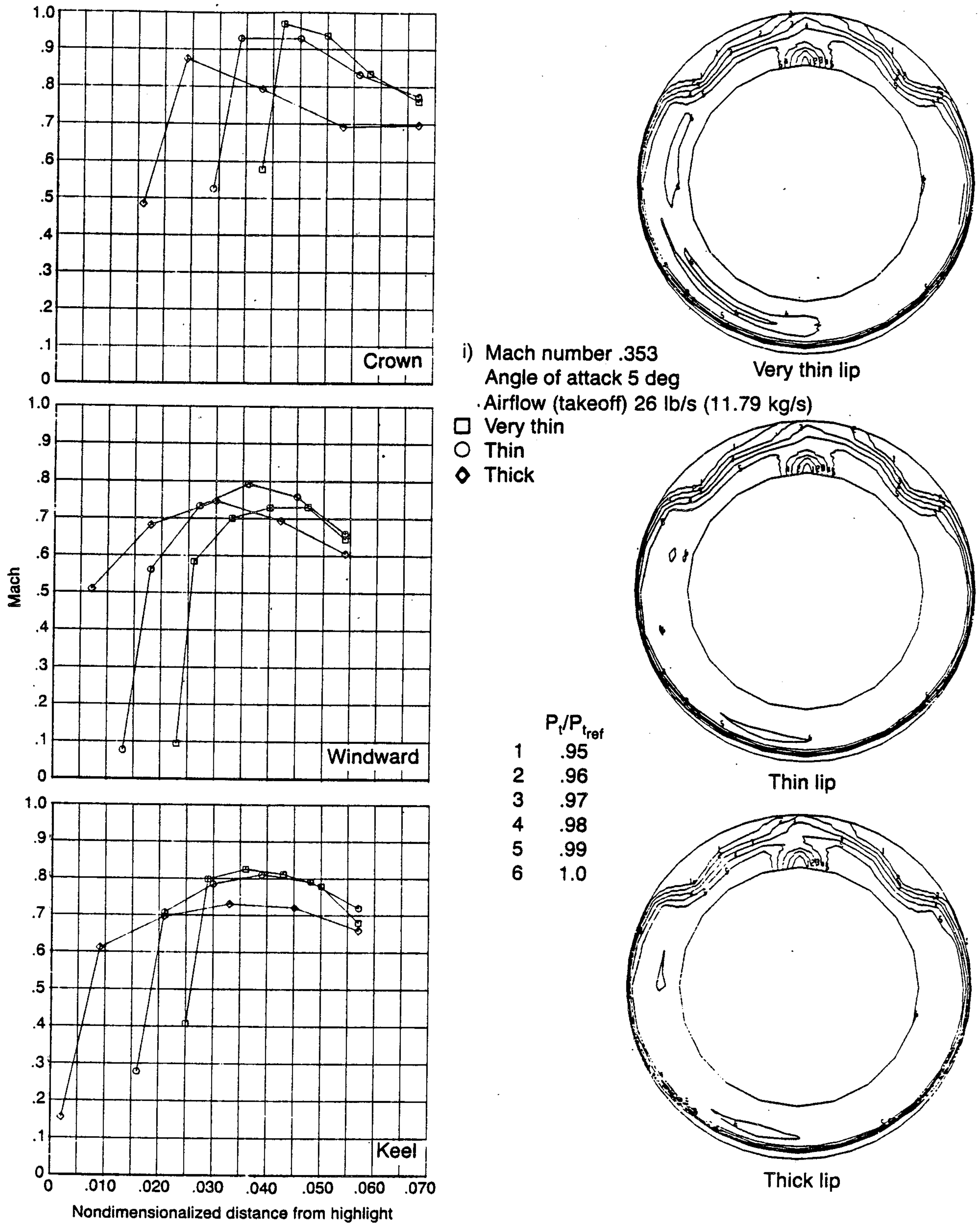

Figure 27. Lip Thickness Comparison—Duct Surface Mach Number and Compressor Face Pressures for Very Thin, Thin, and Thick Lips With 16.2% Diffuser and 3.7-Aspect-Ratio Duct (Concluded)

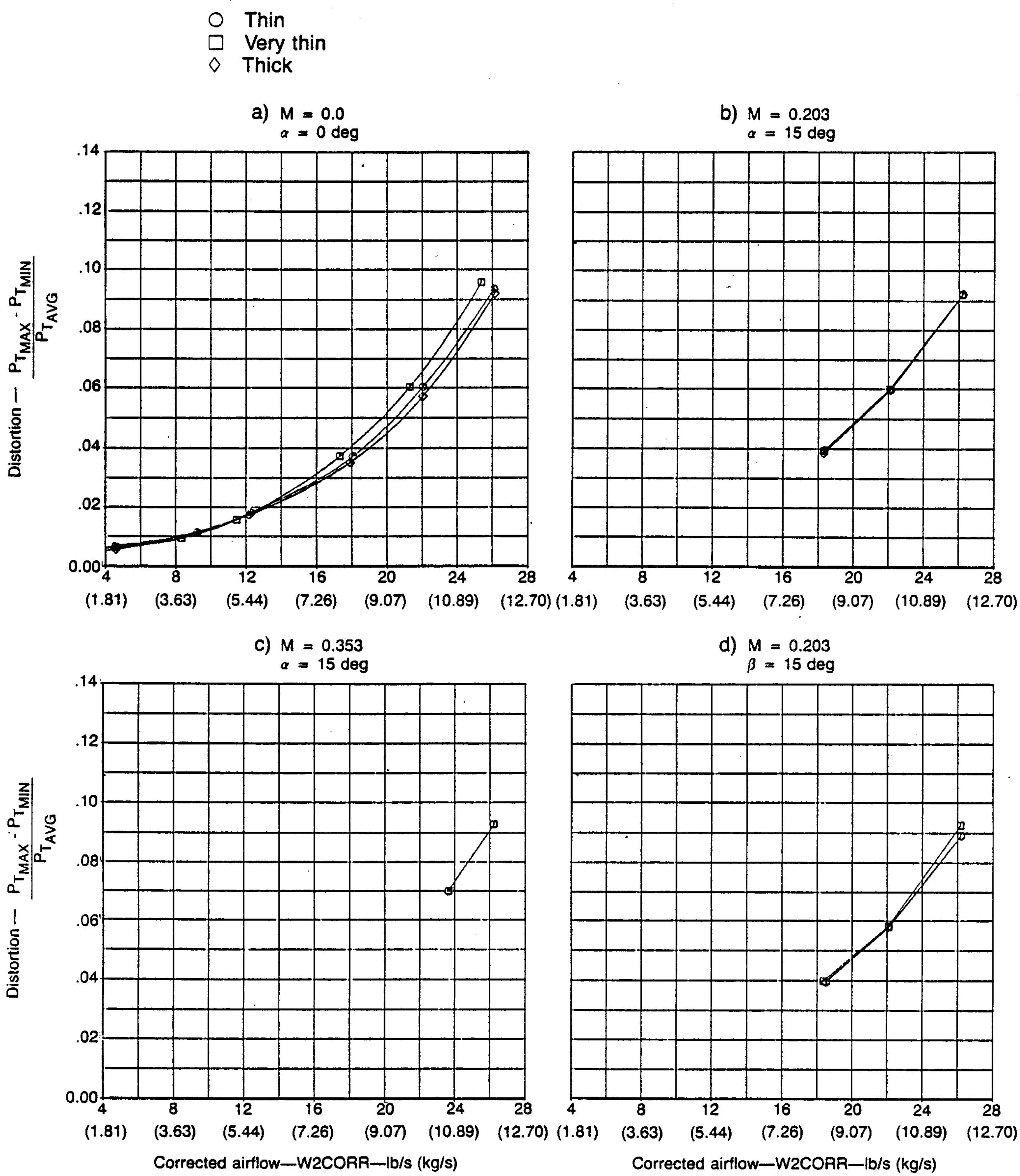

Figure 28. Compressor Face Distortion Comparison for Very Thin, Thin, and Thick Lips

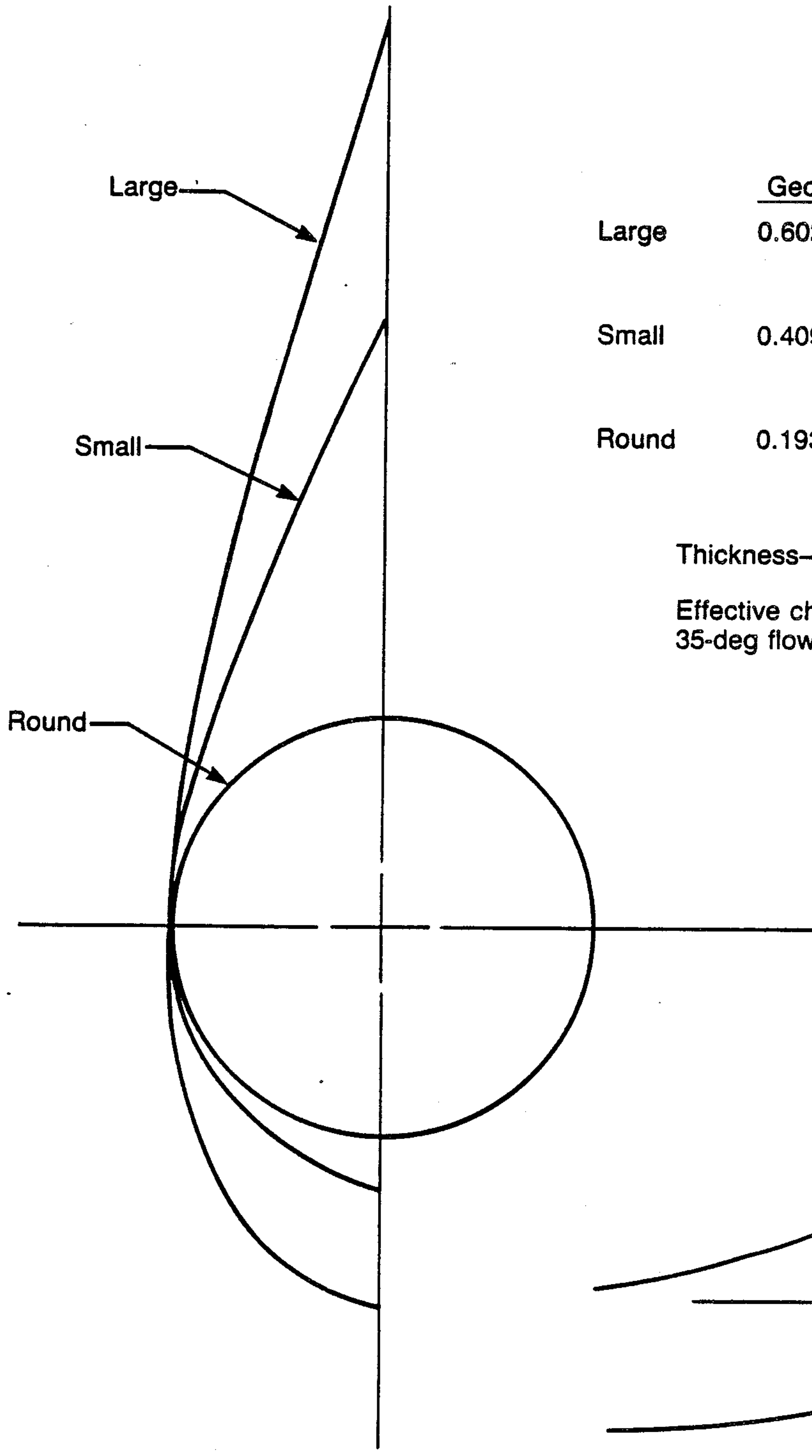

	CHORD	
	Geometric	Effective
Large	0.602 (0.183)	1.050 (0.320)
Small	0.409 (0.125)	0.713 (0.217)
Round	0.193 (0.059)	0.336 (0.102)

Thickness—0.193 (0.059)

Effective chord based on
35-deg flow angle across fairing

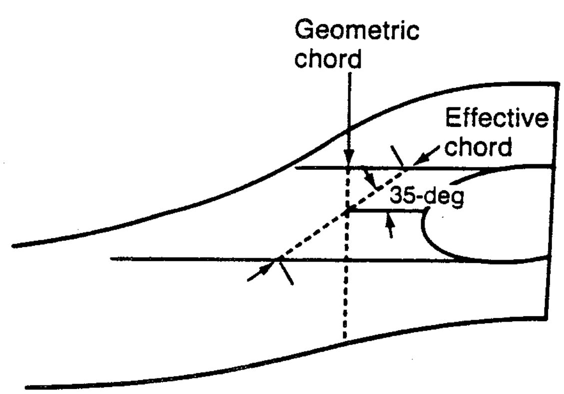

Figure 29. Shaft Fairing Cross Sections

Figure 30. Small and Large Shaft Fairings (the Largest Was Not Tested)

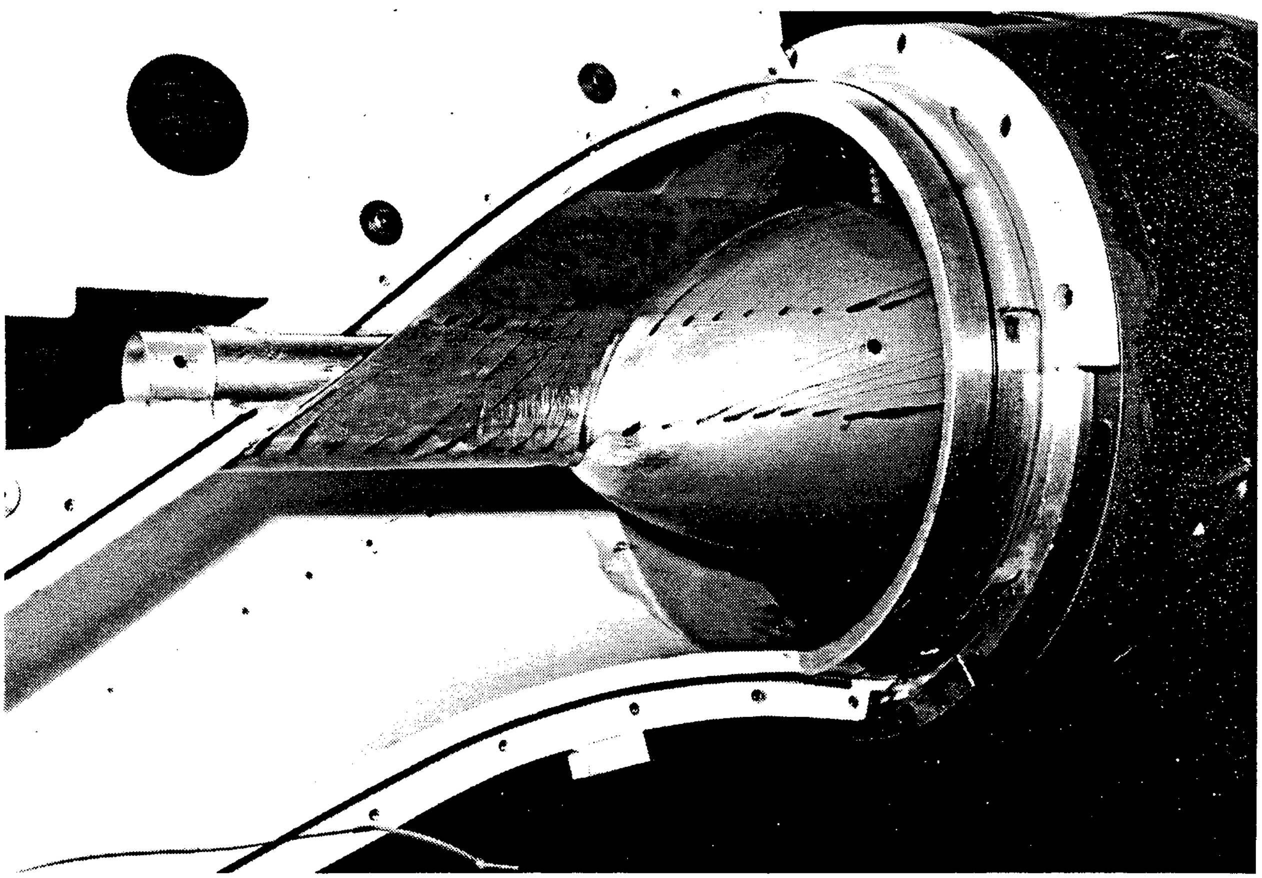

Figure 31. Flow Visualization Streamlines Over Large Shaft Fairing and Compressor-Face Hub Fairing

ORIGINAL PAGE IS
OF POOR QUALITY

ORIGINAL PAGE IS
OF POOR QUALITY

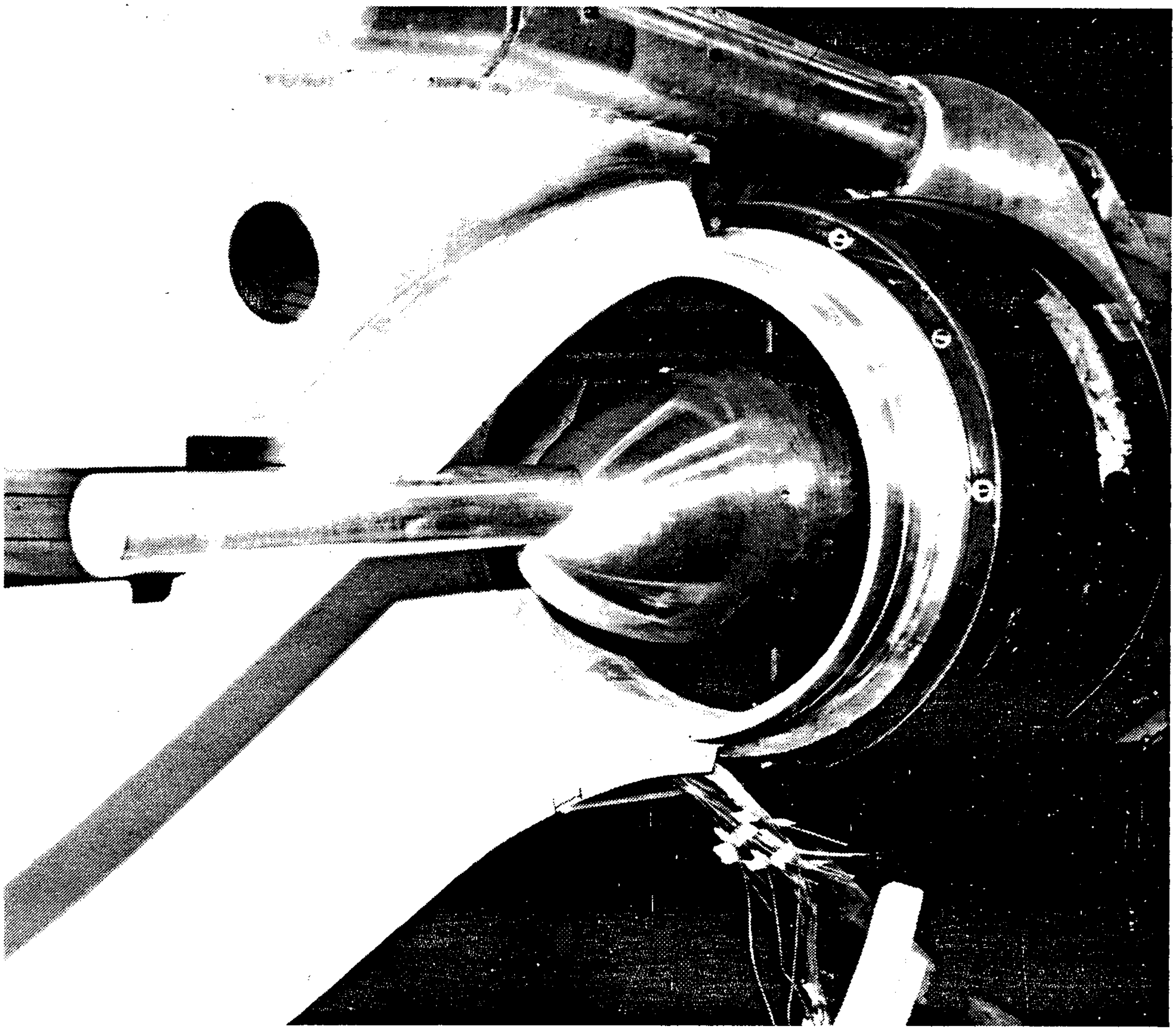

Figure 32. View of Round Shaft and Compressor-Face Hub Fairing

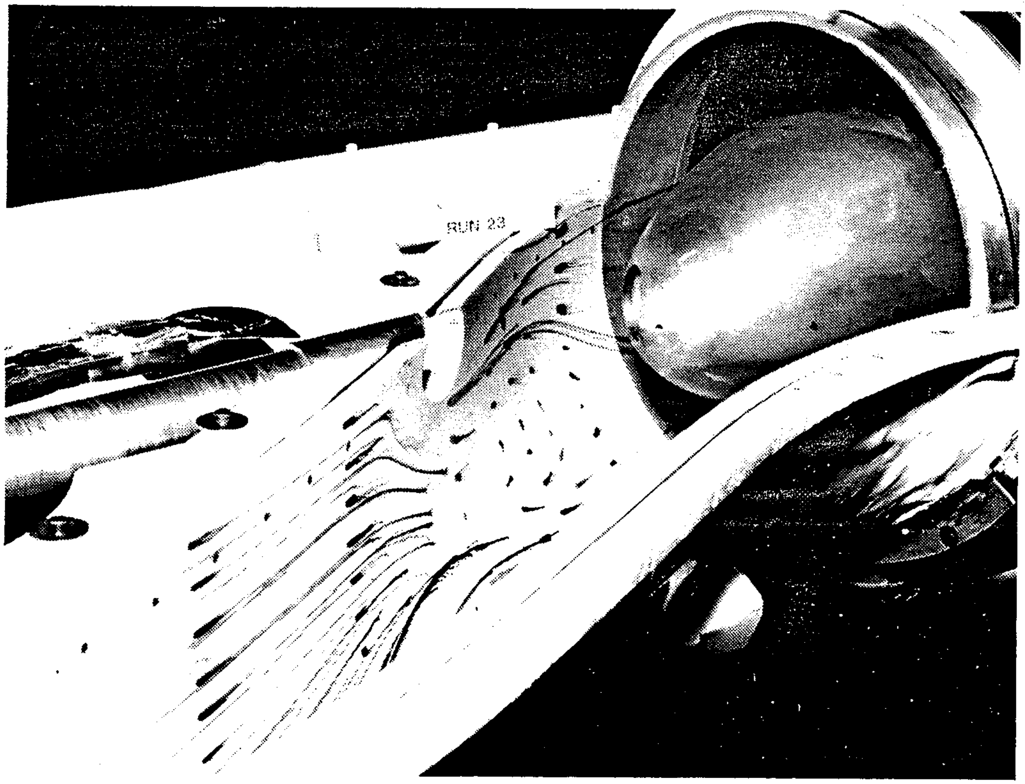

Figure 33. Internal Duct Left Side Showing Separation Bubble (Shaft Fairing Removed for Photography)

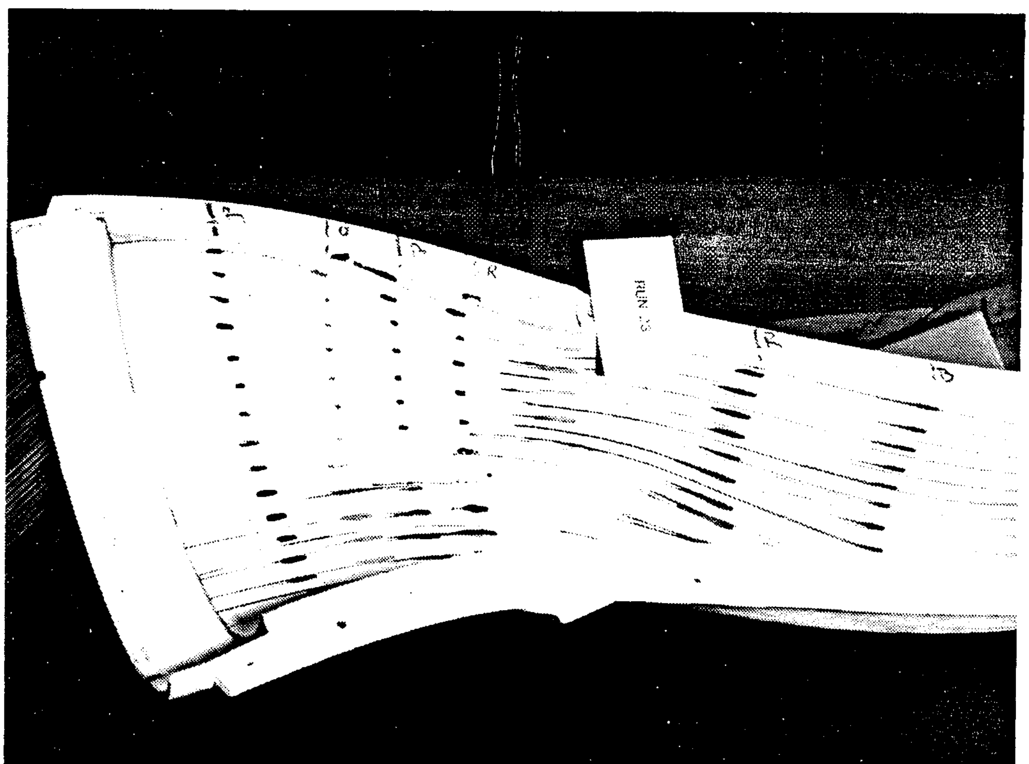

Figure 34. Internal Duct Right Side Showing Separation Bubble

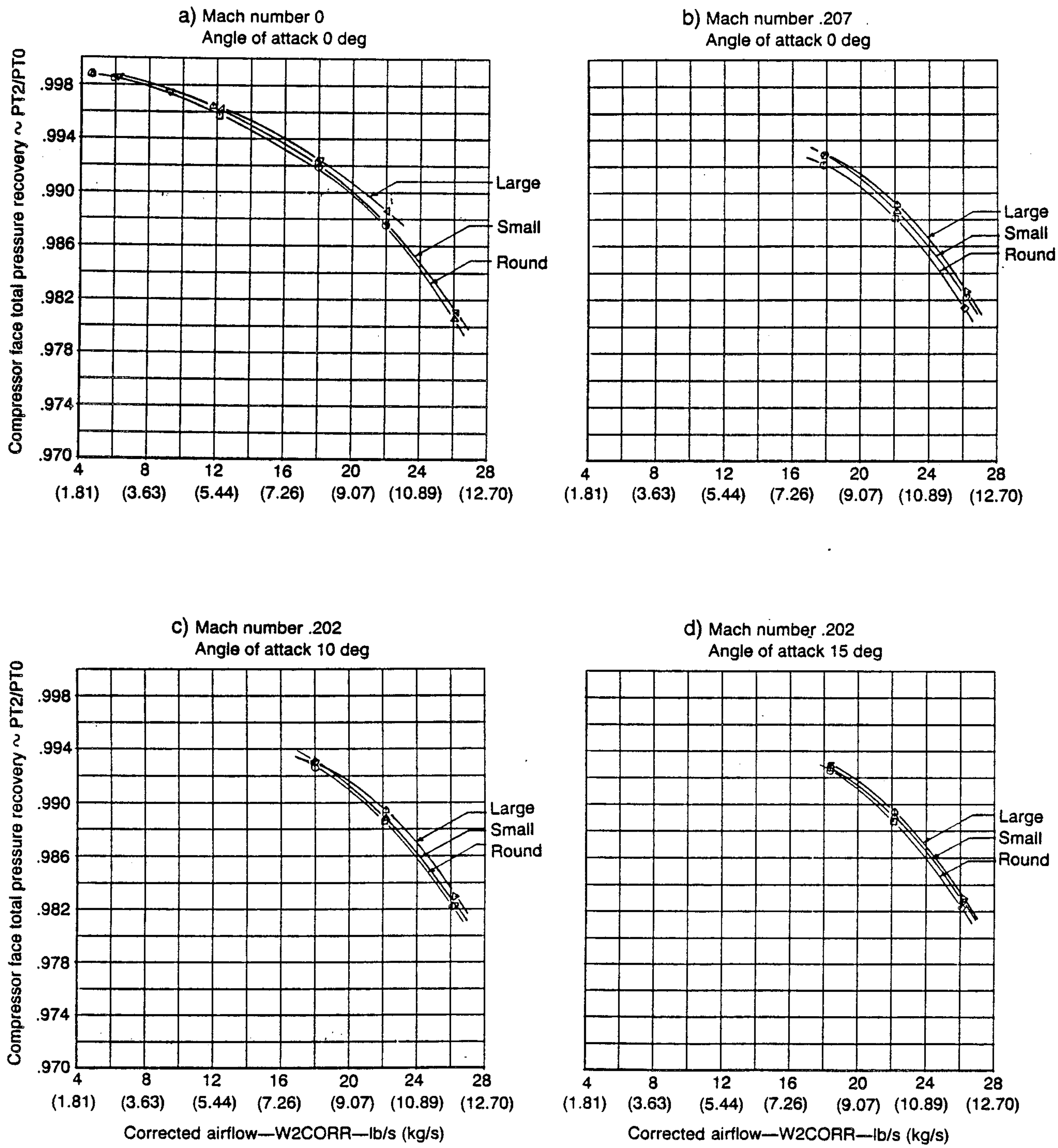

Figure 35. Shaft Fairing Comparison—Compressor Face Pressure Recovery for Round, Small, and Large Shaft Fairings With 16.2% Diffuser, 3.7-Aspect-Ratio Duct, and Thin Lip

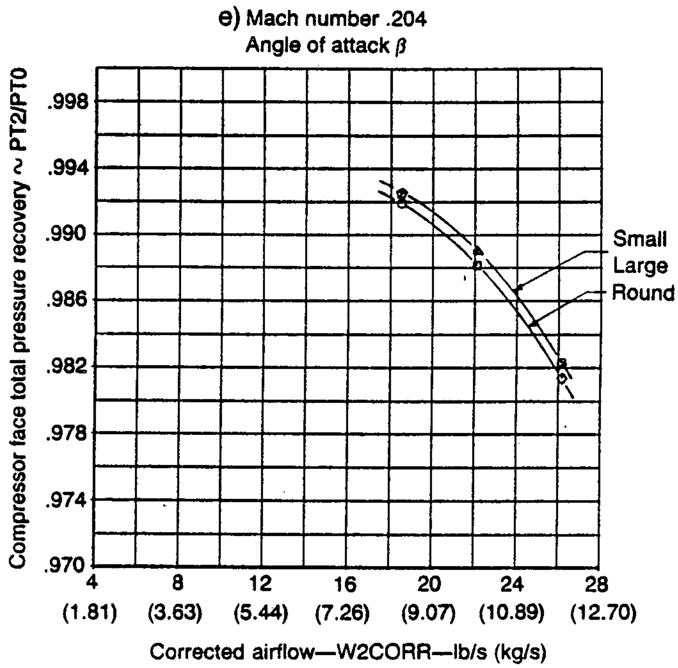

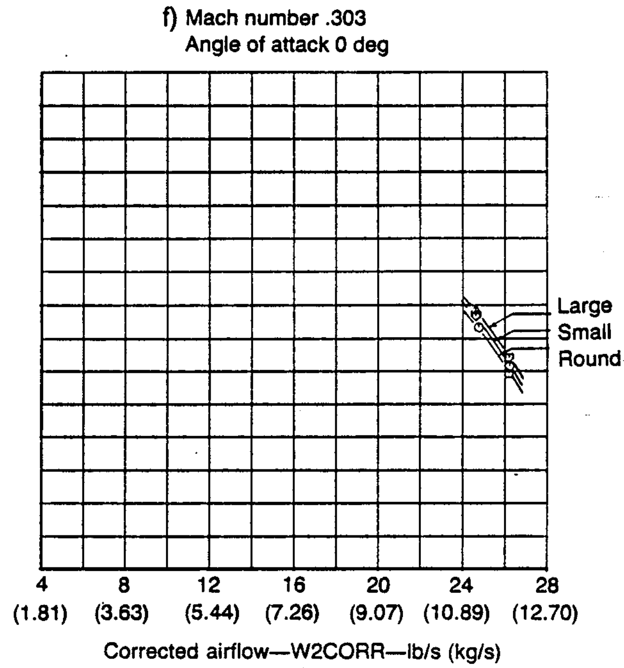

Figure 35. Shaft Fairing Comparison—Compressor Face Pressure Recovery for Round, Small, and Large Shaft Fairings With 16.2% Diffuser, 3.7-Aspect-Ratio Duct, and Thin Lip (Concluded)

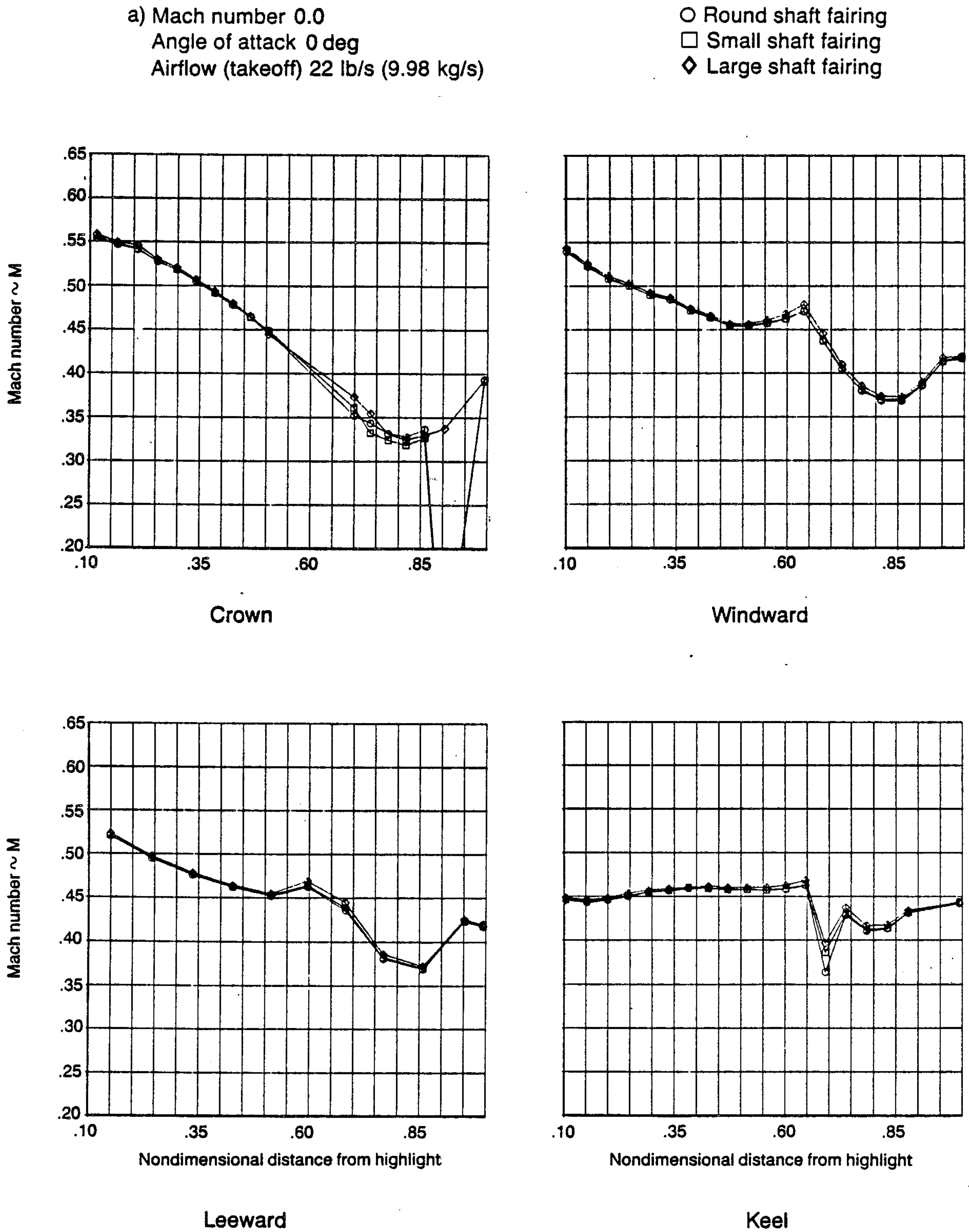

Figure 36. Shaft Fairing Comparison—Duct Surface Mach Number for Round, Small, and Large Shaft Fairings With 16.2% Diffuser, 3.7-Aspect-Ratio Duct, and Thin Lip

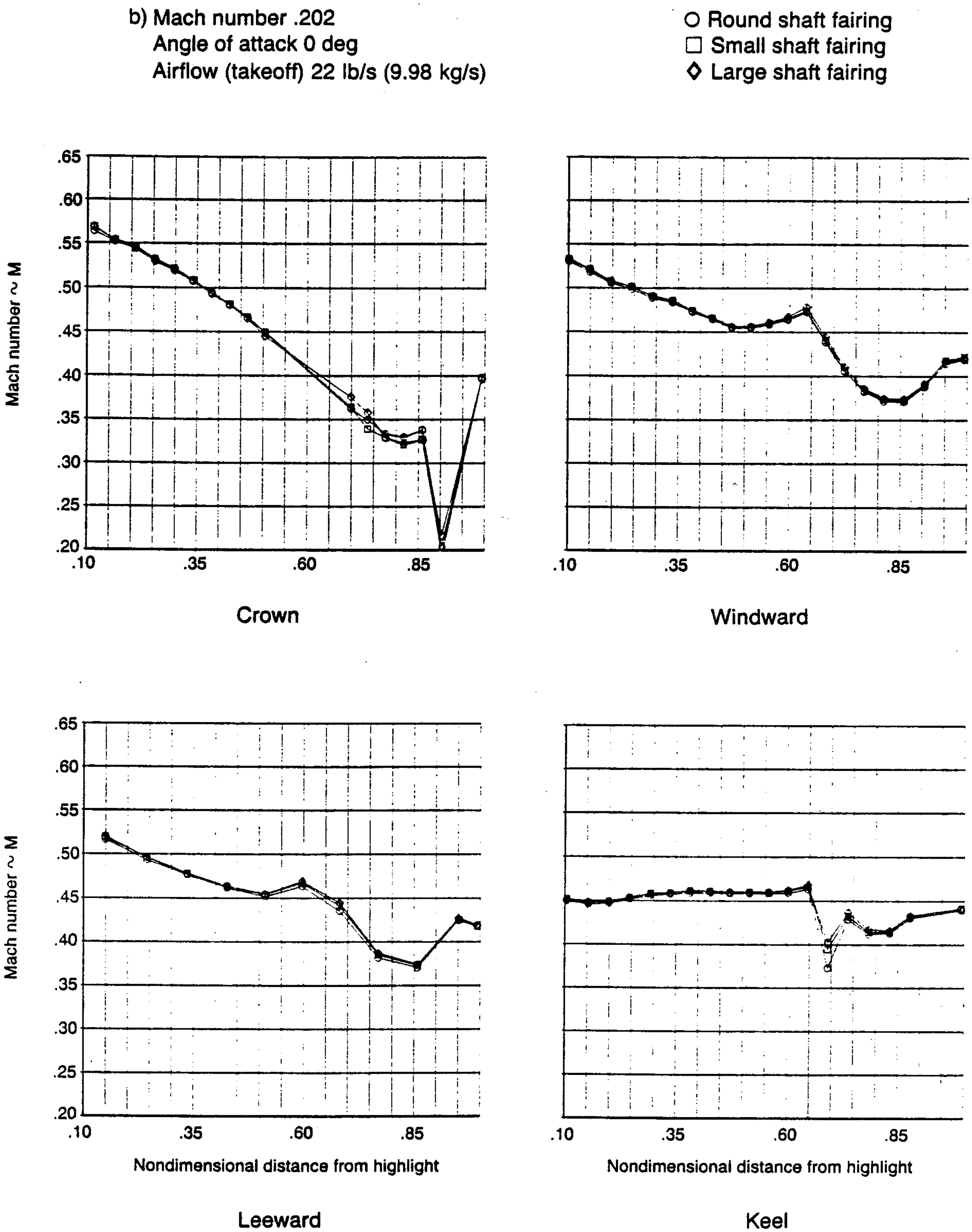

Figure 36. Shaft Fairing Comparison—Duct Surface Mach Number for Round, Small, and Large Shaft Fairings With 16.2% Diffuser, 3.7-Aspect-Ratio Duct, and Thin Lip (Continued)

c) Mach number .202
Angle of attack 10 deg
Airflow (takeoff) 22 lb/s (9.98 kg/s)

O Round shaft fairing
□ Small shaft fairing
◇ Large shaft fairing

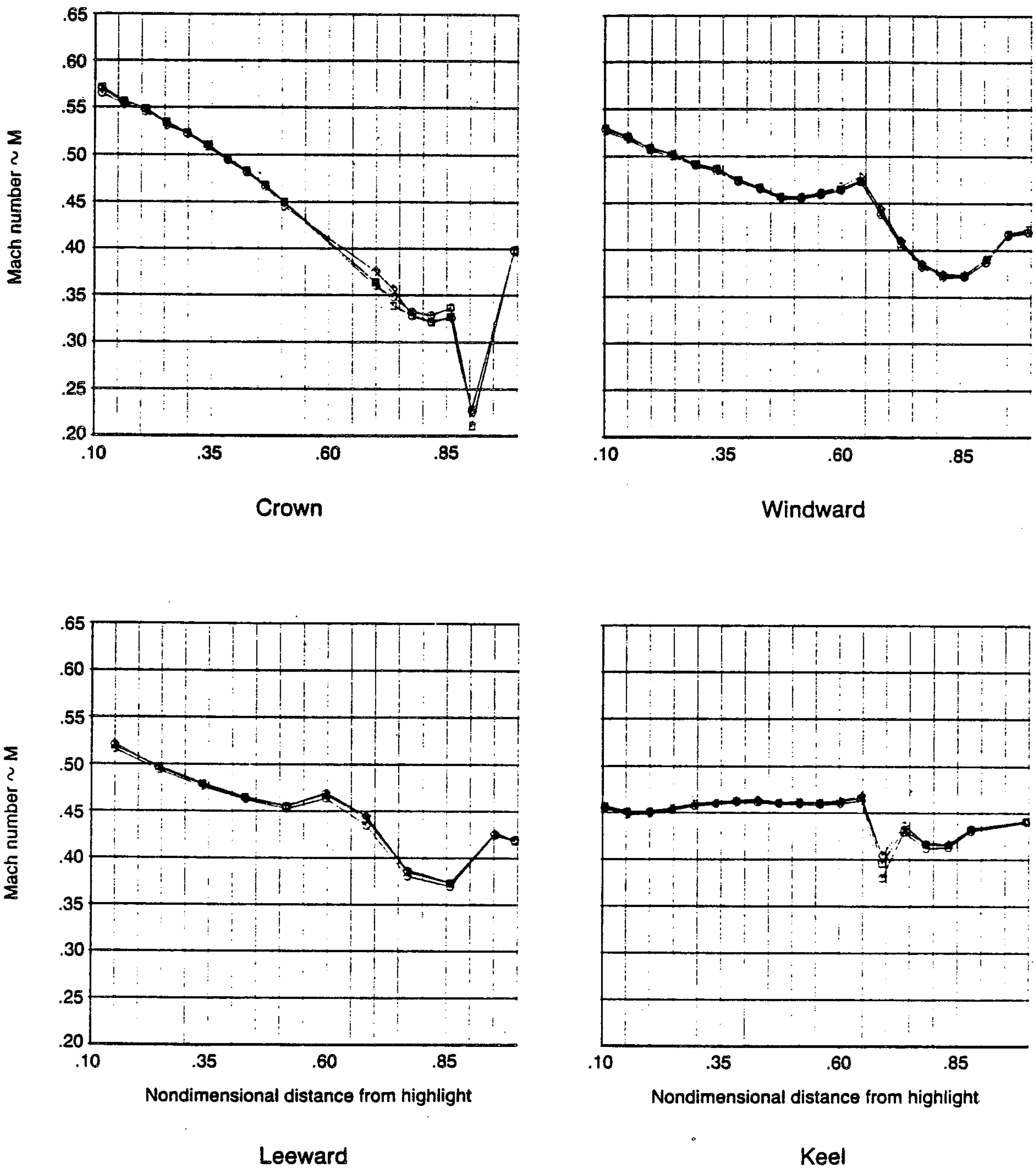

Figure 36. Shaft Fairing Comparison—Duct Surface Mach Number for Round, Small, and Large Shaft Fairings With 16.2% Diffuser, 3.7-Aspect-Ratio Duct, and Thin Lip (Continued)

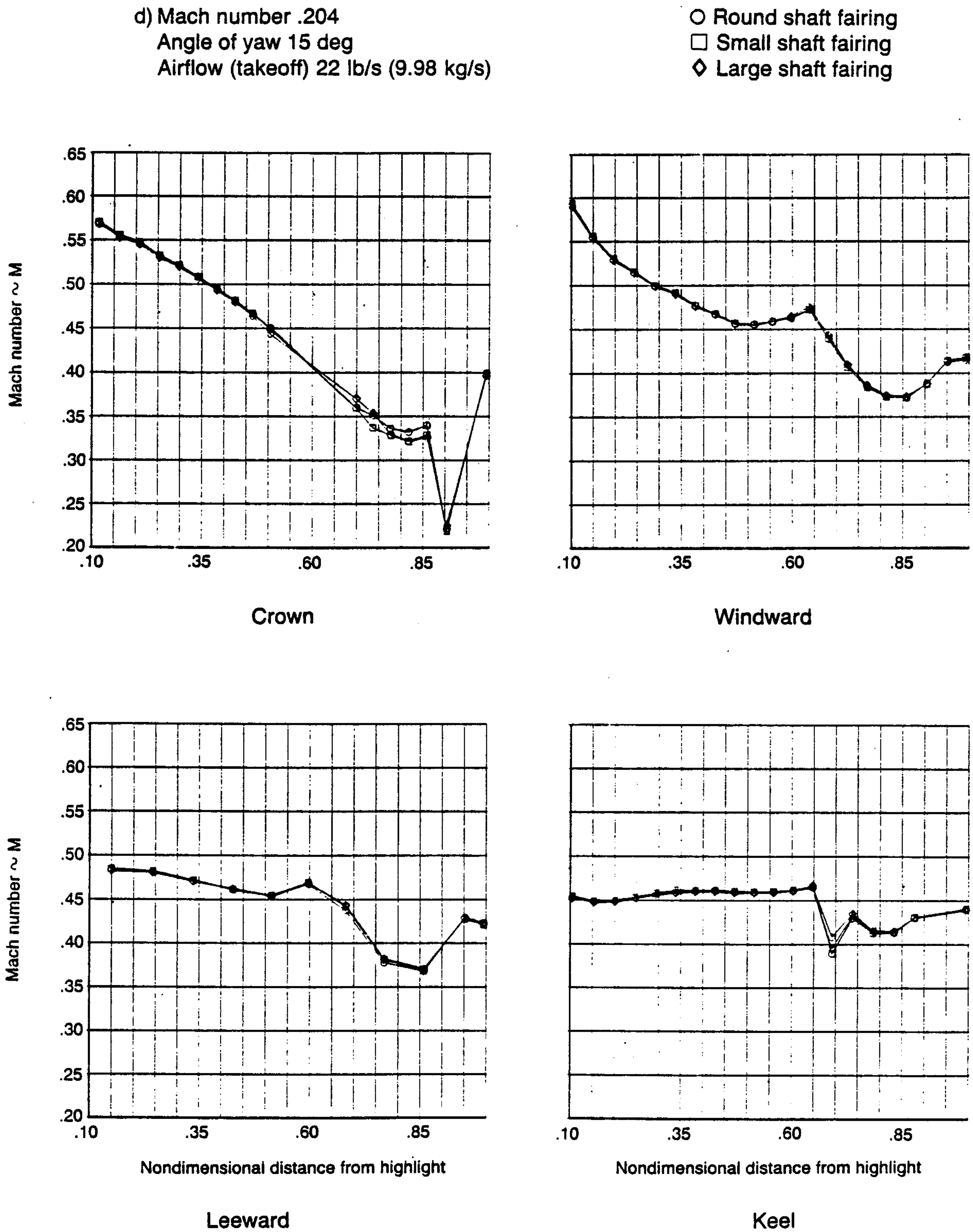

Figure 36. Shaft Fairing Comparison—Duct Surface Mach Number for Round, Small, and Large Shaft Fairings With 16.2% Diffuser, 3.7-Aspect-Ratio Duct, and Thin Lip (Continued)

e) Mach number .202
Angle of attack 15 deg
Airflow (takeoff) 22 lb/s (9.98 kg/s)

O Round shaft fairing
□ Small shaft fairing
◇ Large shaft fairing

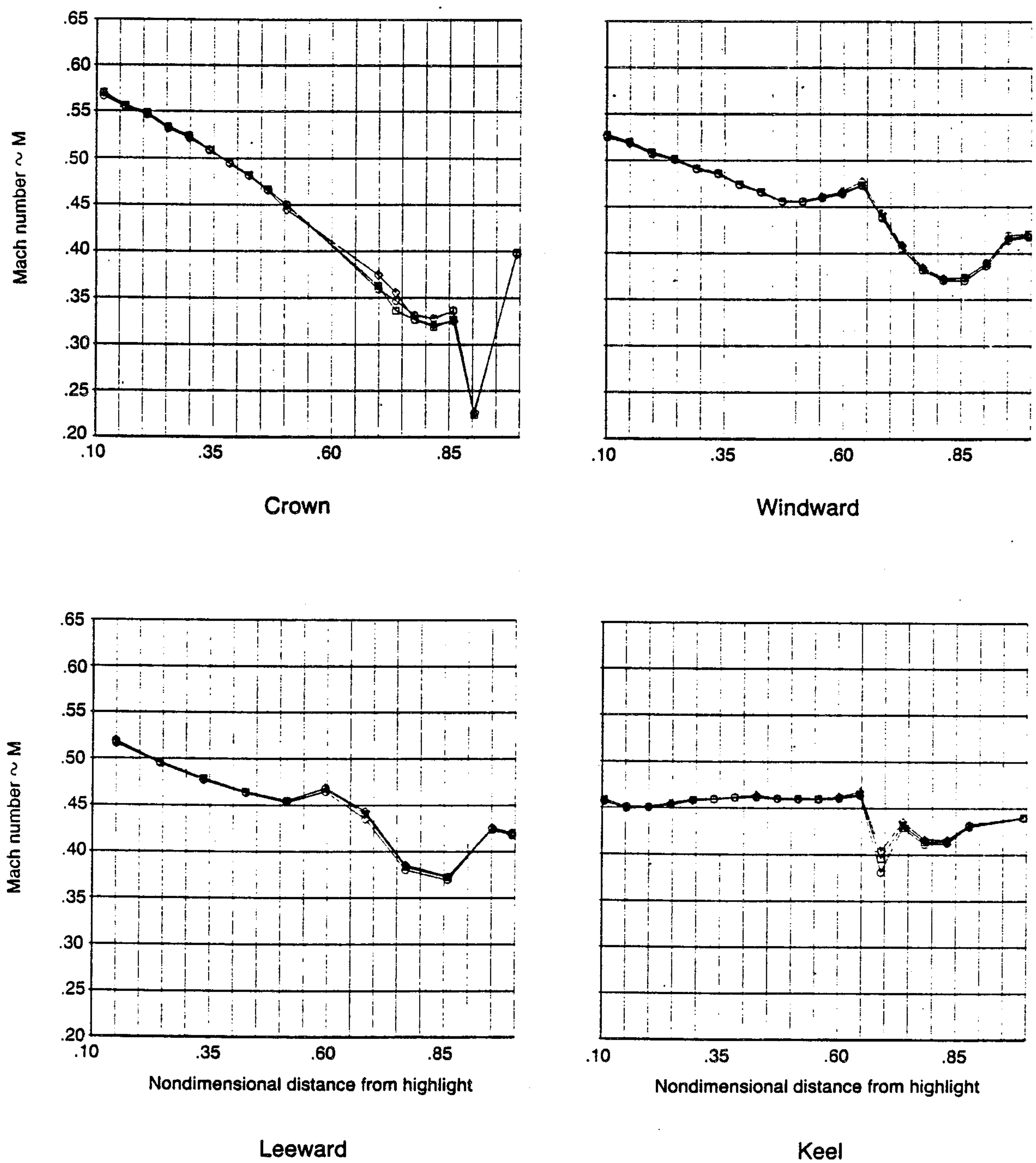

Figure 36. Shaft Fairing Comparison—Duct Surface Mach Number for Round, Small, and Large Shaft Fairings With 16.2% Diffuser, 3.7-Aspect-Ratio Duct, and Thin Lip (Continued)

f) Mach number .303
Angle of attack 0 deg
Airflow (takeoff) 26 lb/s (11.79 kg/s)

O Round shaft fairing
□ Small shaft fairing
◇ Large shaft fairing

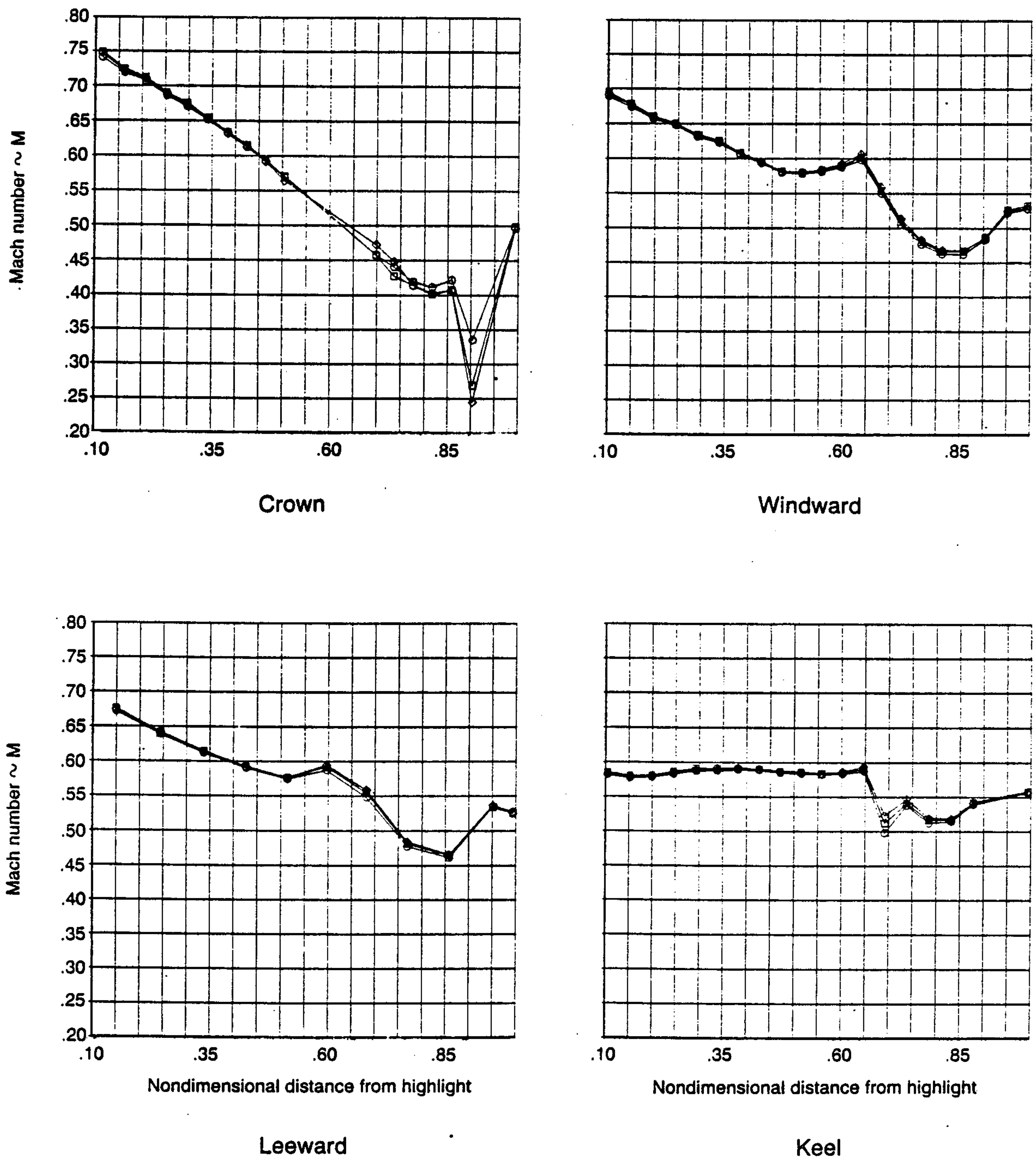

Figure 36. Shaft Fairing Comparison—Duct Surface Mach Number for Round, Small, and Large Shaft Fairings With 16.2% Diffuser, 3.7-Aspect-Ratio Duct, and Thin Lip (Continued)

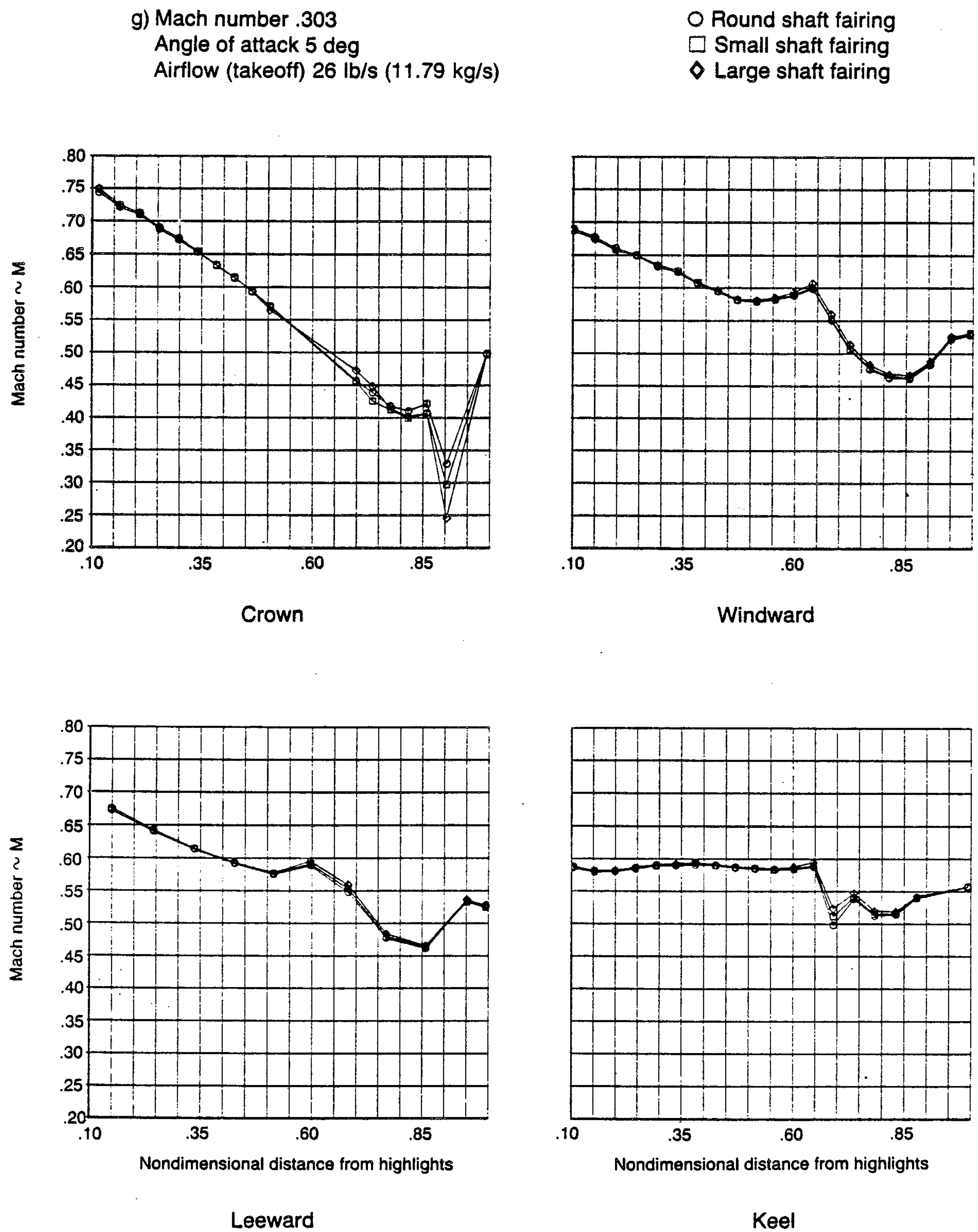

Figure 36. Shaft Fairing Comparison—Duct Surface Mach Number for Round, Small, and Large Shaft Fairings With 16.2% Diffuser, 3.7-Aspect-Ratio Duct, and Thin Lip (Concluded)

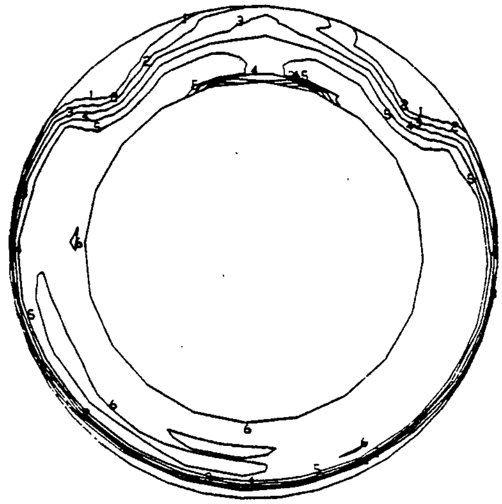

Small shaft fairing

a) Mach number 0.0
Angle of attack 0 deg
Airflow (takeoff) 22 lb/s (9.98 kg/s)

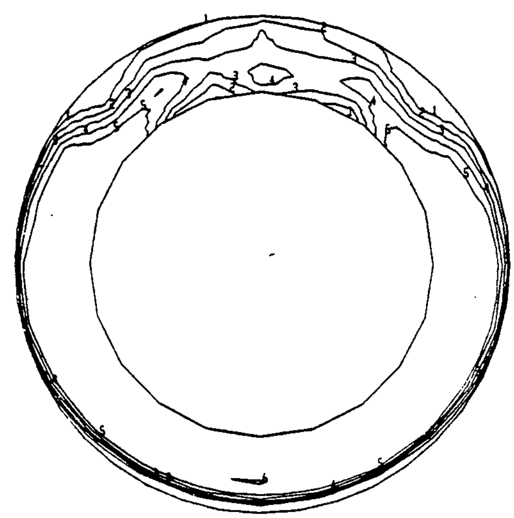

Round shaft fairing

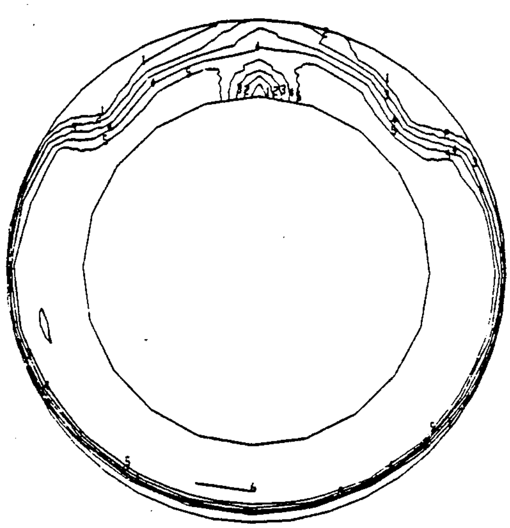

Large shaft fairing

	$P_t/P_{t_{ref}}$
1	.95
2	.96
3	.97
4	.98
5	.99
6	1.0

Figure 37. Shaft Fairing Comparison—Compressor Face Pressures for Round, Small, and Large Shaft Fairings With 16.2% Diffuser, 3.7-Aspect-Ratio Duct, and Thin Lip

b) Mach number .202
Angle of attack 0 deg
Airflow (takeoff) 22 lb/s (9.98 kg/s)

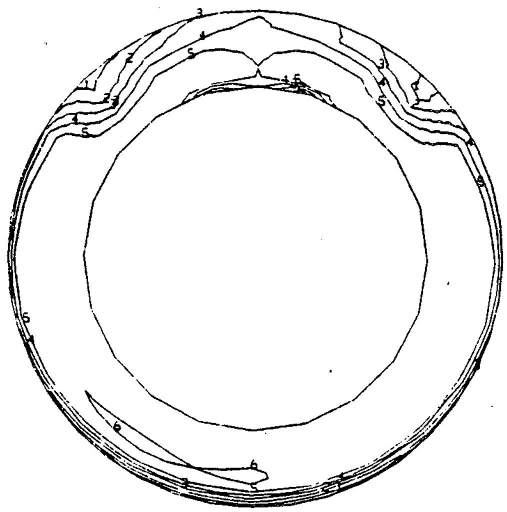

Small shaft fairing

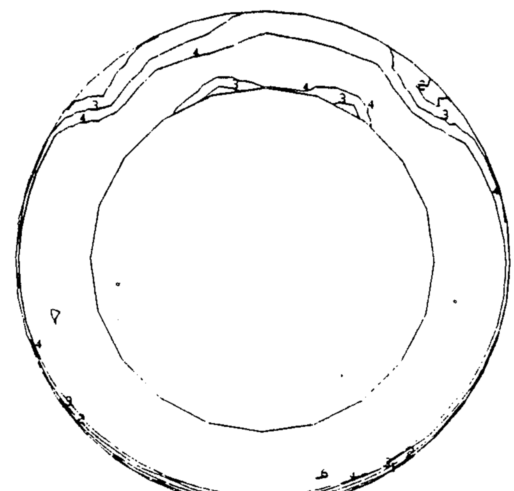

Round shaft fairing

Large shaft fairing

	$P_t/P_{t_{ref}}$
1	.95
2	.96
3	.97
4	.98
5	.99
6	1.0

Figure 37. Shaft Fairing Comparison—Compressor Face Pressures for Round, Small, and Large Shaft Fairings With 16.2% Diffuser, 3.7-Aspect-Ratio Duct, and Thin Lip (Continued)

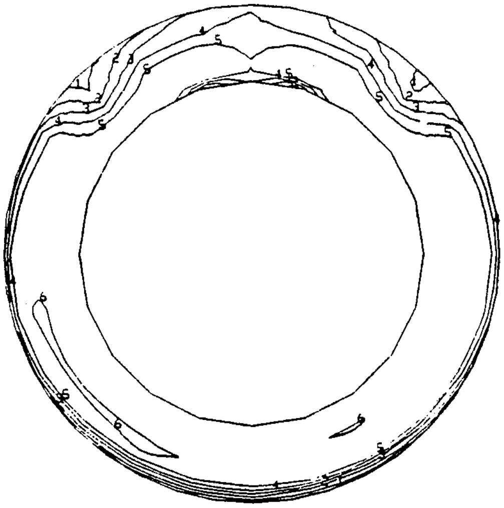

Small shaft fairing

c) Mach number .202
Angle of attack 10 deg
Airflow (takeoff) 22 lb/s (9.98 kg/s)

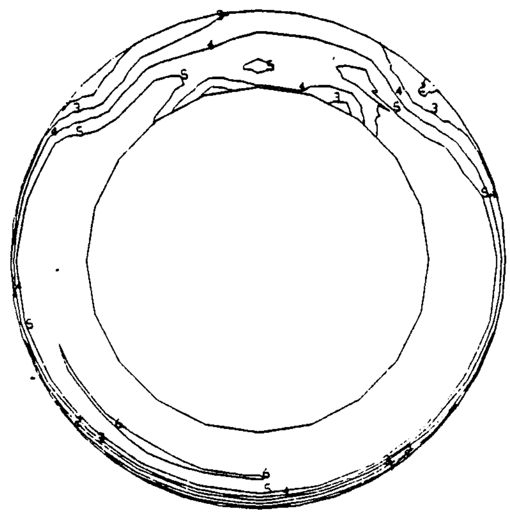

Round shaft fairing

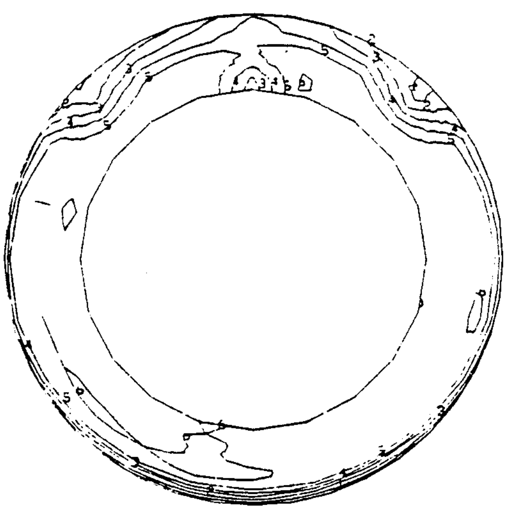

Large shaft fairing

	$P_t/P_{t_{ref}}$
1	.95
2	.96
3	.97
4	.98
5	.99
6	1.0

Figure 37. Shaft Fairing Comparison—Compressor Face Pressures for Round, Small, and Large Shaft Fairings With 16.2% Diffuser, 3.7-Aspect-Ratio Duct, and Thin Lip (Continued)

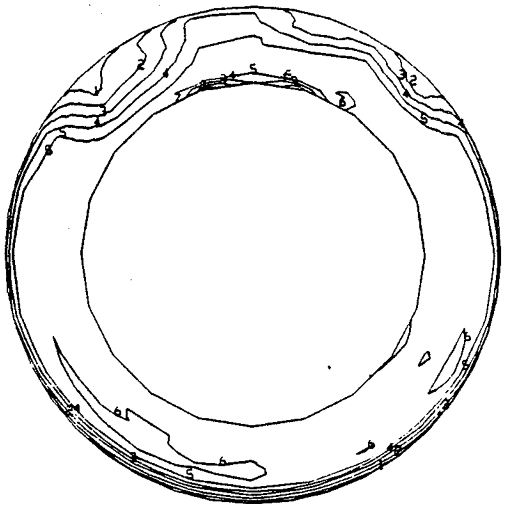

Small shaft fairing

d) Mach number .204
Angle of yaw 15 deg
Airflow (takeoff) 22 lb/s (9.98 kg/s)

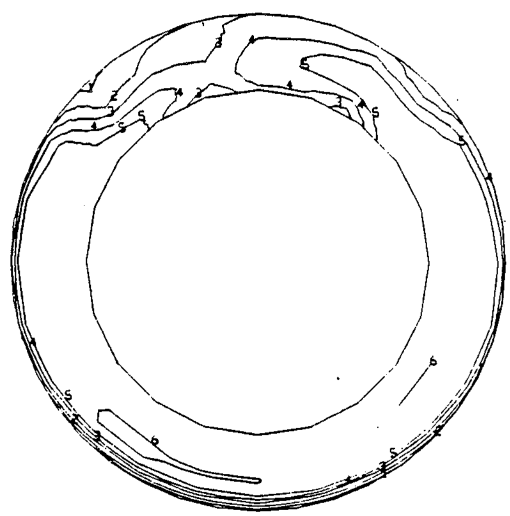

Round shaft fairing

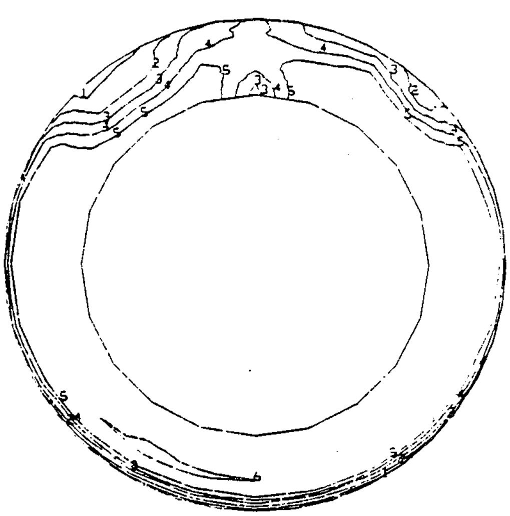

Large shaft fairing

	$P_t/P_{t_{ref}}$
1	.95
2	.96
3	.97
4	.98
5	.99
6	1.0

Figure 37. Shaft Fairing Comparison—Compressor Face Pressures for Round, Small, and Large Shaft Fairings With 16.2% Diffuser, 3.7-Aspect-Ratio Duct, and Thin Lip (Continued)

e) Mach number .202
Angle of attack 15 deg
Airflow (takeoff) 22 lb/s (9.98 kg/s)

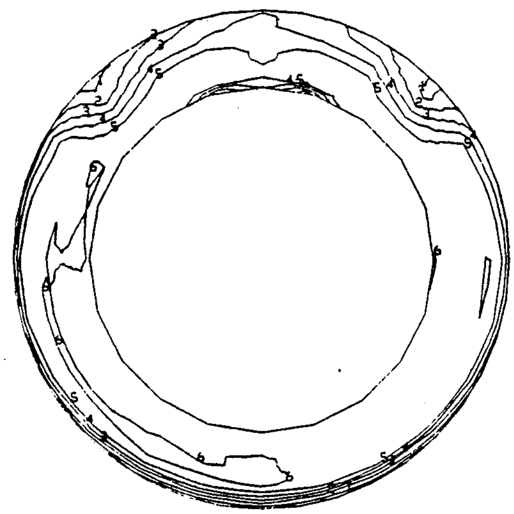

Small shaft fairing

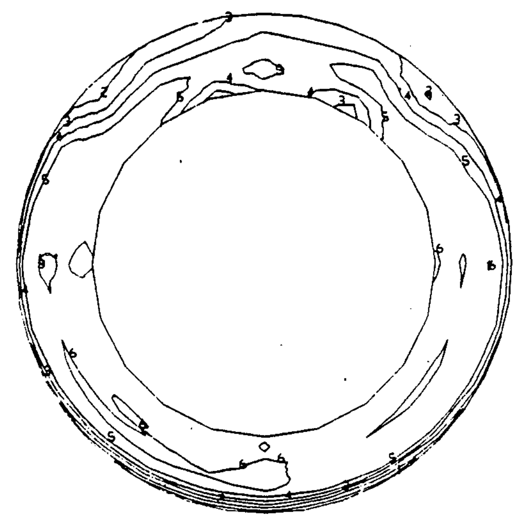

Round shaft fairing

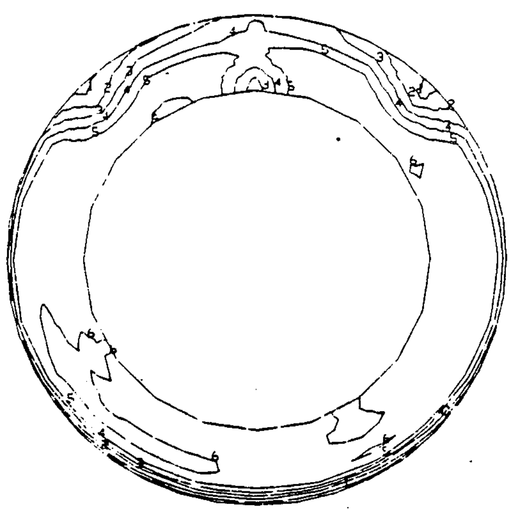

Large shaft fairing

	$P_t/P_{t_{ref}}$
1	.95
2	.96
3	.97
4	.98
5	.99
6	1.0

Figure 37. Shaft Fairing Comparison—Compressor Face Pressures for Round, Small, and Large Shaft Fairings With 16.2% Diffuser, 3.7-Aspect-Ratio Duct, and Thin Lip (Continued)

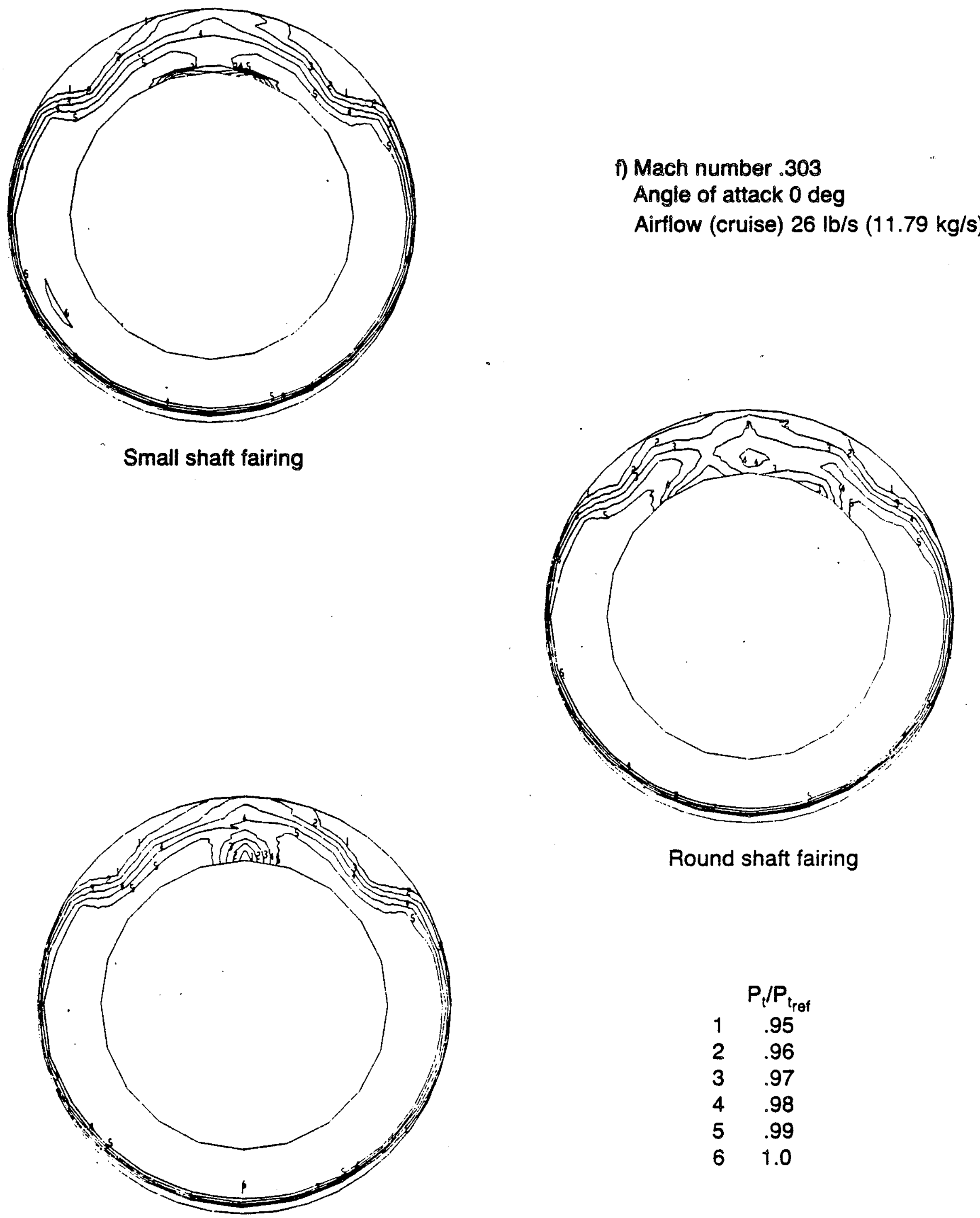

Figure 37. Shaft Fairing Comparison—Compressor Face Pressures for Round, Small, and Large Shaft Fairings With 16.2% Diffuser, 3.7-Aspect-Ratio Duct, and Thin Lip (Continued)

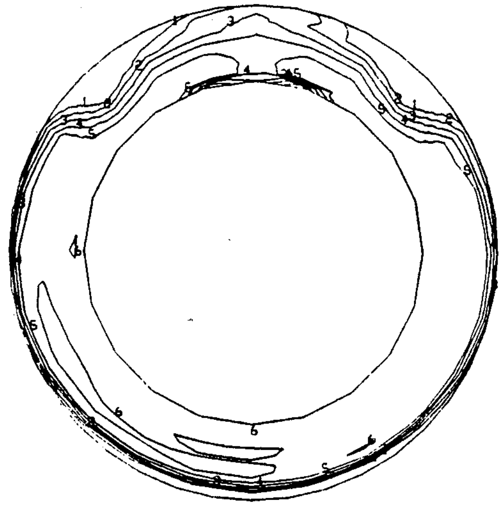

Small shaft fairing

g) Mach number .303
Angle of attack 5 deg
Airflow (cruise) 26 lb/s (11.79 kg/s)

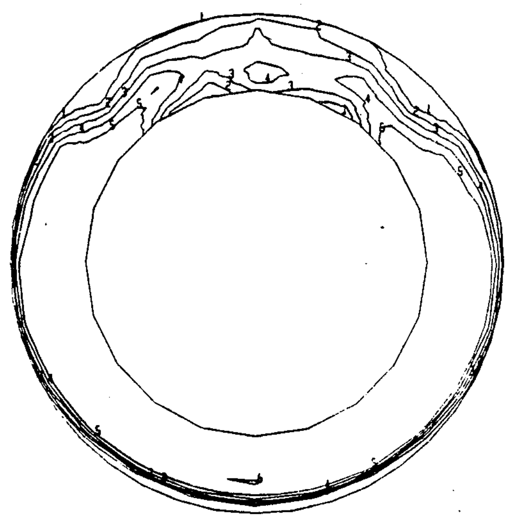

Round shaft fairing

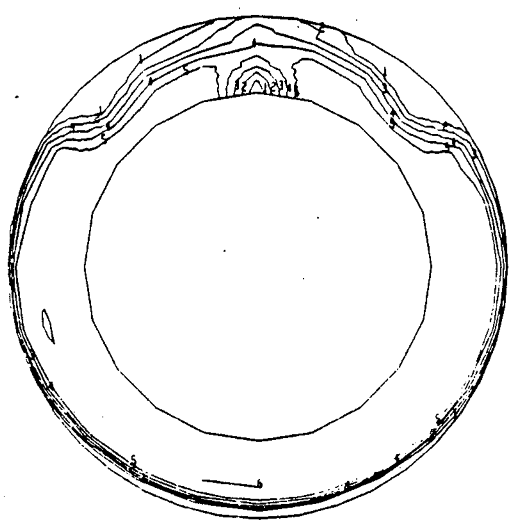

Large shaft fairing

	$P_t/P_{t_{ref}}$
1	.95
2	.96
3	.97
4	.98
5	.99
6	1.0

Figure 37. Shaft Fairing Comparison—Compressor Face Pressures for Round, Small, and Large Shaft Fairings With 16.2% Diffuser, 3.7-Aspect-Ratio Duct, and Thin Lip (Concluded)

C-2

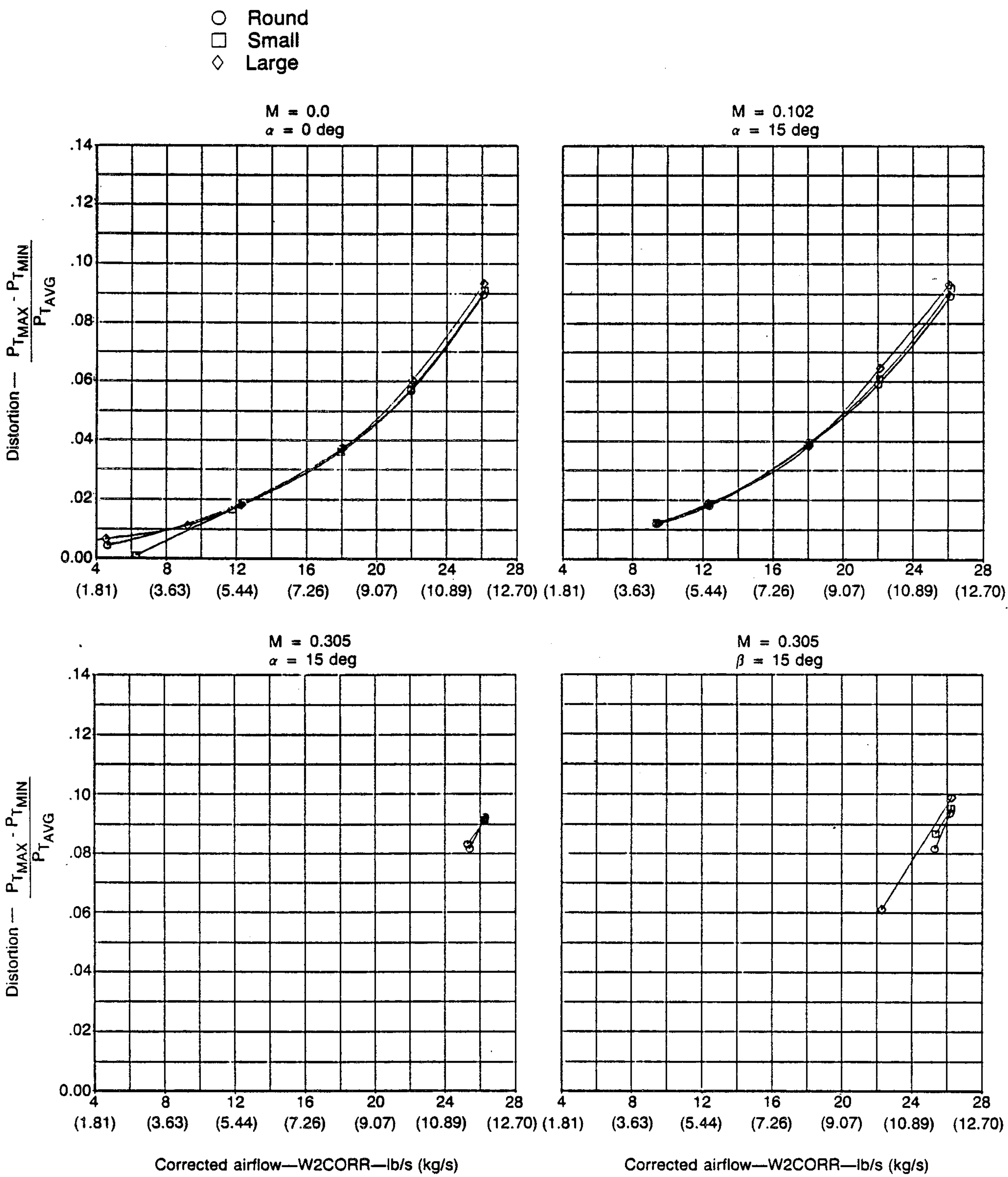

Figure 38. Compressor Face Distortion Comparison for Round, Small, and Large Shaft Fairings

a) Mach number .102
Angle of attack 0 deg
Angle of yaw 0 deg
Airflow 16.9 lb/s (7.67 kg/s)

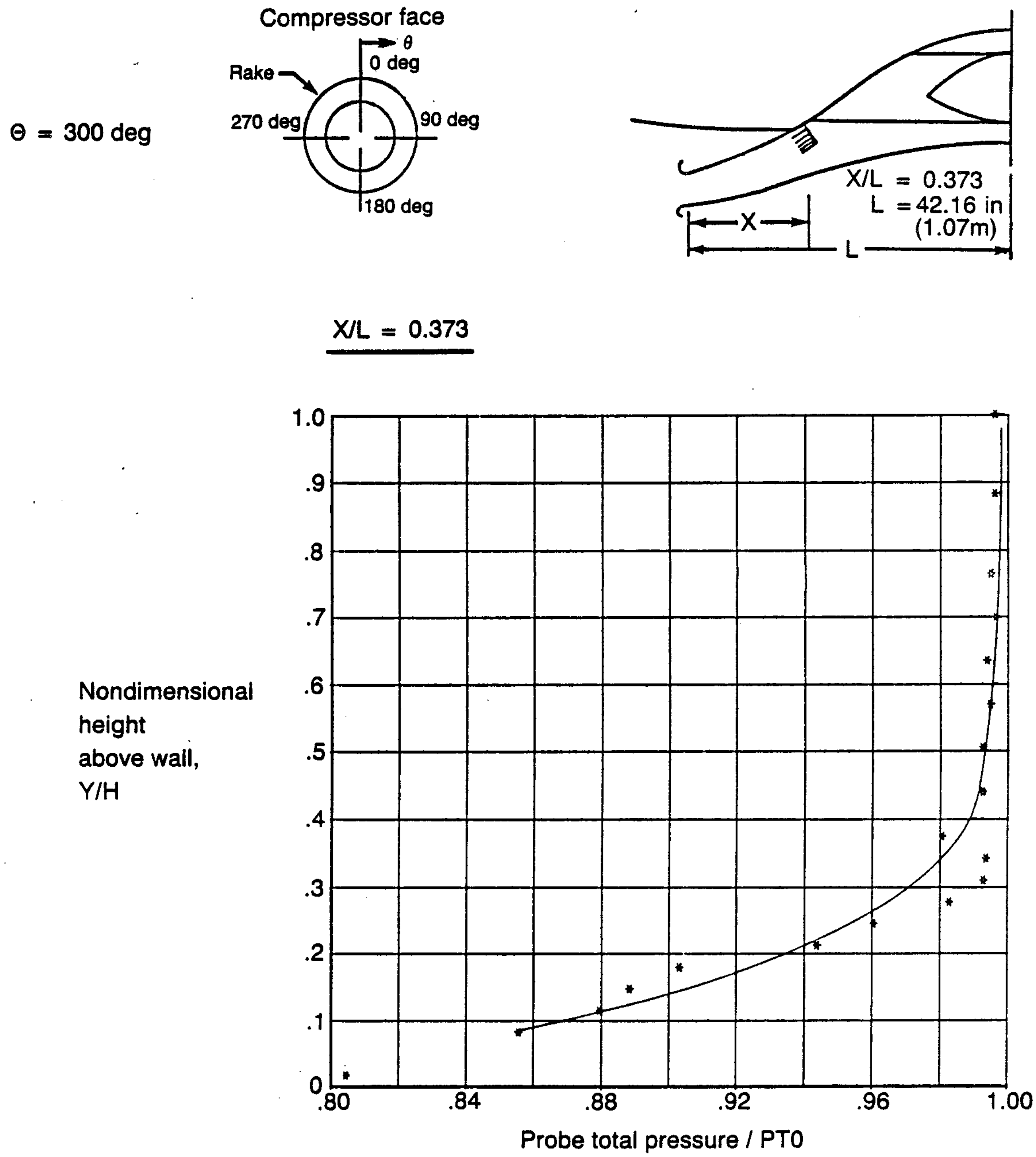

Figure 39. Diffuser Boundary-Layer Profiles for 16.2% Diffuser and 3.7-Aspect-Ratio Duct With Thin Lip and Large Shaft Fairing

b) Mach number .102
Angle of attack 0 deg
Angle of yaw 0 deg
Airflow 16.9 lb/s (7.67 kg/s)

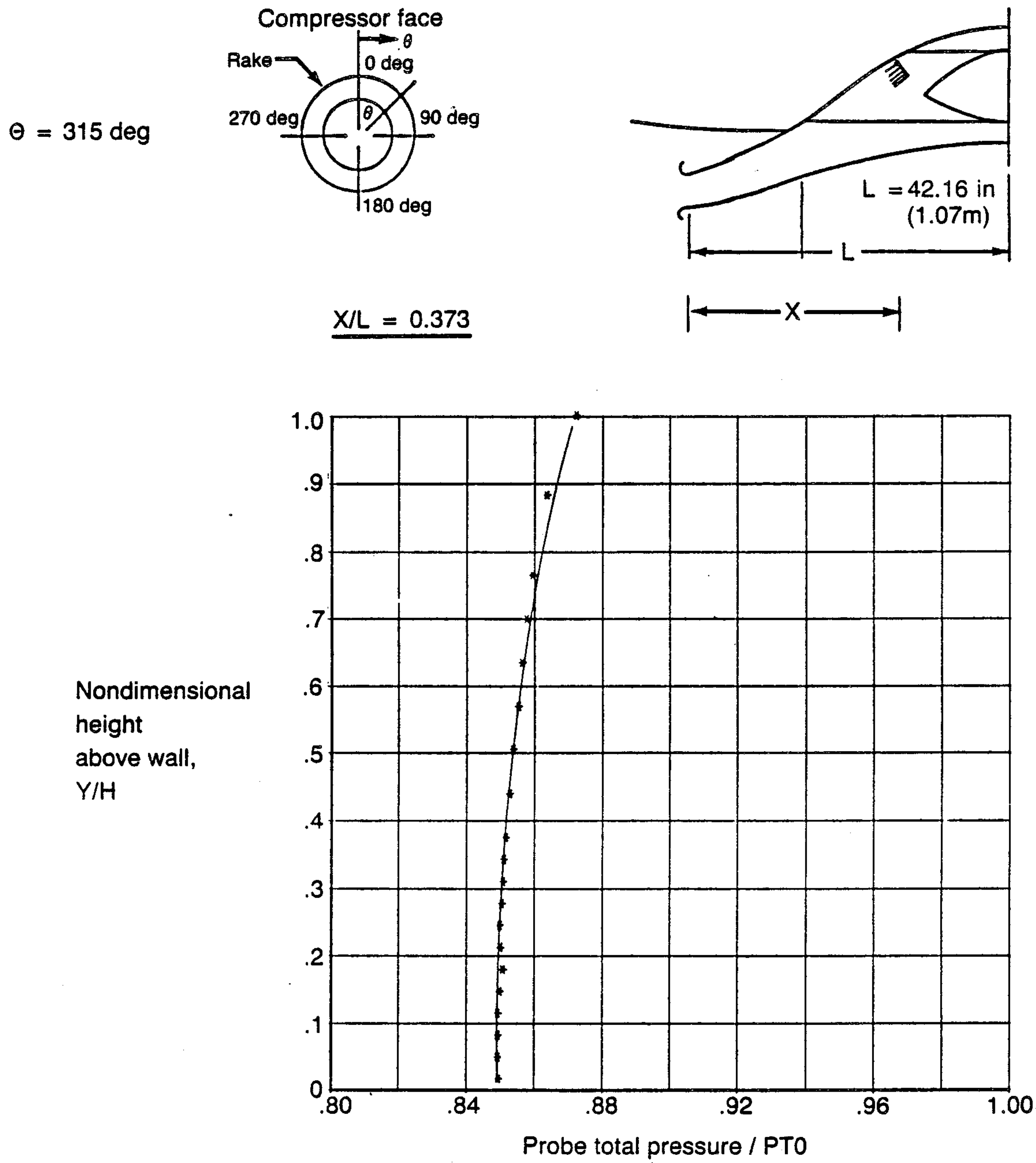

Figure 39. Diffuser Boundary-Layer Profiles for 16.2% Diffuser and 3.7-Aspect-Ratio Duct With Thin Lip and Large Shaft Fairing (Continued)

c) Mach number .102
Angle of attack 0 deg
Angle of yaw 15 deg
Airflow 18.7 lb/s (8.48 kg/s)

Θ = 300 deg

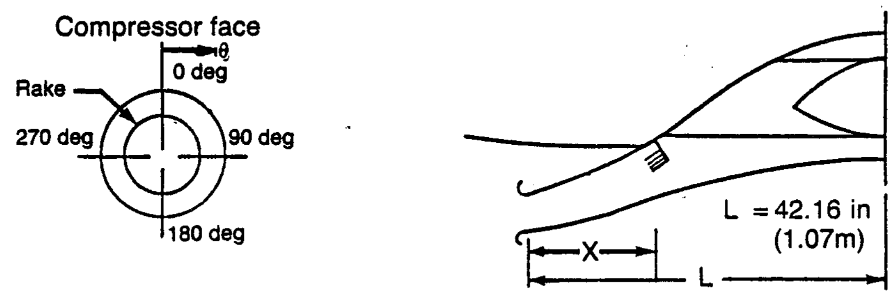

X/L = 0.373

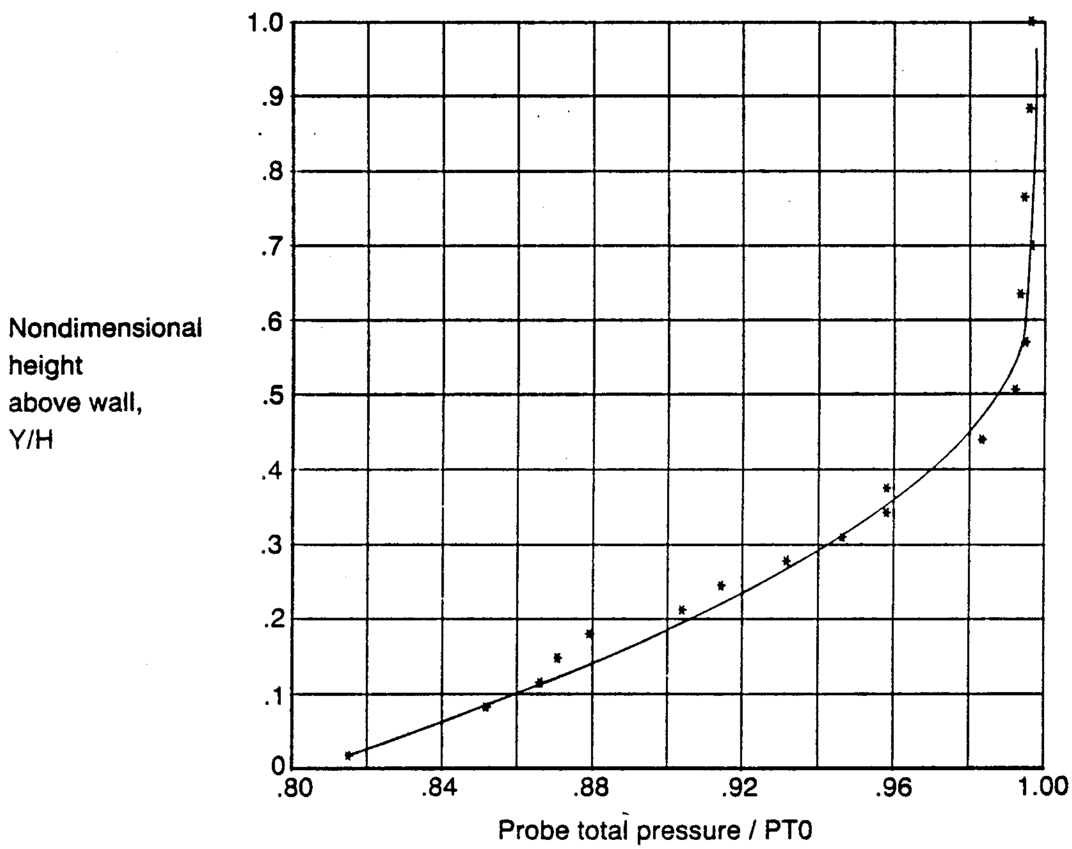

Figure 39. Diffuser Boundary-Layer Profiles for 16.2% Diffuser and 3.7-Aspect-Ratio Duct With Thin Lip and Large Shaft Fairing (Continued)

d) Mach number .102
Angle of attack 0 deg
Angle of yaw 15 deg
Airflow 18.7 lb/s (8.48 kg/s)

Θ = 315 deg

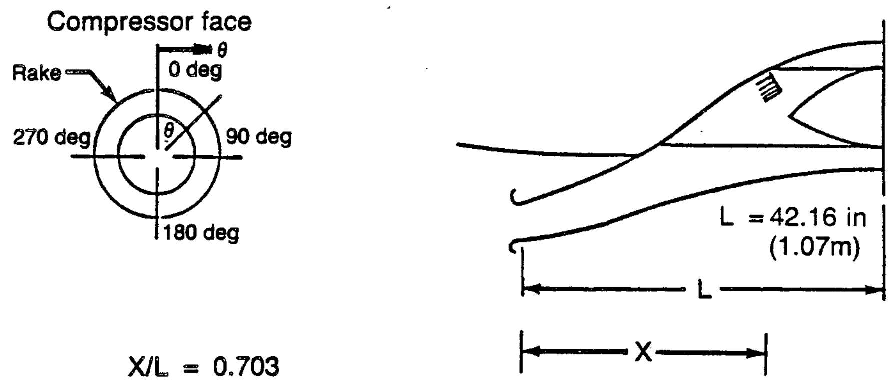

X/L = 0.703

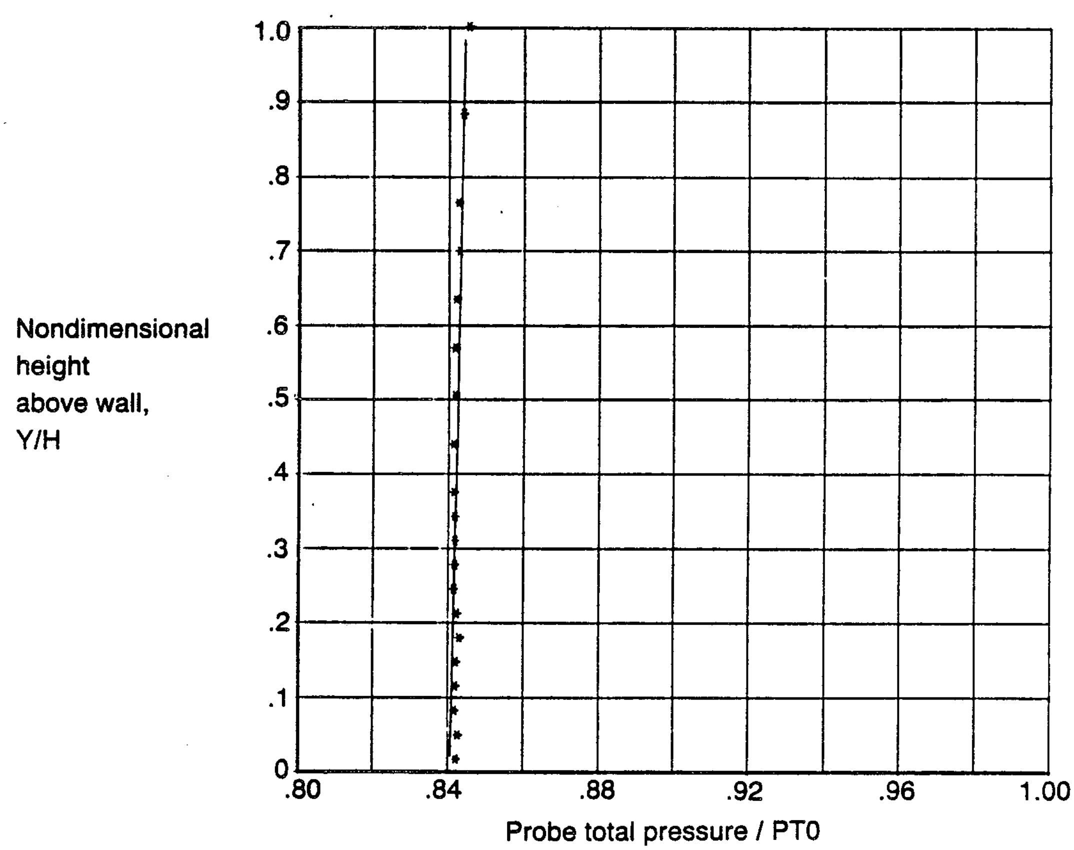

Figure 39. Diffuser Boundary-Layer Profiles for 16.2% Diffuser and 3.7-Aspect-Ratio Duct With Thin Lip and Large Shaft Fairing (Continued)

e) Mach number .203
Angle of attack 0 deg
Angle of yaw 0 deg
Airflow 18.5 lb/s (8.39 kg/s)

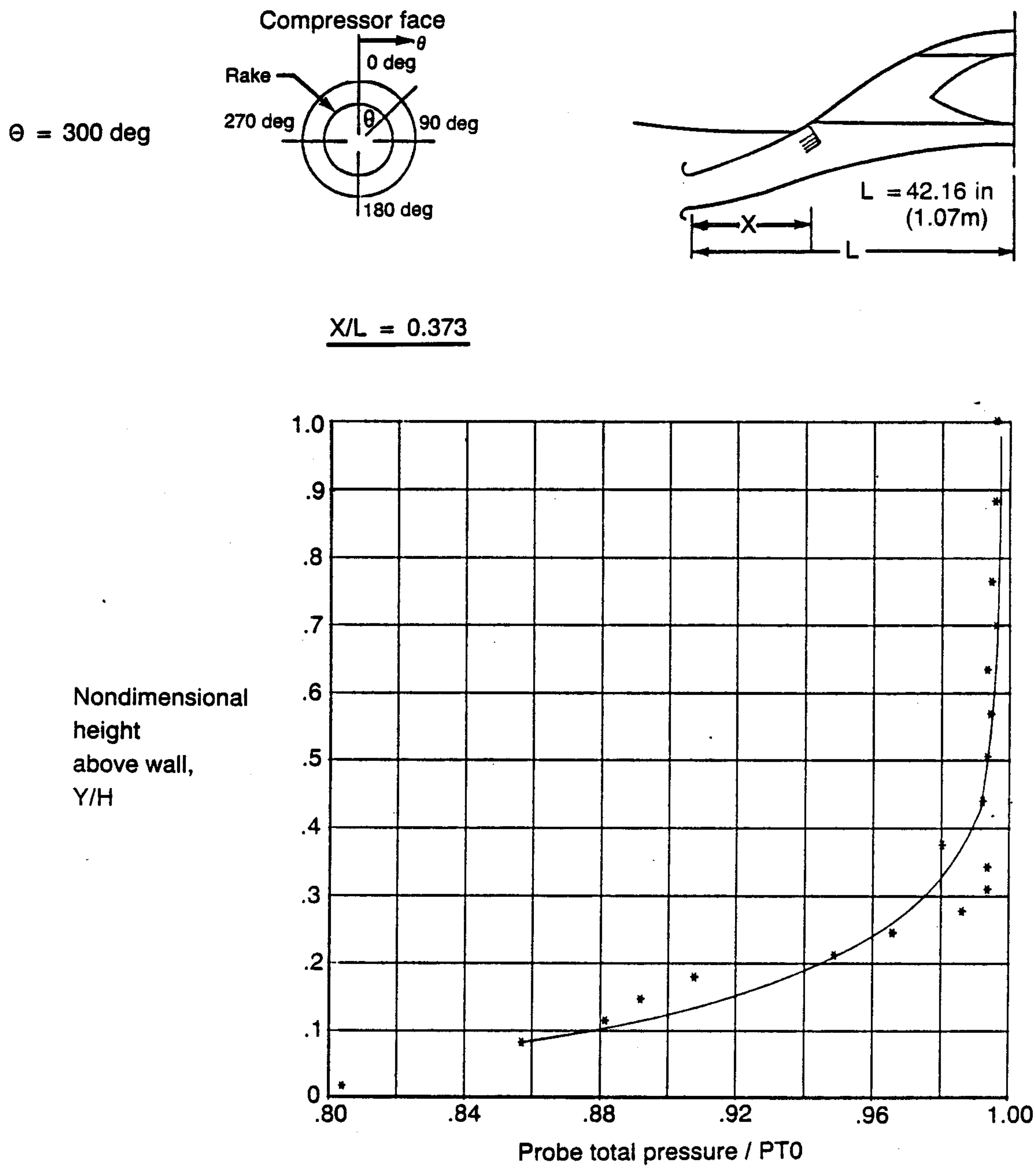

Figure 39. Diffuser Boundary-Layer Profiles for 16.2% Diffuser and 3.7-Aspect-Ratio Duct With Thin Lip and Large Shaft Fairing (Continued)

f) Mach number .203
Angle of attack 0 deg
Angle of yaw 0 deg
Airflow 18.5 lb/s (8.39 kg/s)

Θ = 315 deg

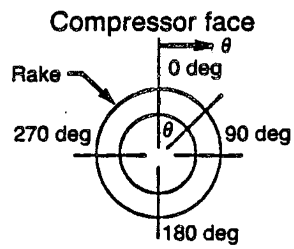

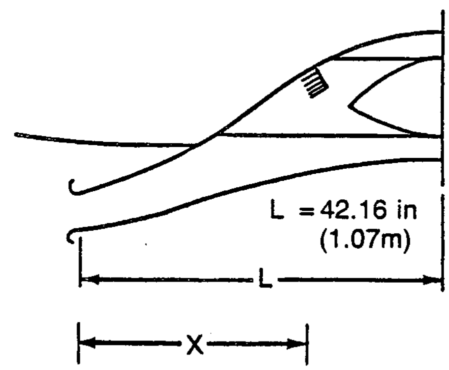

X/L = 0.703

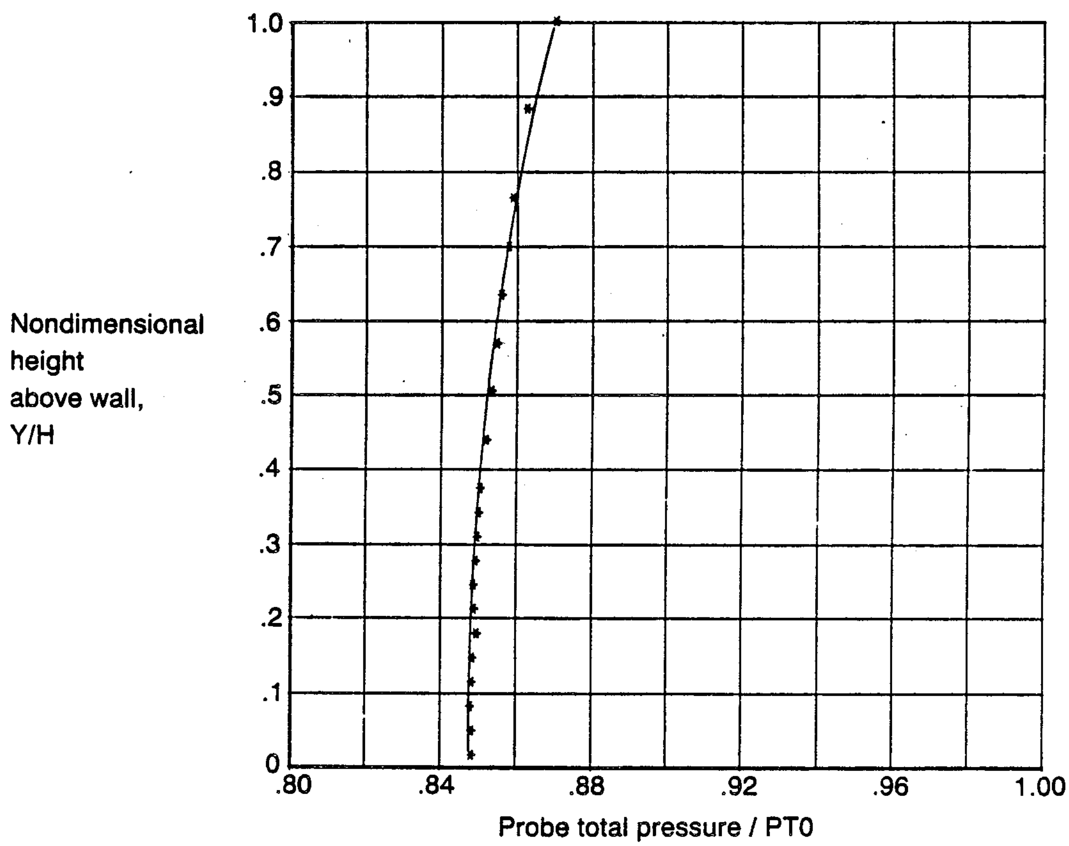

Figure 39. Diffuser Boundary-Layer Profiles for 16.2% Diffuser and 3.7-Aspect-Ratio Duct With Thin Lip and Large Shaft Fairing (Continued)

g) Mach number .203
Angle of attack 0 deg
Angle of yaw 15 deg
Airflow 17.0 lb/s (7.71 kg/s)

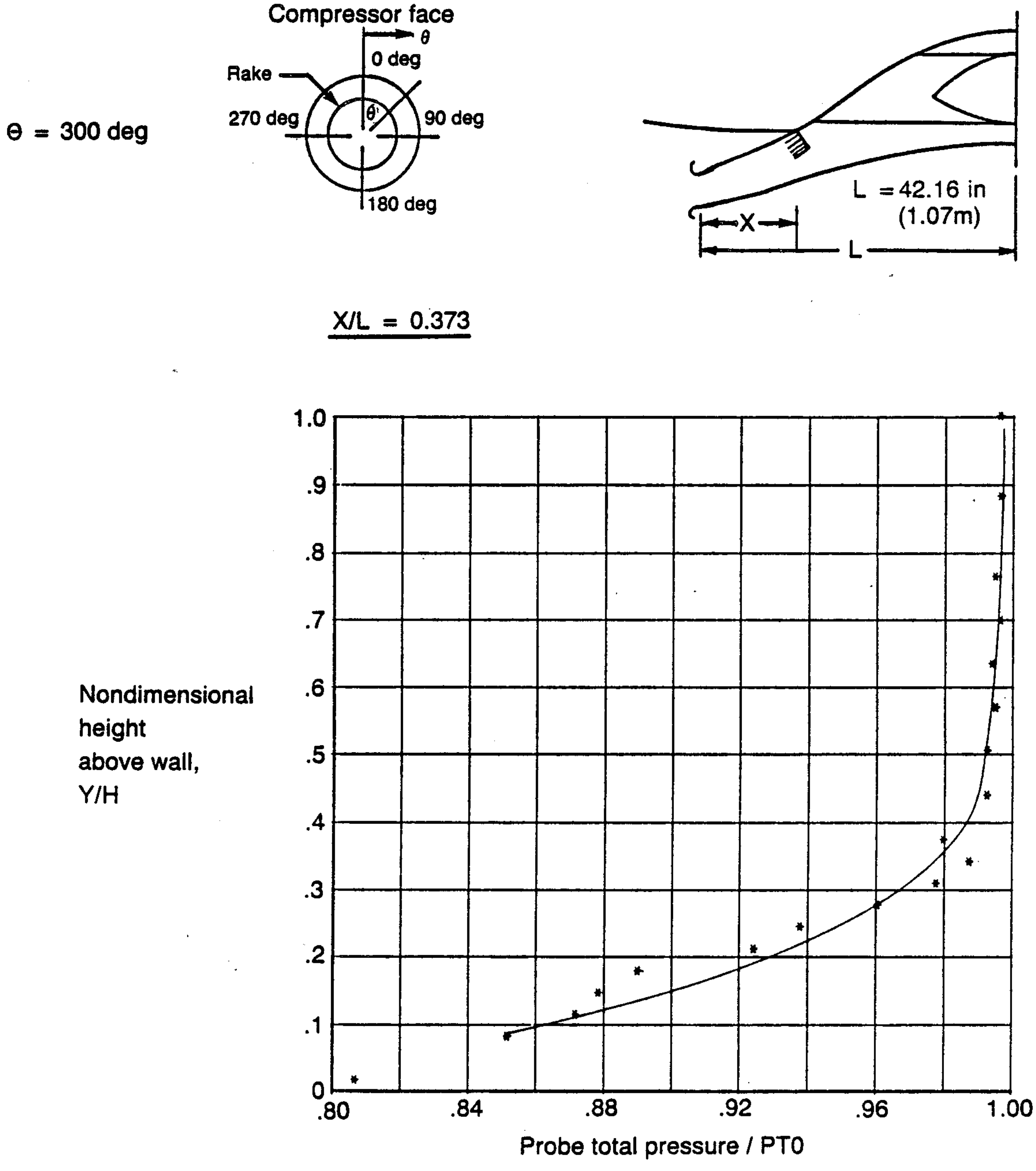

Figure 39. Diffuser Boundary-Layer Profiles for 16.2% Diffuser and 3.7-Aspect-Ratio Duct With Thin Lip and Large Shaft Fairing (Continued)

h) Mach number .203
Angle of attack 0 deg
Angle of yaw 15 deg
Airflow 17.0 lb/s (7.71 kg/s)

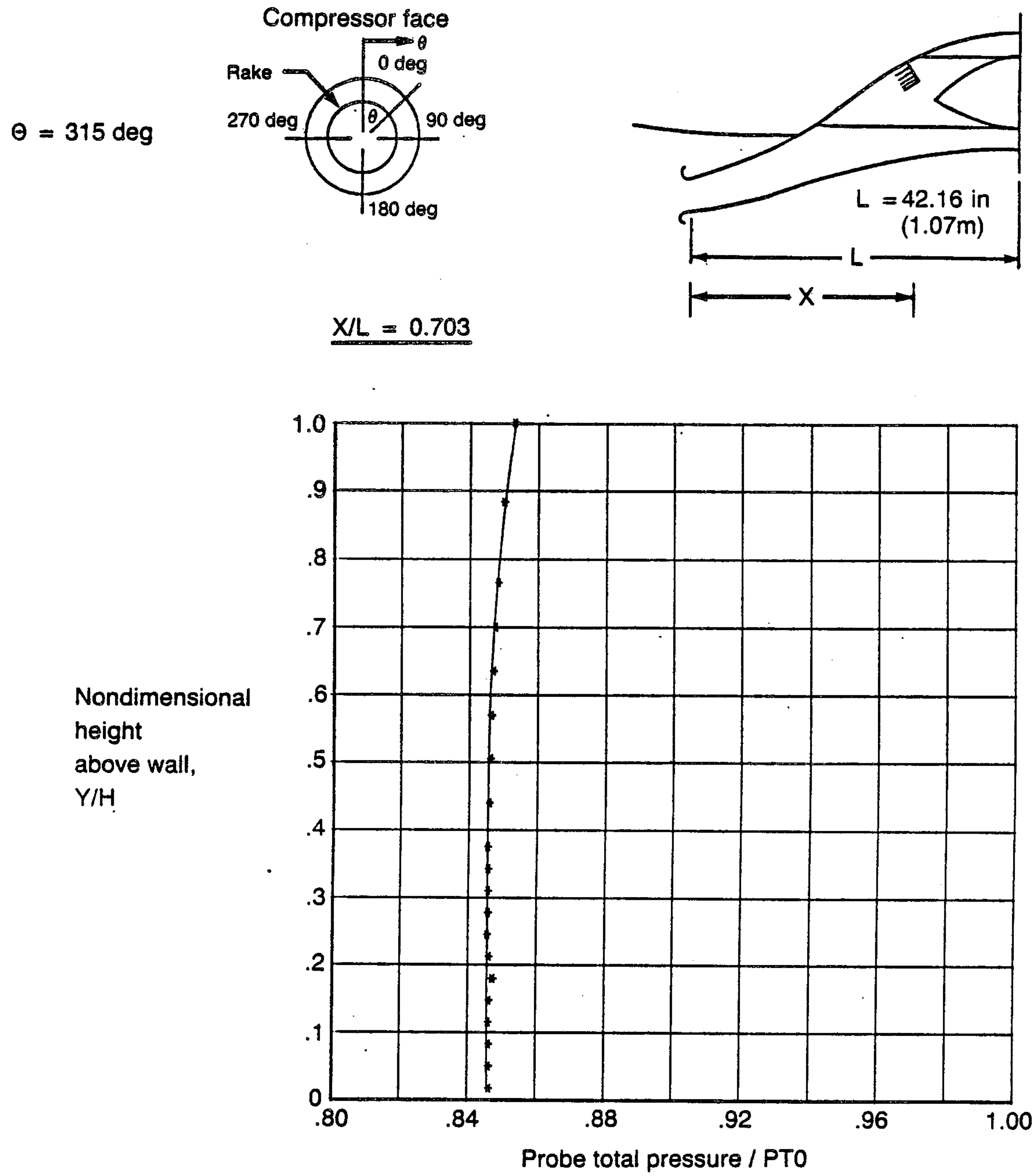

Figure 39. Diffuser Boundary-Layer Profiles for 16.2% Diffuser and 3.7-Aspect-Ratio Duct With Thin Lip and Large Shaft Fairing (Concluded)

a) Mach number .353
Angle of attack 0 deg
Angle of yaw 0 deg
Airflow 23.2 lb/s (10.52 kg/s)

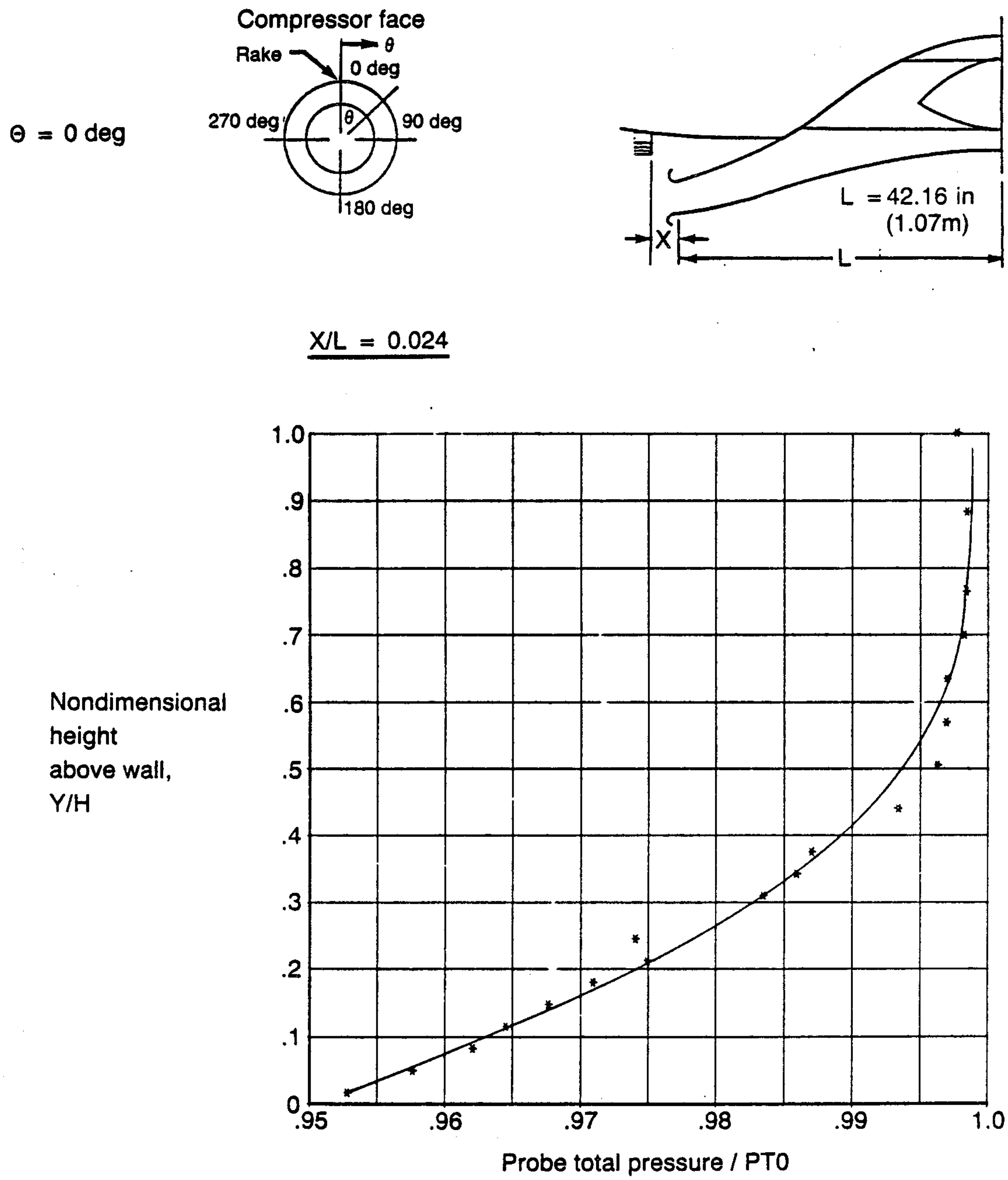

Figure 40. Spinner Boundary-Layer Profile for 10% Diffuser and 3.7-Aspect-Ratio Duct With Thin Lip and Small Shaft Fairing

b) Mach number .304
Angle of attack 0 deg
Angle of yaw 0 deg
Airflow 20.81 lb/s (9.44 kg/s)

Θ = 0 deg

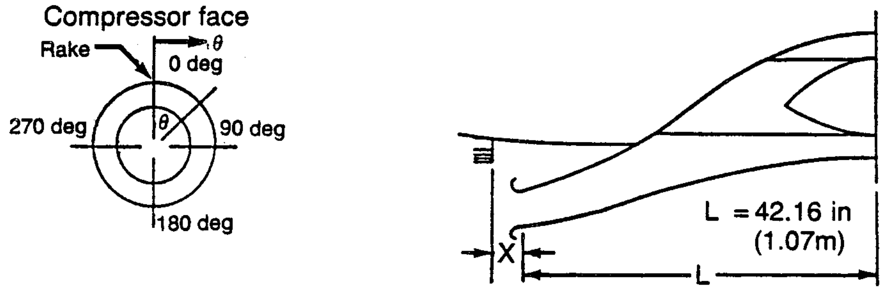

X/L = 0.024

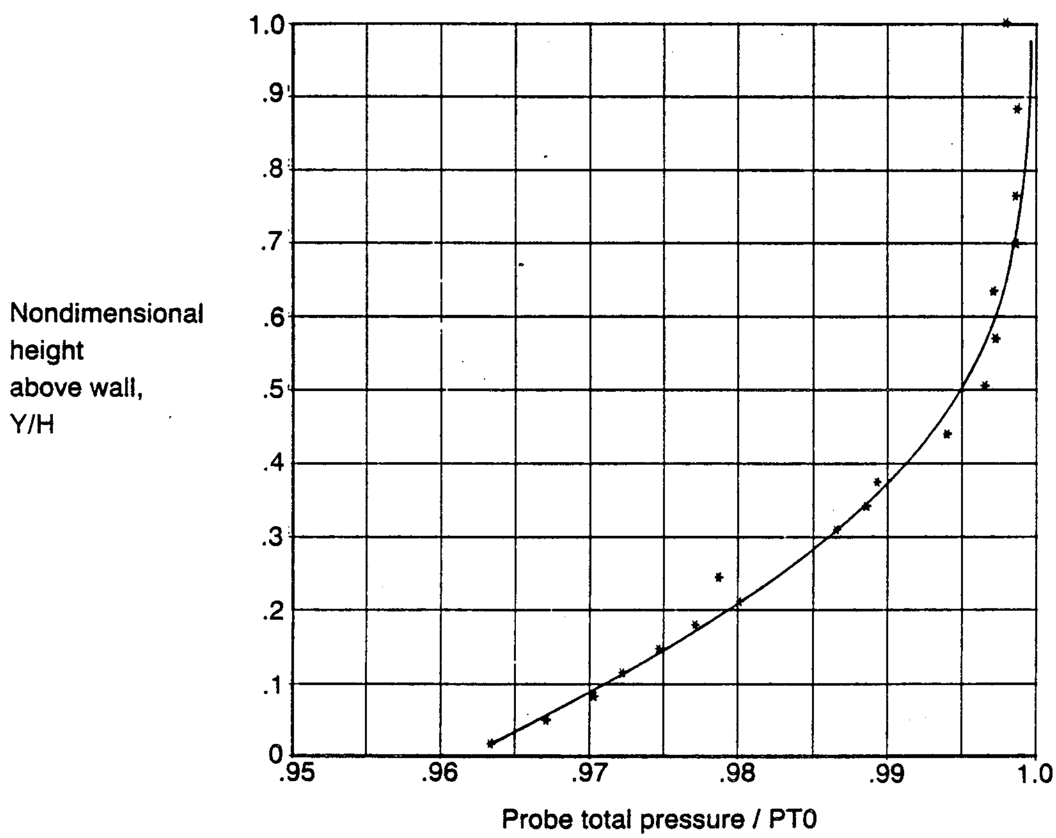

Figure 40. Spinner Boundary-Layer Profile for 10% Diffuser and 3.7-Aspect-Ratio Duct With Thin Lip and Small Shaft Fairing (Continued)

c) Mach number .203
Angle of attack 0 deg
Angle of yaw 0 deg
Airflow 14.9 lb/s (6.76 kg/s)

Θ = 0 deg

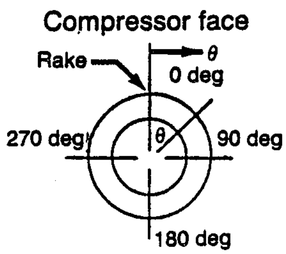

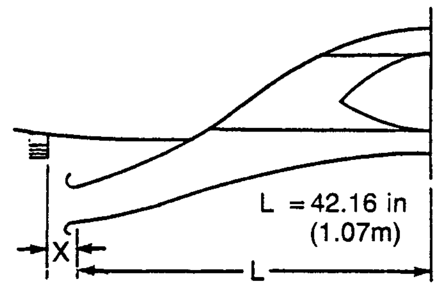

X/L = 0.024

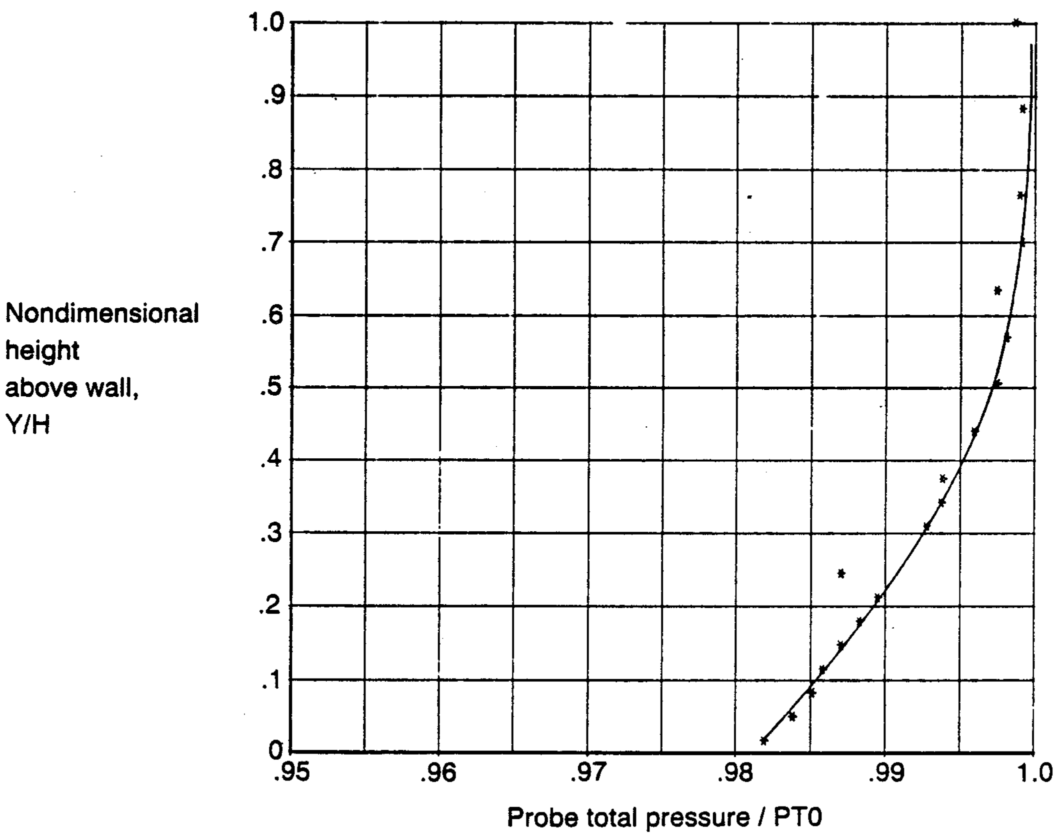

Figure 40. Spinner Boundary-Layer Profile for 10% Diffuser and 3.7-Aspect-Ratio Duct With Thin Lip and Small Shaft Fairing (Continued)

d) Mach number .101
Angle of attack 0 deg
Angle of yaw 0 deg
Airflow 7.6 lb/s (3.45 kg/s)

Θ = 0 deg

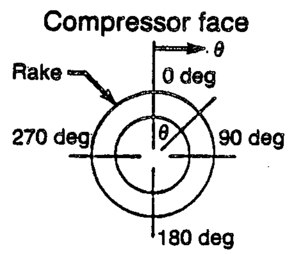

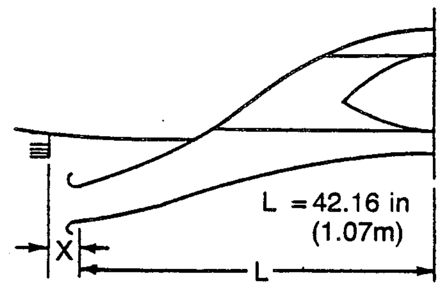

X/L = 0.024

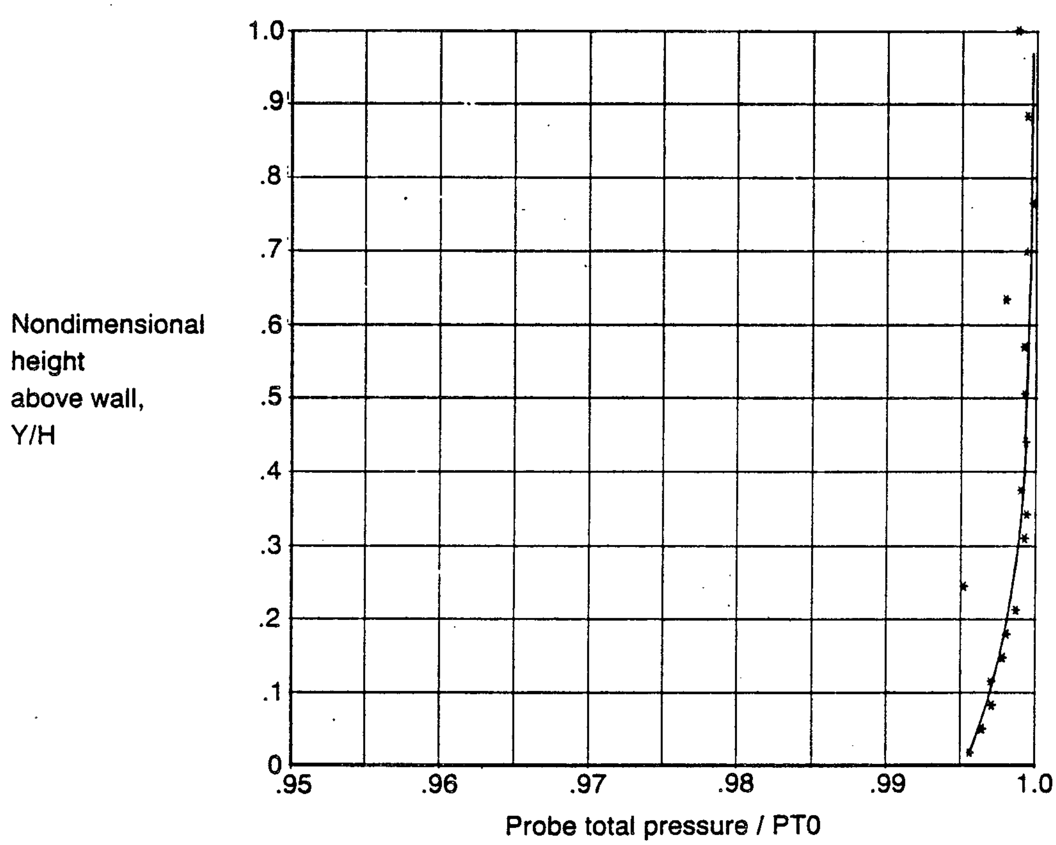

Figure 40. Spinner Boundary-Layer Profile for 10% Diffuser and 3.7-Aspect-Ratio Duct With Thin Lip and Small Shaft Fairing (Concluded)

APPENDIX A

PRECEDING PAGE BLANK NOT FILMED

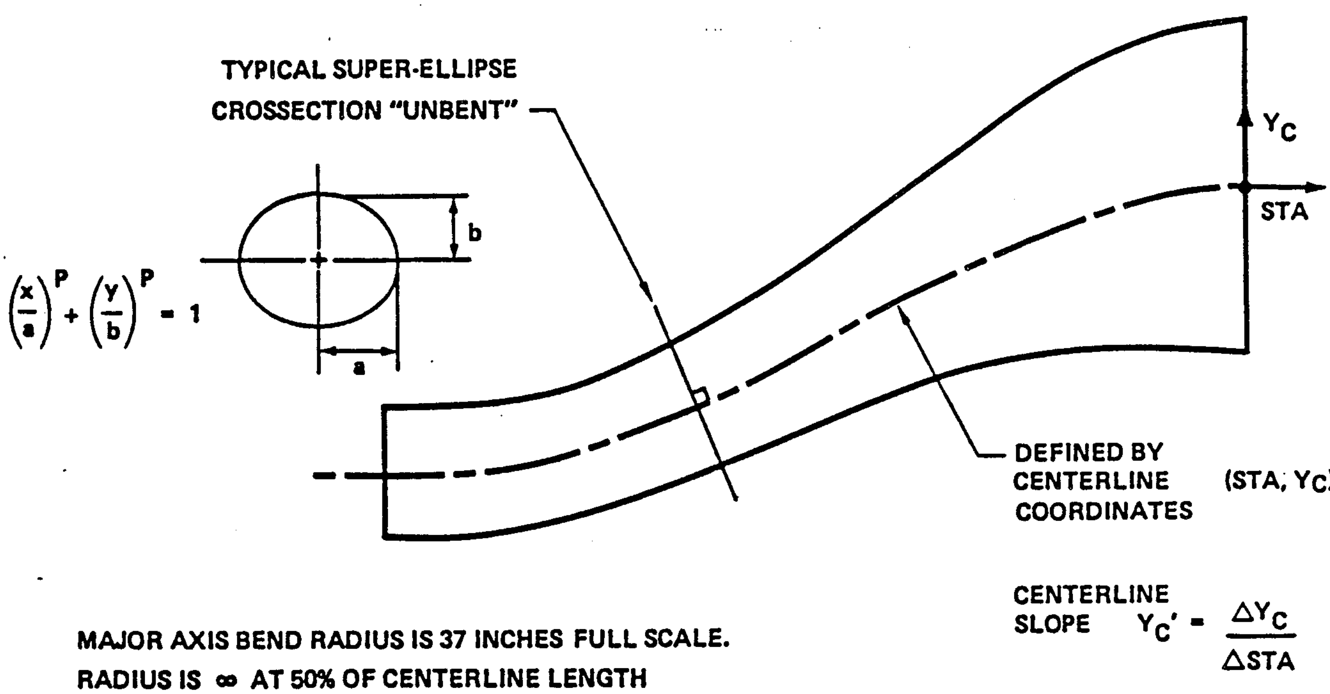

TYPICAL DUCT SIDE VIEW

Figure A-1. Sketch of Duct for Geometry Definition

ORIGINAL PAGE IS
OF POOR QUALITY

Table A-1. High Aspect Ratio S-Duct—16.2% Diffusion

THROAT TO COMPRESSOR FACE — **Dimensions in Inches - Full Scale**

CENTERLINE COORDINATES			CENTERLINE SLOPES			SUPER ELLIPSE EQUATION VARIABLES			CROSS SECTIONAL
STA	X_C	Y_C	X_C'	Y_C'	Z_C'	A	B	P	AREA
-68.0000	0.0000	-22.4000	0.0000	-0.0075	0.0000	16.0000	4.2882	3.2069	245.5827
-66.8341	0.0000	-22.4790	0.0000	-0.0483	0.0000	15.9974	4.2899	3.2053	245.6194
-65.6664	0.0000	-22.5131	0.0000	-0.0103	0.0000	15.9896	4.2951	3.2005	245.7200
-64.4980	0.0000	-22.5035	0.0000	0.0264	0.0000	15.9773	4.3035	3.1927	245.9059
-63.3300	0.0000	-22.4520	0.0000	0.0617	0.0000	15.9599	4.3152	3.1819	246.1507
-62.1660	0.0000	-22.3602	0.0000	0.0956	0.0000	15.9379	4.3301	3.1603	246.4598
-61.0049	0.0000	-22.2302	0.0000	0.1281	0.0000	15.9111	4.3460	3.1520	246.8306
-59.8403	0.0000	-22.0039	0.0000	0.1592	0.0000	15.8798	4.3691	3.1340	247.2612
-58.6973	0.0000	-21.8634	0.0000	0.1869	0.0000	15.8439	4.3932	3.1140	247.7404
-57.5522	0.0000	-21.6309	0.0000	0.2171	0.0000	15.8034	4.4203	3.0928	248.2902
-56.4137	0.0000	-21.3603	0.0000	0.2439	0.0000	15.7585	4.4504	3.0686	248.8843
-55.2820	0.0000	-21.0778	0.0000	0.2693	0.0000	15.7090	4.4835	3.0420	249.5280
-54.1572	0.0000	-20.7613	0.0000	0.2933	0.0000	15.6551	4.5196	3.0100	250.2216
-53.0395	0.0000	-20.4207	0.0000	0.3160	0.0000	15.5966	4.5587	2.9892	250.9000
-51.9260	0.0000	-20.0578	0.0000	0.3373	0.0000	15.5338	4.6008	2.9601	251.7443
-50.8251	0.0000	-19.6744	0.0000	0.3573	0.0000	15.4664	4.6460	2.9302	252.5699
-49.7281	0.0000	-19.2721	0.0000	0.3760	0.0000	15.3945	4.6943	2.9006	253.4339
-48.6376	0.0000	-18.8525	0.0000	0.3934	0.0000	15.3180	4.7457	2.8690	254.3320
-47.5533	0.0000	-18.4170	0.0000	0.4096	0.0000	15.2369	4.8002	2.8379	255.2620
-46.4749	0.0000	-17.9671	0.0000	0.4246	0.0000	15.1510	4.8570	2.8075	256.2200
-45.4021	0.0000	-17.5041	0.0000	0.4364	0.0000	15.0605	4.9166	2.7762	257.2007
-44.3345	0.0000	-17.0293	0.0000	0.4510	0.0000	14.9652	4.9827	2.7440	258.2023
-43.2717	0.0000	-16.5438	0.0000	0.4624	0.0000	14.8652	5.0561	2.7134	259.2264
-42.2133	0.0000	-16.0488	0.0000	0.4720	0.0000	14.7608	5.1209	2.6824	260.2757
-41.1589	0.0000	-15.5454	0.0000	0.4820	0.0000	14.6521	5.1953	2.6509	261.3528
-40.1080	0.0000	-15.0345	0.0000	0.4941	0.0000	14.5392	5.2734	2.6210	262.4607
-39.0602	0.0000	-14.5173	0.0000	0.4971	0.0000	14.4223	5.3553	2.5910	263.6019
-38.0152	0.0000	-13.9946	0.0000	0.5030	0.0000	14.3015	5.4411	2.5607	264.7742
-36.9724	0.0000	-13.4675	0.0000	0.5079	0.0000	14.1762	5.5307	2.5321	265.9561
-35.9315	0.0000	-12.9367	0.0000	0.5117	0.0000	14.0459	5.6239	2.5037	267.1707
-34.8919	0.0000	-12.4032	0.0000	0.5145	0.0000	13.9101	5.7205	2.4752	268.2414
-33.8533	0.0000	-11.8679	0.0000	0.5162	0.0000	13.7683	5.8203	2.4482	269.2914
-32.8151	0.0000	-11.3316	0.0000	0.5168	0.0000	13.6207	5.9232	2.4218	270.2636
-31.7771	0.0000	-10.7952	0.0000	0.5165	0.0000	13.4692	6.0302	2.3954	271.2206
-30.7386	0.0000	-10.2596	0.0000	0.5150	0.0000	13.3165	6.1424	2.3701	272.2767
-29.6994	0.0000	-9.7255	0.0000	0.5126	0.0000	13.1647	6.2607	2.3460	273.4970
-28.6589	0.0000	-9.1939	0.0000	0.5090	0.0000	13.0161	6.3865	2.3220	274.9622
-27.6166	0.0000	-8.6657	0.0000	0.5045	0.0000	12.8789	6.5240	2.2985	277.0829
-26.5722	0.0000	-8.1417	0.0000	0.4988	0.0000	12.7776	6.6866	2.2709	280.0891
-25.5253	0.0000	-7.6228	0.0000	0.4921	0.0000	12.7125	6.8764	2.2555	286.5177
-24.4753	0.0000	-7.1101	0.0000	0.4843	0.0000	12.6769	7.0916	2.2346	293.7765
-23.4219	0.0000	-6.6045	0.0000	0.4754	0.0000	12.6646	7.3302	2.2146	302.4733
-22.3646	0.0000	-6.1071	0.0000	0.4654	0.0000	12.6695	7.5900	2.1960	312.4156
-21.3031	0.0000	-5.6188	0.0000	0.4543	0.0000	12.6865	7.8687	2.1779	323.4121
-20.2368	0.0000	-5.1409	0.0000	0.4420	0.0000	12.7112	8.1642	2.1603	335.2901
-19.1655	0.0000	-4.6745	0.0000	0.4265	0.0000	12.7403	8.4743	2.1434	347.8958
-18.0888	0.0000	-4.2209	0.0000	0.4139	0.0000	12.7711	8.7968	2.1282	361.0766
-17.0061	0.0000	-3.7813	0.0000	0.3980	0.0000	12.8013	9.1292	2.1135	374.6779
-15.9173	0.0000	-3.3571	0.0000	0.3809	0.0000	12.8293	9.4689	2.0946	388.5483
-14.8222	0.0000	-2.9499	0.0000	0.3626	0.0000	12.8539	9.8131	2.0863	402.5344
-13.7203	0.0000	-2.5611	0.0000	0.3429	0.0000	12.8744	10.1587	2.0737	416.4628
-12.6116	0.0000	-2.1924	0.0000	0.3220	0.0000	12.8905	10.5022	2.0620	430.2367
-11.4959	0.0000	-1.8454	0.0000	0.2997	0.0000	12.9020	10.8399	2.0524	443.6356
-10.3731	0.0000	-1.5220	0.0000	0.2761	0.0000	12.9093	11.1677	2.0430	456.5167
-9.2433	0.0000	-1.2241	0.0000	0.2511	0.0000	12.9128	11.4813	2.0345	468.7252
-8.1066	0.0000	-0.9536	0.0000	0.2247	0.0000	12.9134	11.7761	2.0267	480.0945
-6.9633	0.0000	-0.7125	0.0000	0.1968	0.0000	12.9119	12.0471	2.0200	490.4657
-5.8139	0.0000	-0.5030	0.0000	0.1676	0.0000	12.9091	12.2894	2.0141	499.6790
-4.6587	0.0000	-0.3270	0.0000	0.1369	0.0000	12.9059	12.4980	2.0092	507.5746
-3.4900	0.0000	-0.1867	0.0000	0.1048	0.0000	12.9031	12.6679	2.0054	513.9932
-2.3349	0.0000	-0.0842	0.0000	0.0712	0.0000	12.9011	12.7944	2.0026	518.7753
-1.1682	0.0000	-0.0213	0.0000	0.0363	0.0000	12.9007	12.8730	2.0009	521.7616
0.0000	0.0000	0.0000	0.0000	0.0000	0.0000	12.9060	12.9000	2.0003	522.7924

Table A-1. Low Aspect Ratio S-Duct—16.2% Diffusion (Continued)

THROAT TO COMPRESSOR FACE Dimensions in Inches - Full scale

CENTERLINE COORDINATES			CENTERLINE SLOPES			SUPER ELLIPSE EQUATION VARIABLES			CROSS SECTIONAL AREA
STA	X_C	Y_C	X_C'	Y_C'	Z_C'	A	B	P	
-68.0000	0.0000	-22.4000	0.0000	-0.0875	0.0000	12.0000	5.7176	3.2069	245.5827
-66.8343	0.0000	-22.4790	0.0000	-0.0403	0.0000	11.9990	5.7195	3.2053	245.6194
-65.6604	0.0000	-22.5131	0.0000	-0.0103	0.0000	11.9962	5.7249	3.2005	245.7200
-64.4900	0.0000	-22.5035	0.0000	0.0264	0.0000	11.9915	5.7340	3.1927	245.9059
-63.3100	0.0000	-22.4520	0.0000	0.0617	0.0000	11.9850	5.7464	3.1819	246.1507
-62.1600	0.0000	-22.3602	0.0000	0.0956	0.0000	11.9767	5.7622	3.1683	246.4598
-61.0049	0.0000	-22.2302	0.0000	0.1261	0.0000	11.9666	5.7813	3.1520	246.8308
-59.8403	0.0000	-22.0639	0.0000	0.1592	0.0000	11.9548	5.8035	3.1346	247.2617
-58.6973	0.0000	-21.8034	0.0000	0.1889	0.0000	11.9413	5.8289	3.1148	247.7484
-57.5522	0.0000	-21.6309	0.0000	0.2171	0.0000	11.9260	5.8574	3.0928	248.2902
-56.4137	0.0000	-21.3663	0.0000	0.2439	0.0000	11.9089	5.8889	3.0686	248.8843
-55.2620	0.0000	-21.0778	0.0000	0.2693	0.0000	11.8901	5.9235	3.0426	249.5280
-54.1572	0.0000	-20.7613	0.0000	0.2933	0.0000	11.8696	5.9609	3.0168	250.2216
-53.0395	0.0000	-20.4207	0.0000	0.3166	0.0000	11.8474	6.0014	2.9892	250.9600
-51.9288	0.0000	-20.0570	0.0000	0.3373	0.0000	11.8234	6.0447	2.9601	251.7443
-50.8251	0.0000	-19.6744	0.0000	0.3573	0.0000	11.7977	6.0908	2.9302	252.5699
-49.7281	0.0000	-19.2721	0.0000	0.3766	0.0000	11.7702	6.1398	2.9000	253.4339
-48.6376	0.0000	-18.8575	0.0000	0.3934	0.0000	11.7408	6.1916	2.8698	254.3328
-47.5533	0.0000	-18.4170	0.0000	0.4096	0.0000	11.7097	6.2461	2.8379	255.2628
-46.4749	0.0000	-17.9671	0.0000	0.4246	0.0000	11.6766	6.3033	2.8075	256.2200
-45.4021	0.0000	-17.5041	0.0000	0.4364	0.0000	11.6416	6.3631	2.7762	257.2007
-44.3345	0.0000	-17.0293	0.0000	0.4510	0.0000	11.6047	6.4256	2.7440	258.2023
-43.2717	0.0000	-16.5438	0.0000	0.4624	0.0000	11.5659	6.4907	2.7134	259.2264
-42.2133	0.0000	-16.0400	0.0000	0.4726	0.0000	11.5254	6.5584	2.6824	260.2757
-41.1589	0.0000	-15.5454	0.0000	0.4878	0.0000	11.4833	6.6289	2.6509	261.3528
-40.1000	0.0000	-15.0345	0.0000	0.4901	0.0000	11.4390	6.7021	2.6210	262.4607
-39.0602	0.0000	-14.5173	0.0000	0.4971	0.0000	11.3950	6.7780	2.5910	263.6019
-38.0152	0.0000	-13.9946	0.0000	0.5030	0.0000	11.3468	6.8567	2.5607	264.7742
-36.9724	0.0000	-13.4675	0.0000	0.5079	0.0000	11.3009	6.9378	2.5321	265.9561
-35.9315	0.0000	-12.9367	0.0000	0.5117	0.0000	11.2509	7.0209	2.5037	267.1207
-34.8919	0.0000	-12.4032	0.0000	0.5145	0.0000	11.1983	7.1057	2.4752	268.2414
-33.8533	0.0000	-11.8679	0.0000	0.5162	0.0000	11.1427	7.1917	2.4482	269.2914
-32.8151	0.0000	-11.3316	0.0000	0.5168	0.0000	11.0842	7.2787	2.4218	270.2636
-31.7771	0.0000	-10.7952	0.0000	0.5165	0.0000	11.0242	7.3677	2.3954	271.2206
-30.7380	0.0000	-10.2596	0.0000	0.5150	0.0000	10.9649	7.4597	2.3761	272.2767
-29.6994	0.0000	-9.7255	0.0000	0.5126	0.0000	10.9681	7.5559	2.3460	273.4978
-28.6589	0.0000	-9.1939	0.0000	0.5090	0.0000	10.8556	7.6576	2.3220	274.9822
-27.6166	0.0000	-8.6657	0.0000	0.5045	0.0000	10.8143	7.7696	2.2985	277.0029
-26.5722	0.0000	-8.1417	0.0000	0.4980	0.0000	10.8051	7.9073	2.2769	280.0891
-25.5253	0.0000	-7.6226	0.0000	0.4921	0.0000	10.8289	8.0725	2.2555	286.5177
-24.4753	0.0000	-7.1101	0.0000	0.4843	0.0000	10.8845	8.2624	2.2346	293.7765
-23.4219	0.0000	-6.6045	0.0000	0.4754	0.0000	10.9550	8.4740	2.2146	302.4733
-22.3646	0.0000	-6.1071	0.0000	0.4654	0.0000	11.0478	8.7042	2.1963	312.4156
-21.3031	0.0000	-5.6180	0.0000	0.4543	0.0000	11.1542	8.9497	2.1779	323.4121
-20.2360	0.0000	-5.1409	0.0000	0.4420	0.0000	11.2708	9.2077	2.1603	335.2901
-19.1655	0.0000	-4.6745	0.0000	0.4285	0.0000	11.3944	9.4754	2.1434	347.8958
-18.0000	0.0000	-4.2269	0.0000	0.4139	0.0000	11.5223	9.7502	2.1282	361.0760
-17.0001	0.0000	-3.7813	0.0000	0.3980	0.0000	11.6523	10.0294	2.1135	374.6779
-15.9173	0.0000	-3.3571	0.0000	0.3809	0.0000	11.7823	10.3103	2.0996	388.5483
-14.8222	0.0000	-2.9499	0.0000	0.3626	0.0000	11.9106	10.5903	2.0861	402.5344
-13.7203	0.0000	-2.5611	0.0000	0.3429	0.0000	12.0355	10.8668	2.0737	416.4020
-12.6116	0.0000	-2.1924	0.0000	0.3220	0.0000	12.1558	11.1369	2.0626	430.2367
-11.4959	0.0000	-1.8454	0.0000	0.2997	0.0000	12.2783	11.3980	2.0524	443.6356
-10.3731	0.0000	-1.5220	0.0000	0.2761	0.0000	12.3779	11.6472	2.0430	456.5187
-9.2433	0.0000	-1.2241	0.0000	0.2511	0.0000	12.4777	11.8817	2.0345	468.7252
-8.1066	0.0000	-0.9536	0.0000	0.2247	0.0000	12.5689	12.0988	2.0267	480.0945
-6.9633	0.0000	-0.7125	0.0000	0.1968	0.0000	12.6580	12.2957	2.0200	490.4657
-5.8119	0.0000	-0.5030	0.0000	0.1676	0.0000	12.7225	12.4696	2.0141	499.6790
-4.6507	0.0000	-0.3270	0.0000	0.1369	0.0000	12.7834	12.6177	2.0092	507.5746
-3.4900	0.0000	-0.1567	0.0000	0.1048	0.0000	12.8326	12.7374	2.0054	513.9932
-2.3349	0.0000	-0.0842	0.0000	0.0712	0.0000	12.8692	12.8261	2.0026	518.7753
-1.1682	0.0000	-0.0213	0.0000	0.0363	0.0000	12.8920	12.8811	2.0009	521.7616
0.0000	0.0000	0.0000	0.0000	0.0000	0.0000	12.9000	12.9000	2.0003	522.7924

ORIGINAL PAGE IS
OF POOR QUALITY

ORIGINAL PAGE IS
OF POOR QUALITY

Table A-1. High Aspect Ratio S-Duct— 10 % Diffusion (Concluded)

THROAT TO COMPRESSOR FACE **Dimensions in Inches - Full Scale**

CENTERLINE COORDINATES			CENTERLINE SLOPES			SUPER ELLIPSE EQUATION VARIABLES			CROSS SECTIONAL
STA	X_C	Y_C	X_C'	Y_C'	Z_C'	A	B	P	AREA
-68.0000	0.0000	-22.4000	0.0000	-0.0075	0.0000	16.5797	4.4436	3.2067	263.7000
-66.8343	0.0000	-22.4796	0.0000	-0.0483	0.0000	16.5765	4.4453	3.2051	263.7225
-65.6664	0.0000	-22.5131	0.0000	-0.0103	0.0000	16.5671	4.4502	3.2003	263.7892
-64.4980	0.0000	-22.5035	0.0000	0.0264	0.0000	16.5515	4.4582	3.1925	263.8988
-63.3308	0.0000	-22.4520	0.0000	0.0617	0.0000	16.5301	4.4694	3.1817	264.0497
-62.1660	0.0000	-22.3602	0.0000	0.0956	0.0000	16.5020	4.4836	3.1681	264.2406
-61.0049	0.0000	-22.2302	0.0000	0.1291	0.0000	16.4699	4.5008	3.1519	264.4699
-59.8483	0.0000	-22.0639	0.0000	0.1592	0.0000	16.4314	4.5209	3.1344	264.7363
-58.6973	0.0000	-21.8634	0.0000	0.1889	0.0000	16.3874	4.5439	3.1140	265.0362
-57.5522	0.0000	-21.6309	0.0000	0.2171	0.0000	16.3381	4.5696	3.0926	265.3743
-56.4137	0.0000	-21.3683	0.0000	0.2439	0.0000	16.2835	4.5987	3.0685	265.7427
-55.2820	0.0000	-21.0778	0.0000	0.2693	0.0000	16.2235	4.6304	3.0425	266.1420
-54.1572	0.0000	-20.7613	0.0000	0.2933	0.0000	16.1584	4.6649	3.0160	266.5703
-53.0395	0.0000	-20.4207	0.0000	0.3160	0.0000	16.0881	4.7024	2.9891	267.0260
-51.9288	0.0000	-20.0578	0.0000	0.3373	0.0000	16.0127	4.7427	2.9599	267.5074
-50.8251	0.0000	-19.6744	0.0000	0.3573	0.0000	15.9322	4.7860	2.9301	268.0132
-49.7281	0.0000	-19.2721	0.0000	0.3760	0.0000	15.8467	4.8323	2.9005	268.5430
-48.6376	0.0000	-18.8525	0.0000	0.3934	0.0000	15.7563	4.8815	2.8697	269.0972
-47.5533	0.0000	-18.4170	0.0000	0.4096	0.0000	15.6611	4.9339	2.8378	269.6757
-46.4749	0.0000	-17.9671	0.0000	0.4246	0.0000	15.5611	4.9893	2.8074	270.2774
-45.4021	0.0000	-17.5041	0.0000	0.4384	0.0000	15.4562	5.0479	2.7761	270.8957
-44.3345	0.0000	-17.0293	0.0000	0.4510	0.0000	15.3463	5.1096	2.7439	271.5229
-43.2717	0.0000	-16.5438	0.0000	0.4624	0.0000	15.2313	5.1745	2.7133	272.1509
-42.2133	0.0000	-16.0498	0.0000	0.4726	0.0000	15.1111	5.2425	2.6823	272.7755
-41.1589	0.0000	-15.5454	0.0000	0.4828	0.0000	14.9861	5.3138	2.6500	273.4057
-40.1080	0.0000	-15.0345	0.0000	0.4901	0.0000	14.8568	5.3886	2.6209	274.0538
-39.0602	0.0000	-14.5173	0.0000	0.4971	0.0000	14.7237	5.4672	2.5909	274.7325
-38.0152	0.0000	-13.9946	0.0000	0.5030	0.0000	14.5870	5.5490	2.5606	275.4539
-36.9724	0.0000	-13.4675	0.0000	0.5079	0.0000	14.4474	5.6365	2.5320	276.2307
-35.9315	0.0000	-12.9367	0.0000	0.5117	0.0000	14.3049	5.7276	2.5036	277.0645
-34.8919	0.0000	-12.4032	0.0000	0.5145	0.0000	14.1587	5.8227	2.4751	277.9153
-33.8533	0.0000	-11.8679	0.0000	0.5162	0.0000	14.0076	5.9214	2.4481	278.7320
-32.8151	0.0000	-11.3316	0.0000	0.5168	0.0000	13.8506	6.0231	2.4217	279.4639
-31.7771	0.0000	-10.7952	0.0000	0.5165	0.0000	13.6888	6.1277	2.3954	280.0602
-30.7386	0.0000	-10.2596	0.0000	0.5150	0.0000	13.5153	6.2341	2.3701	280.4699
-29.6994	0.0000	-9.7255	0.0000	0.5126	0.0000	13.3395	6.3439	2.3460	280.8094
-28.6589	0.0000	-9.1939	0.0000	0.5090	0.0000	13.1779	6.4659	2.3220	281.8631
-27.6166	0.0000	-8.6657	0.0000	0.5045	0.0000	13.0467	6.6091	2.2985	284.3508
-26.5722	0.0000	-8.1417	0.0000	0.4988	0.0000	12.9399	6.7716	2.2760	288.0706
-25.5253	0.0000	-7.6228	0.0000	0.4921	0.0000	12.8469	6.9491	2.2555	292.6075
-24.4753	0.0000	-7.1101	0.0000	0.4843	0.0000	12.7581	7.1370	2.2346	297.5514
-23.4219	0.0000	-6.6045	0.0000	0.4754	0.0000	12.6650	7.3304	2.2146	302.4923
-22.3646	0.0000	-6.1071	0.0000	0.4654	0.0000	12.5597	7.5242	2.1960	307.0201
-21.3031	0.0000	-5.6188	0.0000	0.4543	0.0000	12.4390	7.7153	2.1779	310.9170
-20.2368	0.0000	-5.1409	0.0000	0.4420	0.0000	12.3155	7.9101	2.1603	314.7402
-19.1655	0.0000	-4.6745	0.0000	0.4285	0.0000	12.2043	8.1170	2.1434	319.2354
-18.0890	0.0000	-4.2209	0.0000	0.4139	0.0000	12.1191	8.3477	2.1282	325.1513
-17.0061	0.0000	-3.7813	0.0000	0.3980	0.0000	12.0747	8.6111	2.1135	333.3556
-15.9173	0.0000	-3.3571	0.0000	0.3809	0.0000	12.0924	8.9251	2.0996	345.1959
-14.8222	0.0000	-2.9499	0.0000	0.3626	0.0000	12.1807	9.2992	2.0863	361.4746
-13.7203	0.0000	-2.5611	0.0000	0.3429	0.0000	12.3010	9.7070	2.0737	380.3340
-12.6116	0.0000	-2.1924	0.0000	0.3220	0.0000	12.4230	10.1213	2.0626	399.5981
-11.4959	0.0000	-1.8454	0.0000	0.2997	0.0000	12.5307	10.5280	2.0524	416.4727
-10.3731	0.0000	-1.5220	0.0000	0.2761	0.0000	12.6232	10.9203	2.0430	436.5096
-9.2433	0.0000	-1.2241	0.0000	0.2511	0.0000	12.6980	11.2904	2.0344	453.2602
-8.1066	0.0000	-0.9536	0.0000	0.2247	0.0000	12.7545	11.6312	2.0267	468.3512
-6.9633	0.0000	-0.7125	0.0000	0.1968	0.0000	12.7961	11.9391	2.0200	481.7111
-5.8139	0.0000	-0.5030	0.0000	0.1676	0.0000	12.8270	12.2112	2.0141	493.3435
-4.6587	0.0000	-0.3270	0.0000	0.1369	0.0000	12.8508	12.4447	2.0092	503.2521
-3.4988	0.0000	-0.1867	0.0000	0.1046	0.0000	12.8704	12.6350	2.0054	511.3947
-2.3349	0.0000	-0.0842	0.0000	0.0712	0.0000	12.8856	12.7792	2.0026	517.5461
-1.1682	0.0000	-0.0213	0.0000	0.0363	0.0000	12.8961	12.8690	2.0009	521.4357
0.0000	0.0000	0.0000	0.0000	0.0000	0.0000	12.9000	12.9000	2.0003	522.7924

Table A-2. High Aspect Ratio Duct—16.2% Diffusion Thick Lip Inlet Configuration Lines

Dimensions in Inches - Full Scale

COWL — Trailing Edge to Highlight

CROWN	
STA	Y
-59.83333	-15.39761
-60.93586	-15.31816
-62.49201	-15.28063
-64.02750	-15.29641
-65.43357	-15.35498
-66.66133	-15.44761
-67.69991	-15.56182
-68.56009	-15.68834
-69.26224	-15.82050
-69.82912	-15.95394
-70.28193	-16.08593
-70.63881	-16.21489
-70.91439	-16.33985
-71.11993	-16.46008
-71.26365	-16.57455
-71.35100	-16.68088
-71.38425	-16.76766

KEEL	
STA	Y
-61.02148	-31.28414
-62.31799	-31.11611
-63.85703	-30.88284
-65.36662	-30.60164
-66.74099	-30.29881
-67.93401	-29.99439
-68.93698	-29.70158
-69.76212	-29.42761
-70.43065	-29.17553
-70.96674	-28.94568
-71.38876	-28.73706
-71.71783	-28.54810
-71.96752	-28.37718
-72.14906	-28.22308
-72.27071	-28.08539
-72.33827	-27.96551
-72.35596	-27.87429

LIP — Highlight to Throat

CROWN	
STA	Y
-71.38425	-16.76766
-71.38583	-16.84448
-71.37707	-16.92242
-71.35750	-17.00166
-71.32626	-17.08238
-71.28217	-17.16471
-71.22357	-17.24866
-71.14841	-17.33409
-71.05408	-17.42061
-70.93752	-17.50756
-70.79510	-17.59386
-70.62273	-17.67803
-70.41565	-17.75818
-70.16806	-17.83218
-69.87112	-17.89807
-69.50482	-17.95620
-68.91418	-18.01644
-67.82626	-18.12812

KEEL	
STA	Y
-72.35596	-27.87429
-72.33518	-27.76040
-72.29265	-27.64812
-72.22745	-27.53729
-72.13813	-27.42787
-72.02262	-27.32001
-71.87833	-27.21415
-71.70218	-27.11104
-71.48073	-27.01189
-71.24051	-26.91842
-70.94841	-26.83298
-70.61234	-26.75853
-70.23209	-26.69865
-69.81020	-26.65679
-69.35275	-26.63681
-68.86956	-26.64137
-68.37374	-26.67188

Table A-3. High Aspect Ratio Duct—16.2% Diffusion Very Thin Lip Inlet Configuration Lines

Dimension in Inches - Full Scale

COWL - Trailing Edge to Highlight

STA	Y
-64.33655	-30.24138
-64.97638	-30.16103
-65.74897	-30.02259
-66.53190	-29.84328
-67.27586	-29.63621
-67.95379	-29.41362
-68.55207	-29.18517
-69.06759	-28.95862
-69.50276	-28.73862
-69.86379	-28.52845
-70.15776	-28.32983
-70.39207	-28.14379
-70.57276	-27.97034
-70.70552	-27.81034
-70.79466	-27.66431
-70.84328	-27.53517
-70.85448	-27.43552

LIP - Highlight to Throat

STA	Y
-70.84241	-27.36931
-70.81759	-27.30397
-70.77966	-27.23948
-70.72776	-27.17586
-70.66052	-27.11310
-70.57672	-27.05155
-70.47431	-26.99155
-70.35138	-26.93397
-70.20586	-26.87966
-70.03586	-26.83000
-69.84052	-26.78672
-69.61931	-26.75172
-69.37414	-26.72741
-69.10810	-26.71586
-68.82707	-26.71845
-68.53879	-26.73621
-65.82448	-26.87328

Table A-4. High Aspect Ratio Duct—16.2% Diffusion Thin Lip Inlet Configuration Lines

Dimensions in Inches - Full Scale

COWL — Trailing Edge to Highlight

CROWN		KEEL	
STA	Y	STA	Y
-61.55017	-15.31227	-62.89059	-30.63328
-62.44890	-15.26248	-63.78430	-30.52626
-63.53452	-15.25053	-64.85551	-30.34961
-64.62685	-15.28290	-65.92563	-30.12795
-65.65256	-15.35369	-66.92346	-29.88013
-66.57326	-15.45381	-67.81278	-29.62166
-67.37389	-15.57403	-68.58037	-29.36423
-68.05435	-15.70646	-69.22751	-29.11565
-68.62291	-15.84610	-69.76335	-28.88038
-69.09136	-15.98572	-70.20028	-28.68056
-69.47212	-16.12548	-70.55097	-28.46880
-69.77669	-16.26258	-70.82710	-28.26890
-70.01480	-16.39578	-71.03847	-28.09637
-70.19430	-16.52409	-71.19296	-27.93886
-70.32104	-16.64617	-71.29659	-27.79661
-70.39896	-16.75929	-71.35368	-27.67167
-70.42941	-16.85118	-71.36770	-27.57589

LIP — Highlight to Throat

CROWN		KEEL	
STA	Y	STA	Y
-70.42941	-16.85118	-71.36770	-27.57589
-70.43039	-16.92802	-71.35208	-27.49026
-70.42223	-17.00596	-71.32010	-27.40585
-70.40260	-17.08520	-71.27109	-27.32253
-70.37142	-17.16592	-71.20393	-27.24026
-70.32733	-17.24825	-71.11710	-27.15917
-70.25874	-17.33220	-71.00861	-27.07958
-70.19357	-17.41763	-70.87617	-27.00206
-70.09924	-17.50415	-70.71719	-26.92751
-69.98268	-17.59109	-70.52907	-26.85723
-69.84025	-17.67739	-70.30946	-26.79300
-69.68789	-17.76156	-70.05679	-26.73703
-69.46082	-17.84171	-69.77090	-26.69193
-69.21322	-17.91671	-69.45371	-26.66064
-68.91629	-17.98161	-69.10979	-26.64551
-68.54999	-18.03874	-68.74651	-26.64896
-67.95935	-18.09898	-68.37374	-26.67188
-67.62526	-18.12812		

ORIGINAL PAGE IS
OF POOR QUALITY

ORIGINAL PAGE IS
OF POOR QUALITY

Table A-5. Low Aspect Ratio Duct—16.2% Diffusion Thin Lip Inlet Configuration Lines

Dimensions in Inches - Full Scale

COWL – Trailing Edge to Highlight

CROWN	
STA	Y
-61.37220	-13.27804
-62.20104	-13.23728
-63.21157	-13.24109
-64.24527	-13.29500
-65.23716	-13.39317
-66.14958	-13.52652
-66.96329	-13.68638
-67.67200	-13.86105
-68.27771	-14.04642
-68.78700	-14.23813
-69.20840	-14.42828
-69.55067	-14.61412
-69.82181	-14.79761
-70.02856	-14.97496
-70.17612	-15.14397
-70.26794	-15.30047
-70.30482	-15.42722

KEEL	
STA	Y
-63.06856	-32.86751
-63.88189	-32.56373
-64.88641	-32.38451
-65.89503	-32.15192
-66.85480	-31.88299
-67.73021	-31.59323
-68.50397	-31.29548
-69.17141	-30.99842
-69.73573	-30.71168
-70.20435	-30.43842
-70.58632	-30.17599
-70.89077	-29.93156
-71.12593	-29.70378
-71.29874	-29.49322
-71.41470	-29.30115
-71.47797	-29.13109
-71.49228	-28.99985

LIP – Highlight to Throat

CROWN	
STA	Y
-70.30482	-15.42722
-70.30641	-15.50408
-70.29766	-15.58200
-70.27308	-15.66123
-70.24684	-15.74196
-70.20275	-15.82429
-70.14416	-15.90824
-70.06899	-15.99366
-69.97466	-16.08019
-69.85809	-16.16713
-69.71568	-16.25343
-69.54331	-16.33760
-69.33624	-16.41775
-69.08864	-16.49175
-68.79171	-16.55766
-68.42541	-16.61478
-67.83477	-16.67502
-67.50168	-16.70416

KEEL	
STA	Y
-71.49228	-28.99985
-71.47666	-28.91422
-71.44468	-28.82981
-71.39667	-28.74648
-71.32861	-28.66422
-71.24168	-28.58313
-71.13319	-28.50354
-71.00076	-28.42602
-70.84177	-28.35147
-70.65365	-28.28120
-70.43404	-28.21696
-70.18137	-28.16098
-69.89648	-28.11589
-69.57829	-28.08449
-69.23437	-28.06947
-68.87109	-28.07291
-68.49832	-28.09684

Table A-5. High Aspect Ratio Duct—10% Diffusion Thin Lip Inlet Configuration Lines (Concluded)

Dimensions in Inches - Full Scale

COWL — Trailing Edge to Highlight

CROWN	
STA	Y
-61.31649	-15.05543
-62.24776	-15.00383
-63.37272	-14.99145
-64.50464	-15.02499
-65.56750	-15.09836
-66.52155	-15.20210
-67.35119	-15.32667
-68.05631	-15.46390
-68.64546	-15.60757
-69.13089	-15.75328
-69.52546	-15.89811
-69.84105	-16.04017
-70.08778	-16.17621
-70.27379	-16.31116
-70.40514	-16.43767
-70.48588	-16.55490
-70.51743	-16.65011

KEEL	
STA	Y
-62.70547	-30.93163
-63.63157	-30.82073
-64.74158	-30.63758
-65.85047	-30.40799
-66.88445	-30.15119
-67.80600	-29.88334
-68.60139	-29.61660
-69.27197	-29.35901
-69.82723	-29.11522
-70.27998	-28.88743
-70.64340	-28.67628
-70.92953	-28.48158
-71.14855	-28.30280
-71.30866	-28.13956
-71.41602	-27.99216
-71.47518	-27.86270
-71.48972	-27.76345

LIP — Highlight to Throat

CROWN	
STA	Y
-70.51743	-16.65011
-70.51906	-16.72973
-70.50999	-16.81049
-70.48971	-16.89260
-70.46734	-16.97625
-70.41165	-17.06157
-70.35093	-17.14866
-70.27303	-17.23708
-70.17529	-17.32673
-70.05450	-17.41683
-69.90694	-17.50625
-69.72832	-17.59347
-69.51374	-17.67653
-69.25717	-17.75321
-68.94949	-17.82149
-68.56991	-17.88069
-67.95788	-17.94311
-67.51272	-17.97331

KEEL	
STA	Y
-71.48972	-27.76345
-71.47353	-27.67472
-71.44039	-27.58725
-71.38960	-27.50091
-71.32001	-27.41566
-71.23003	-27.33163
-71.11761	-27.24916
-70.98038	-27.16883
-70.81564	-27.09158
-70.62070	-27.01876
-70.39314	-26.95220
-70.13132	-26.89419
-69.83607	-26.84746
-69.50639	-26.81494
-69.14999	-26.79937
-68.77356	-26.80293
-68.38728	-26.82669

Table A-6. Shaft Fairing Configuration Lines

SMALL SHAFT FAIRING

X	Y
.04241	.40810
.60345	.49621
.10586	.63276
.21172	.87362
.42328	1.18776
.63500	1.40328
.84672	1.56466
1.27000	1.78603
1.69345	1.91707
2.11672	1.98517
2.5400	2.00534
2.96345	1.98759
3.38672	1.93897
3.81017	1.86466
4.23345	1.76897
4.65672	1.65483
5.08017	1.52483
5.50345	1.38086
5.92690	1.22431
6.35017	1.05603
6.77345	.87655
7.19690	.68586
7.62017	.48379
8.04362	.26948
8.46690	.04207

LARGE SHAFT FAIRING

X	Y
.15517	.63276
.31207	.87414
.62241	1.18793
.93448	1.40345
1.24483	1.56379
1.86724	1.78621
2.48966	1.91724
3.11379	1.98448
3.73621	2.00517
4.98103	1.95517
6.22586	1.76897
7.47069	1.52414
8.71552	1.22414
9.96207	.87586
11.20690	.48448
11.82931	.26897
12.45172	.04138

1. Report No.
CR 179454

2. Government Accession No.

3. Recipient's Catalog No.

4. Title and Subtitle
"An Experimental Evaluation of S-Duct Inlet-Diffuser Configurations for Turboprop Offset Gearbox Applications"

5. Report Date
July 1986

6. Performing Organization Code

7. Author(s)
Paul L. McDill

8. Performing Organization Report No.
D6-53344

10. Work Unit No.

9. Performing Organization Name and Address
Boeing Commercial Airplane Company
P. O. Box 3707
Seattle, WA 98124

11. Contract or Grant No.
Memorandum of Understanding

13. Type of Report and Period Covered
Contractor Report

12. Sponsoring Agency Name and Address
National Aeronautics and Space Administration
Washington, D.C. 20546

14. Sponsoring Agency Code

15. Supplementary Notes

Project Manager - George L. Stefko, Propulsion Systems Division
NASA-Lewis Research Center
Cleveland, Ohio 44135

16. Abstract

A test program, utilizing a large scale model, was run in the NASA-Lewis Research Center 10- by 10-ft wind tunnel to examine the influence on performance of design parameters of turboprop S-duct inlet/diffuser systems. The parametric test program investigated inlet lip thickness, inlet/diffuser cross-sectional geometry, throat design Mach number, and shaft fairing shape.

The test program was run at angles of attack to 15 deg and tunnel Mach numbers to 0.35.

Results of the program indicate that current design techniques can be used to design inlet/diffuser systems with acceptable total pressure recovery, but several of the design parameters, notably lip thickness (contraction ratio) and shaft fairing cross section, must be optimized to prevent excessive distortion at the compressor face.

17. Key Words (Suggested by Author(s))
S-Duct, Inlet Pressure Recovery, Compressor Face Distortion, Contraction Ratio, Diffusion Rate, Shaft Fairing

18. Distribution Statement
Distribution of this document is limited until February 1989

19. Security Classif. (of this report)	20. Security Classif. (of this page)	21. No. of pages	22. Price*
Unclassified	Unclassified		

[redacted]